A Robotic Chewing Device for Food Evaluation

A thesis presented in partial fulfilment of the
requirements for the degree of

Master of Engineering
in
Mechatronics

at
Massey University,
Palmerston North, New Zealand

Darren Lewis

2006

Abstract

The aim of this masters project was to design and develop a prototype of robotic chewing device. This project was required for use in food evaluation as it can provide standardised chewing. The chewing device was required to follow chewing trajectories of a human and apply the same forces that humans apply during chewing. This was achieved by the use of a robotic system that incorporated a mechanical linkage, supporting software and electronics to control it and therefore ensure correct operation. The mechanical linkage used is based on a four-bar linkage mechanism that can closely approximate human chewing trajectories. The linkage also has the ability to be adjusted to achieve a range of chewing trajectories for different food types. This is due to the fact that humans chew foods with different properties differently. The linkage is driven by a single DC motor that is controlled by a control card and a supervisory software program on a computer. This ensures that chewing is performed at the correct speed in the different phases of the chewing cycle and also provides all the necessary controls for operation of the device. Anatomically correct teeth were also used to help closely match the particle size reduction of the human system, while a food retention device was made to keep the food particles on the teeth while chewing.

Acknowledgements

I would first of all like to thank my supervisors Dr. John Bronlund, Assoc. Prof. Peter Xu and Dr. Kylie Foster who have guided me throughout this project and help make it a success.

The technicians at the Massey University Institute of Technology and Engineering workshop for their help and support.

Christine Lawrence from Massey University Auckland for her help.

Prof. Jules Kieser, Ionut Ichim and Neil Waddell from the School of Dentistry at the University of Otago for their guidance on the function of teeth.

Flanders, Sebastian, Jonathan for their help and friendliness throughout the year.

And finally Crop and Food New Zealand for funding this project.

Table of contents

List of figures

List of tables

1 Introduction

The aim of this thesis research was to design and implement a robotic chewing device for the evaluation of foods. This required the device to approximate the human chewing cycle. To do so, extensive research was carried out in order to understand how humans chew and the important features that prepare the bolus for swallowing. Once this was done, a mechanical system could be built and controlled to ensure correct operation.

The specific aspects of the food chewing of interest are the grinding of the food sample to form a bolus ready for swallowing. Ideally the robotically chewed bolus would have similar particle size distributions and rheology to human chewed samples.

The tasks of the thesis were identified to be:

- Research the human chewing motion and identify the important aspects of jaw movement that prepare the bolus for swallowing
- Analyse and design a mechanism that is able to reproduce the key aspects of the human masticatory cycle
- Construct the designed mechanism
- Implement a suitable controller for controlling the mechanism

2 Literature review

2.1 Introduction

The literature reviewed in this chapter is to study the operation of the human chewing cycle. This is required to specify the requirements of the chewing device and what important factors need to be considered to ensure that the chewed food sample that the chewing device provides is similar to that of what a human produces.

2.2 Human masticatory system

2.2.1 Overview

The human masticatory system is a complex system that comprises of an upper and lower jaw that have teeth located on them. It also includes a tongue, check and saliva production capability. When mastication is performed, the lower jaw is moved by muscles that are attached between it and the upper jaw. These muscles are responsible for the chewing motion can be broken up into five main muscle groups which are as follows; (Lucas 2004, A)

- The temporalis
- The masseter
- The medial pterygoid
- The lateral pterygoid, and
- The digastric

The digastric muscle is attached between the chin and the bottom of the skull. This is the muscle that is primarily responsible for opening the mouth

The temporalis muscles are attached from the side of the skull to the top of the lower jaw behind the teeth as shown in Figure 2-1. This is a large muscle that is approximately the same length of that of the bicep and consists of vertical and horizontal muscle fibres to help close the mouth and also help to move the lower jaw backward and forward.

The masseter muscles are attached between the cheek on the skull and the lower rear section of the lower jaw as shown in Figure 2-1. These are large muscles that are used to close the mouth and also to move the lower jaw laterally from side to side by contracting one muscle and not the other.

The medial pterygoid muscles are attached on the inside of the skull and the lower jaw as shown in Figure 2-1. These muscles are primarily responsible for the side to side movement of the lower jaw and also help to close the mouth.

The lateral pterygoid muscles are attached between the skull and the lower jaw in a horizontal fashion as shown in Figure 2-1. These muscles are used to move the lower jaw forward and backward.

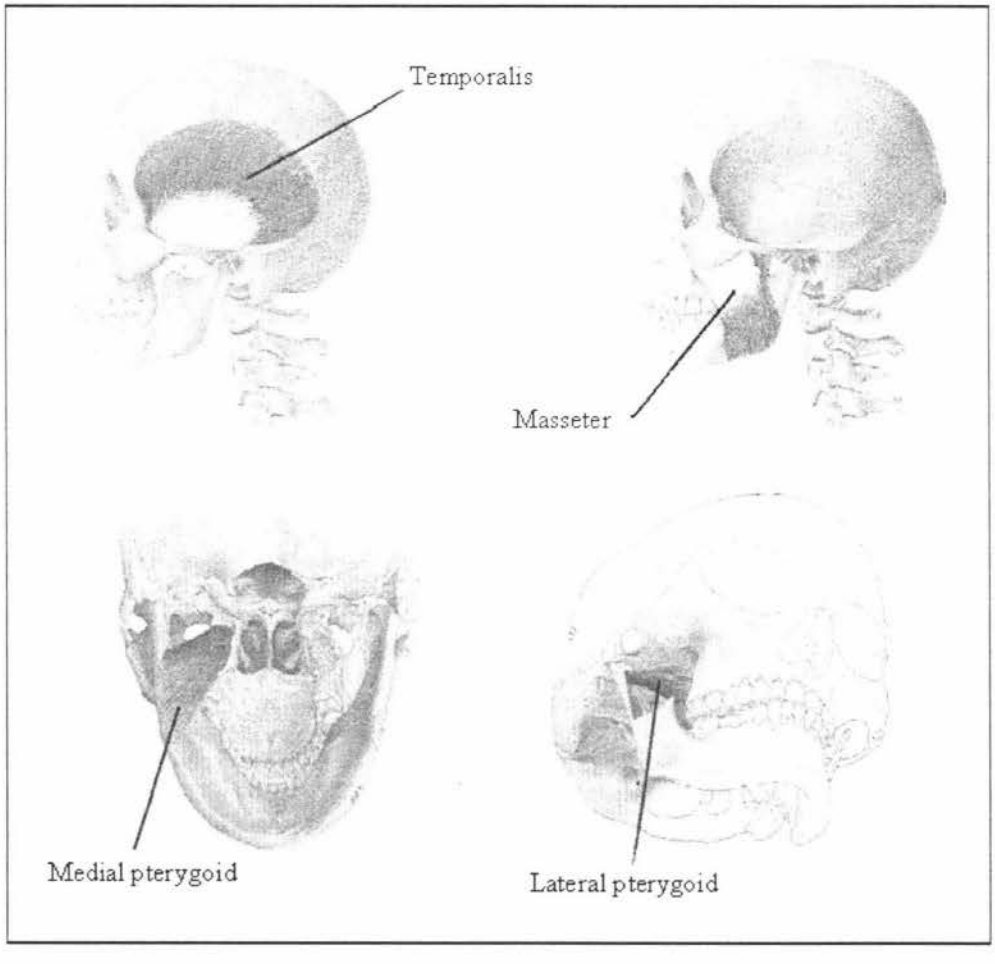

Figure 2-1 The location of muscles that are used in chewing (adapted from Hannam 1997)

Using these muscle groups in different ways allows the lower jaw to move in six degrees of freedom (Koolstra & van Eijden 1999). This allows the lower jaw to perform many complex motions.

The teeth that are in the human mouth are developed to perform specific tasks (Lucas 2004a and 2004c). The front teeth are called incisors and are used to take an initial bite of a piece of food. This piece of food is then broken up further by the pre-molars which are located between the front incisors and the rear molars. When the food particles are sufficiently broken up by each type of teeth the tongue and cheek then move the food to the next type of teeth for further chewing. The tongue is also used to determine when the food particles are sufficiently small enough to move on to the next type of teeth and when it is time to swallow (Lucas 2004b and 2004c). As well as moving the food particles from teeth to teeth the tongue and check also have the task of stopping the food from falling off the teeth during chewing. While all of this is happening saliva is being released by the salivary glands. The main tasks that the saliva performs in mastication include binding the food particles together, stopping the food from sticking to the teeth and also helping to break the food down (Pedersen *et al* 2002).

2.2.2 Jaw geometry

The human jaw consists of an upper and lower jaw. The upper jaw is called the maxilla and is attached to other bones that make up the skull. The lower jaw is called the mandible and is attached to the skull by muscles. This means that the mandible is moved while the skull remains in a fixed location relative to the mandible. Both the maxilla and the mandible have teeth attached to them which the main purpose is of mastication.

The mandible is the largest and strongest bone in the facial skeleton. It consists of a horizontal portion and two vertical portions. The horizontal portion is called the body while the vertical portions are called the rami. The mandible is moved by the muscles attached to it, and pivots around a point on each rami called the 'condyle'. This can be seen in Figure 2-2. While the maxilla is the second largest bone in the facial skeleton and consists of teeth that are designed to compliment the teeth on the mandible (Gray 1918).

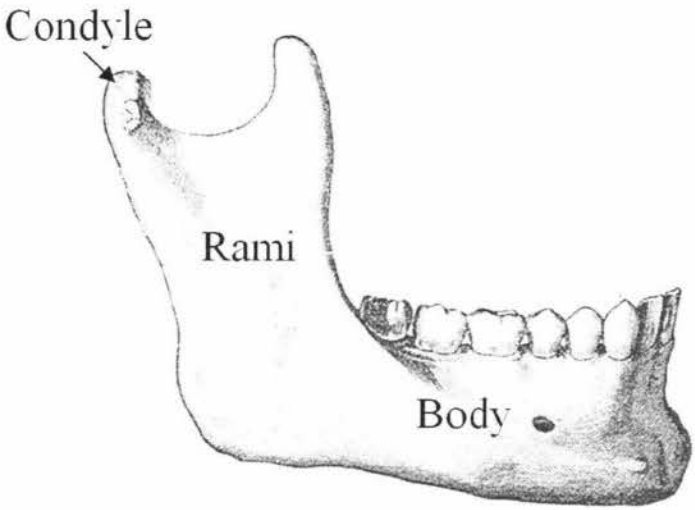

Figure 2-2 The human mandible (adapted from Gray 1918)

The teeth that are located on the mandible and the maxilla make a curve in both the frontal and sagittal planes. The frontal and sagittal planes are referred to throughout this thesis where the frontal plane corresponds to looking at the face while the sagittal plane corresponds to looking at the side of the skull. The curve in the frontal plane is called the 'Curve of Wilson' while the curve in the sagittal plane is called the 'Curve of Spee' (Dawson 1989). These curves can be seen in Figure 2-3.

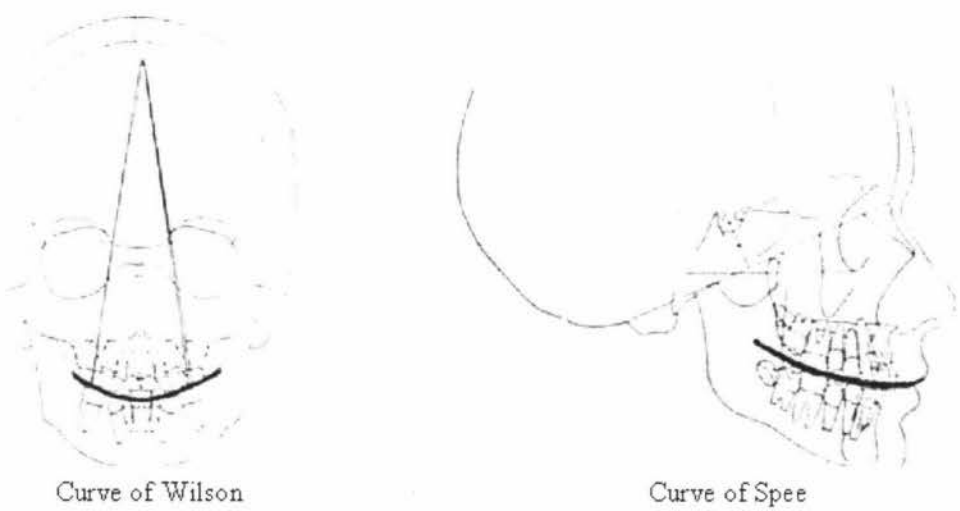

Figure 2-3 The curve of Wilson and the curve of Spee (taken from Palmer 2004)

The curve of Spee has the function of protecting the pre-molars and molars. This is done by allowing the incisors to contact before the molars and pre-molars. By doing this

the strong forces applied by the mastication muscles are removed from the molars and pre-molars (Wynne 2005). This is required to stop excessive wear on the molars and pre-molars so that the ability to chew food is retained over an entire life time. An ideal curve of Spee would extend though the condyle with a radius of approximately four inches (Dawson 1989).

The curve of Wilson allows the teeth to move without any interference at occlusion (Wynne 2005). This can be thought of as ball and socket joint which allows the ball to move freely inside the socket with no excessive interference. Therefore the teeth can move with minimal interference reducing the chance of damaging the teeth.

2.2.3 Teeth shape

Teeth in the human mouth consist of a number of different shapes. The teeth at the front of the mouth have one sharp edge like a blade, while teeth at the back of the mouth consist of peaks called cusps. These different teeth shapes can be classified into incisors, canines and post canines, where the post canine teeth consist of pre-molars and molars. The teeth layout can be seen in Figure 2-4.

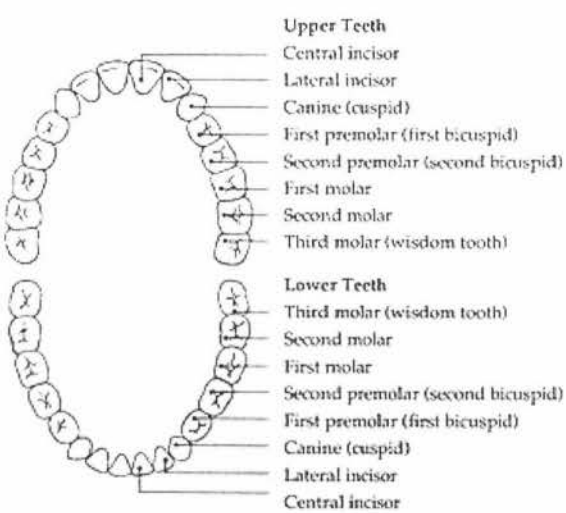

Figure 2-4 Teeth in the human mouth (taken from Oralb)

The incisors and canine teeth are also know as the anterior teeth and work like scissors by cutting the food upon the first bite. This is why these teeth have a blade like edge. The postcanine teeth are also known as the posterior teeth and perform the mastication

(Lucas 2004a). Because the focus of this work is to build a machine to simulate mastication (rather than biting), it should include the four opposing post-canine teeth from one side of the mouth.

As the postcanine teeth are used for mastication they are required to reduce the particle size of the food. The reduction of particle size is required to increase the surface area of the food being chewed. This allows the food to be digested by the enzymes in the stomach more quickly (Lucas 2004b), thereby allowing the energy of the food to be released more quickly.

While the exact operation of every part of the tooth surface is unknown, a common theory can be described. To perform the task of particle size reduction the postcanine teeth are designed to fracture the food being chewed. The simplest way of fracturing a food particle is to apply a point force. This creates a large stress in the food particle from a minimal force. The postcanine teeth are in fact shaped on this principle using cusps to apply point forces. From this idea it may be thought that the sharper the cusps are the better they will fracture the food particle. However the cusps on the post canine teeth are not sharp but instead dull. In fact if the cusps are sharp they are more likely to plastically deform the food particle rather than fracturing it (Lucas 2004c). The cusps can therefore be thought of as being spherical in shape and when pressed onto the food particle an indentation is made. The fracture force resulting from this indentation is proportional to the radius of the spherical cusp (Frank & Lawn 1967). This then would mean that dull cusps will fracture the food particles better than sharp ones. An example of how the cusps of the postcanine teeth fracture food particles and how it can be approximated to a three point bending can be seen in Figure 2-5.

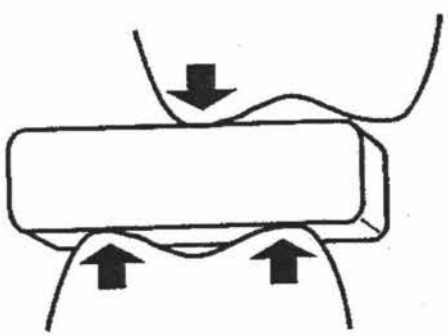

Figure 2-5 Three point bending principle adapted to mastication for fracturing food (adapted from Ashby & Jones 1996)

However not all foods fracture easily. Therefore the teeth require another method to reduce the particle size of the food. A possible solution is that the post-canine teeth also include a sharp blade like edge as used by the anterior teeth. This would give them the ability to cut food particles by moving the blades over each other. The blades of the upper teeth would then have to match the lower teeth. This is due to the fact that the blades must make good contact when they pass over each other. The cusps on the other hand do not need to be as precise as they are used to produce fractures ahead of their path of travel. This explanation of the use of cusps and blades is the most likely solution to apply to the design of the working surfaces of the post-canine teeth (Lucas 2004c). Because the teeth shape is important to the mechanism and effectiveness of food mastication, the chewing device developed in this work must employ realistically shaped teeth.

2.2.4 Forces on teeth

The forces applied on the teeth vary with the type of food that is being chewed. The force applied to a single tooth is also different to that of total force between all the contacting teeth during chewing. On foods such as biscuits, carrots and cooked meats forces range between 70 and 150N on a single tooth (Anderson 1956), while forces on all the contacting teeth range between 190 and 260N (Gibbs *et al* 1981). This is much smaller than the maximum bite force that can be applied to the molars which measures 500 to 700N (Wood & Williams 1981). It is thought that these high forces must be important in the process of thegosis or grinding teeth to sharpen the cusps (Every 1970). From the literature values an estimate of the maximum force that the chewing device in this work is 150N.

2.2.5 Jaw trajectories during chewing

The first stage in the human chewing cycle involves the mandible opening thereby creating a space between the teeth located on skull and the mandible. The tongue then places food particles that need chewing on to the molars on one side of the mouth. The mandible then closes and breaks up these food particles and then the particles fall off the teeth back on to the tongue for positioning on the next cycle. If the food gets stuck to the teeth most of the food would remain un-chewed. Therefore saliva is used to help

stop the food particles from sticking to the teeth and also helps to break down the food. In extreme cases the tongue is used to pick food particles that get stuck off the teeth (Lucas 2004b).

The opening of the mouth in the first stage of the chewing cycle is relatively vertical (Mongini *et al* 1986). The speed of the mandible in the opening phase initially starts slowly and increases as the mouth opens. But when the mouth starts to close, the mandible moves laterally outward and initially closes quickly coming back towards the teeth and then slows for occlusion. This can be seen in Figure 2-6.

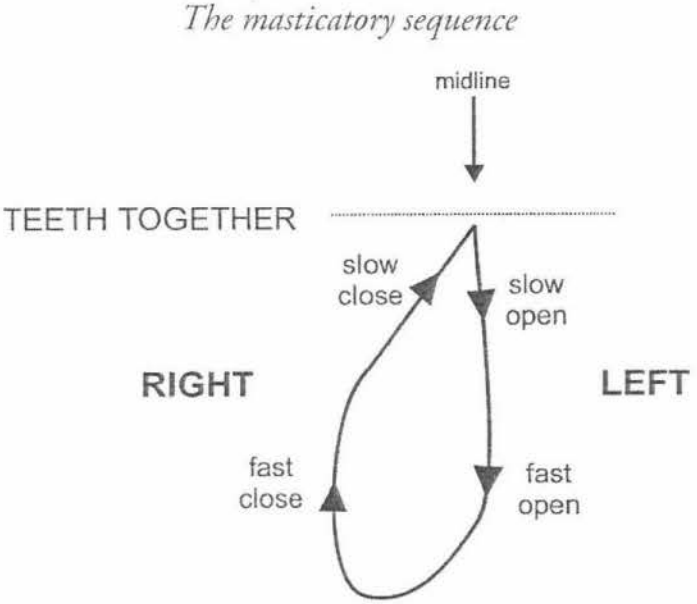

Figure 2-6 The masticatory sequence (taken from Lucas 2004b)

The trajectories of the teeth during chewing need to be characterised for different food properties. This is required to determine how different foods affect the chewing trajectories. The different chewing trajectories are represented in the frontal and sagittal planes which correspond to the planes looking at the front and side of the skull. Some of the many jaw trajectories can be seen below in Figure 2-7 to Figure 2-9.

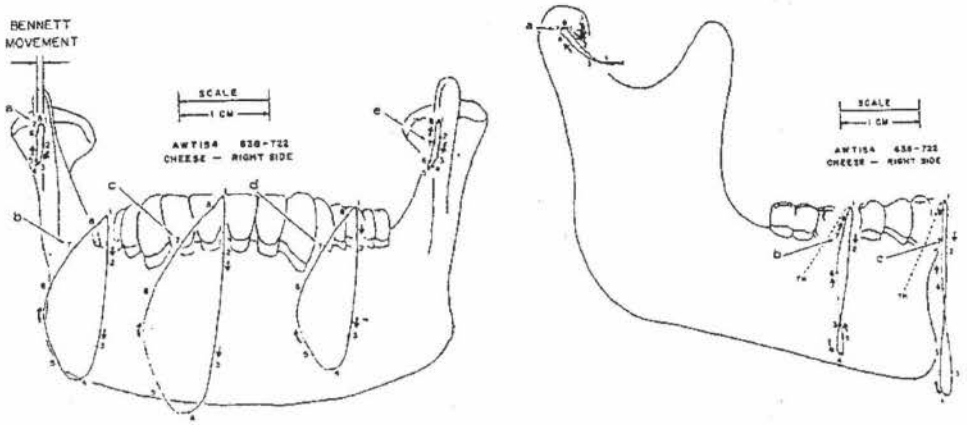

Figure 2-7 Frontal and sagittal trajectories of a typical adult when chewing soft cheese on the right side (taken from Gibbs & Lundeen 1982)

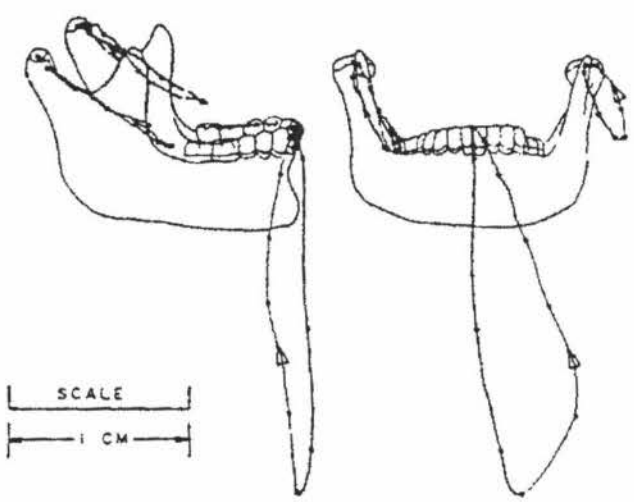

Figure 2-8 Sagittal and frontal trajectories of a typical adult when chewing carrot (taken from Gibbs & Lundeen 1982)

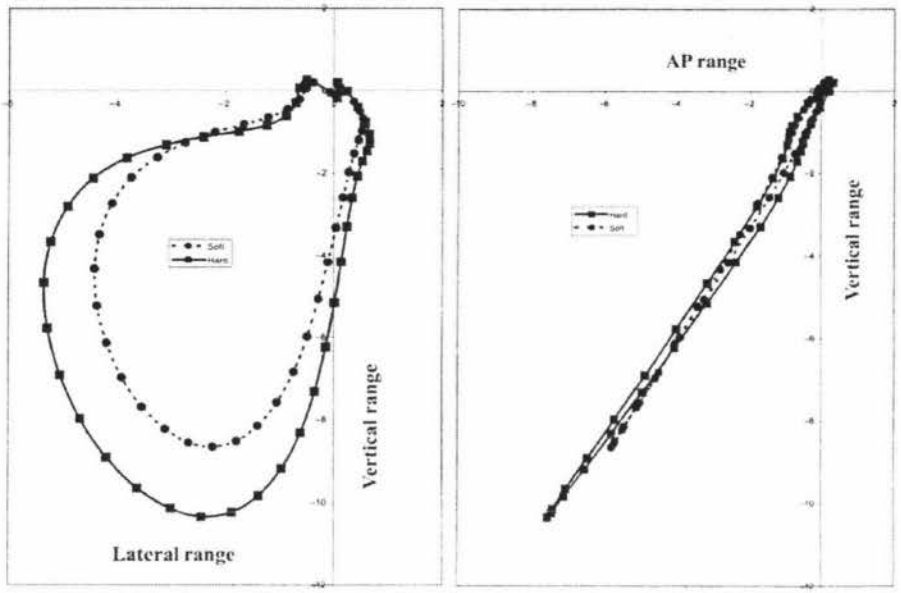

Figure 2-9 Average frontal and sagittal trajectories for a typical adult when chewing hard and soft gum (adapted from Anderson et al, 2002)

It can be seen from these figures that the chewing trajectories vary substantially. It can be seen that the trajectories in the sagittal plane are very close to a straight line. However from the literature reviewed it can vary from a vertical line where the teeth come together at a zero degree angle and a line where the teeth come together at a 30 degree angle. The trajectories in the frontal plane can also be seen to change from vertical profiles where the teeth occlude in a vertical fashion to lateral profiles where the teeth slide across each other in a horizontal fashion. The presence of a straight line trajectory in the sagittal plane presents the opportunity to reproduce the chewing motion with a two-dimensional system. The orientation of this two-dimensional trajectory however should be ideally adjustable from being directly in the sagittal plane (e.g. Figure 2-7) to 30 degrees from this (see Figure 2-9 where there is some movement in the sagittal plane).

The trajectories used to chew different food particles differ depending on both the shape and the texture of the food particles. This is due to the fact that the teeth operate differently depending on the chewing trajectory. If a vertical chewing motion is used, the teeth use their cusps to fracture the food particles. Where as if a more lateral chewing motion is used, the teeth use their sharp edges to function as blades and cut up the food particles (Lucas 2004c). The chewing trajectory used is therefore adjusted to ensure that the teeth are used correctly to chew the desired food particles. The decision

of how to use the teeth, and therefore what chewing trajectory to use can be seen in Figure 2-10**Error! Reference source not found.**. It shows that in the first step of deciding on how to use the teeth, the particle shape is detected and if the particles are thin sheets or rods the teeth are used as blades to cut up the food. If however they are thick blocks, then the texture is examined in the mouth. Lucas describes the texture as being $(R/E)^{0.5}$, where R is the food toughness and E is Young's modulus of elasticity. If $(R/E)^{0.5}$ is low, the teeth use their cusps to fracture the food. If $(R/E)^{0.5}$ is high, then the teeth once again use their sharp edges as blades to cut up the food. The application of this model implies foods that require fracturing include peanuts and biscuits as they are not tough and have a relatively high modulus of elasticity and therefore can be chewed with a vertical chewing motion. While foods that require cutting include meats and vegetables and therefore need to be chewed with a lateral chewing motion.

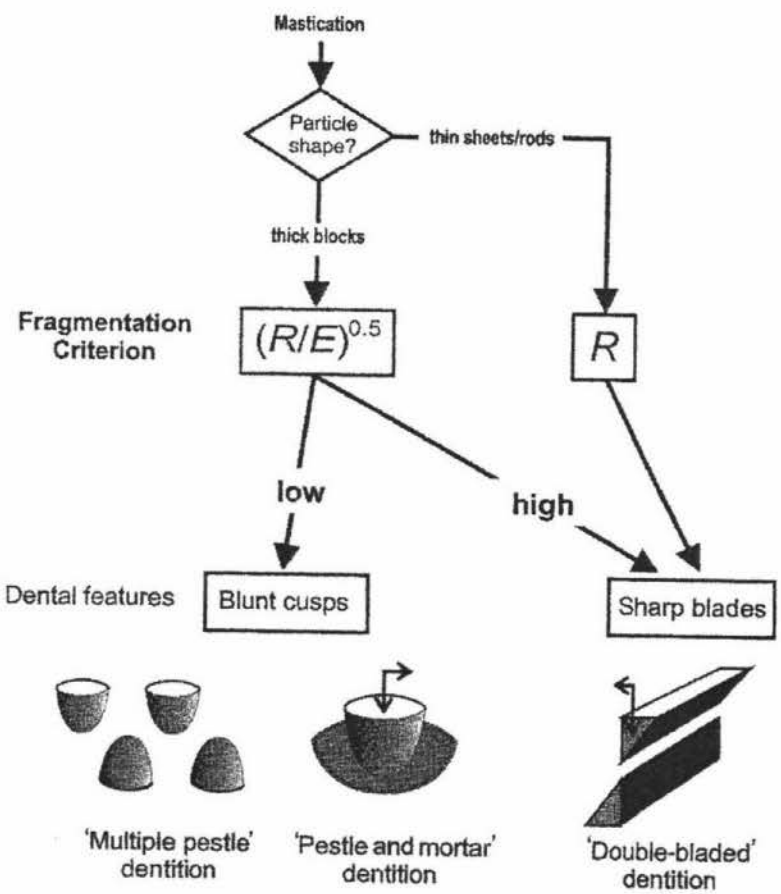

Figure 2-10 The decision of what teeth function to use (adapted from Lucas 2004c)

Due to the fact that chewing is performed on the post canines, the chewing device must follow the trajectories of the post canine teeth. However no data was found on the trajectories of the post canine teeth during chewing. This is most likely due to the fact

that there has been limited research done on this as it is very difficult to accurately measure the trajectories of the post canine teeth while chewing. A method to do this would involve placing a sensor onto these teeth in order to measure the trajectories. However it would not feel natural to the test subject to have such a sensor on the post canine teeth while chewing. Therefore the chewing trajectories measured could in fact be quite different due to the fact that test subject may alter there chewing to compensate for the sensor in their mouth. There was however data available for incisor trajectories. Therefore the relationship between incisor and molar trajectories was investigated. This was done by using a SolidWorks model (J.-S.Pap 2005) of the human mandible and making it move by specifying a known incisor trajectory. This model cen be seen in Figure 2-11. The trajectory of the first molar was then measured and compared with the incisor trajectory. It was found that the trajectory of the first molar where vertically compressed versions of the incisor trajectories. But the entry and exit angle to and from occlusion were not greatly different. A comparison of a single incisor and molar trajectory can be seen in Figure 2-12 Therefore data on the occlusal angles for incisors was used.

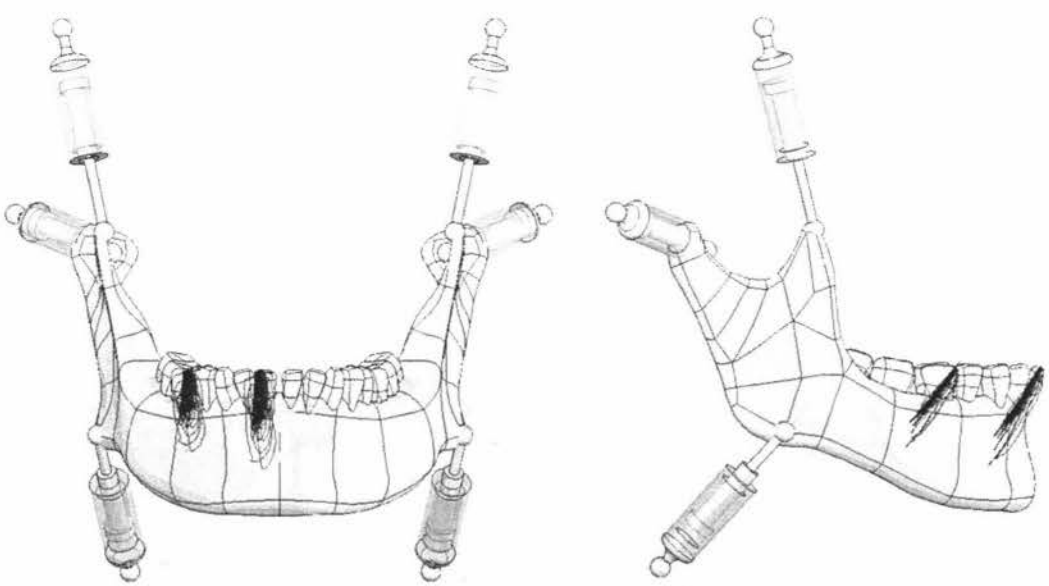

Figure 2-11 J.-S. Pap's SolidWorks model

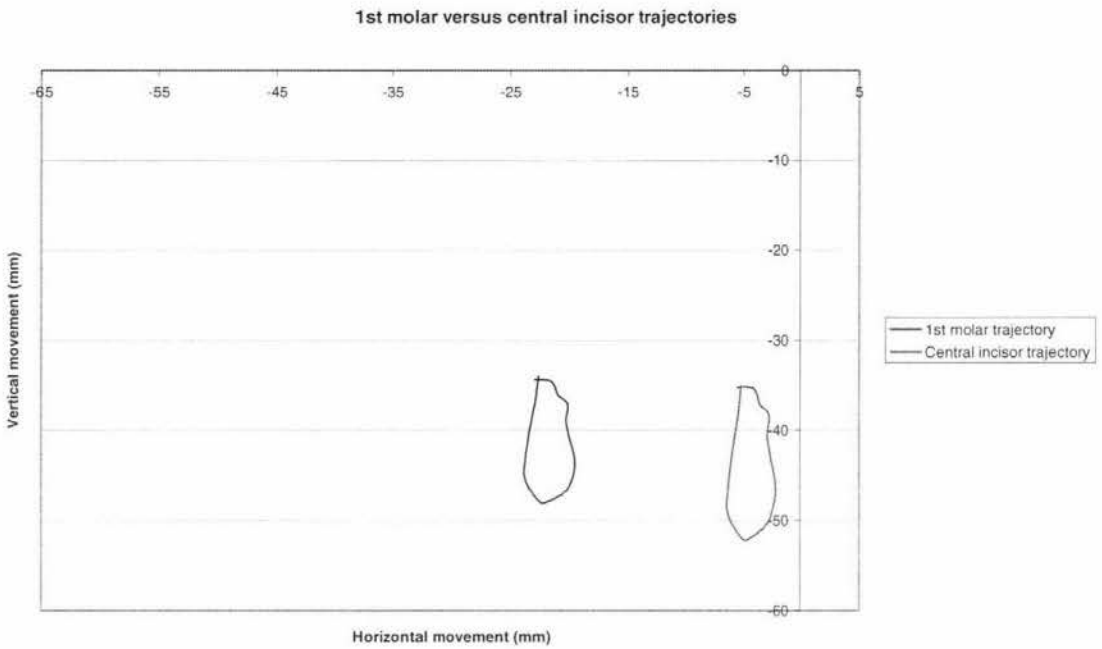

Figure 2-12 Comparison between first molar and incisor chewing trajectories

The angles that the teeth occlude at in the frontal plane can be seen in Table 1 (adapted from Ogawa *et al.* 2001). The data has divided the test subjects into vertical and lateral chewing groups and also includes data on cycle time and velocities.

Table 1 Movement variables for vertical and horizontal chewing motions (adapted from Ogawa *et al.* 2001)

	Lateral chewing	Vertical chewing
Closing angle (degree)	46.6	72.5
Opening angle (degree)	113.1	78
Total angle (degrees)	66.5	5.5
Vertical opening (mm)	14.6	15.1
Lateral displacement in opening (mm)	1.1	0.4
Lateral displacement in closing (mm)	4.0	3.1
Cycle time (s)	0.77	0.7
Occlusal time (s)	0.12	0.16
Opening/closing time (s)	0.65	0.54

Table 1 also shows some times for the opening, closing and occlusal phases of the chewing cycle. The time to complete a chewing cycle remains approximately the same for chewing foods with different properties (Anderson *et al,* 2002). This is due to the fact that the cycle time is controlled by the brain by neural circuitry called "central pattern generators" (Lund 1991). However everything else in the chewing cycle is very variable. Because the trajectory changes for different foods the chewing device being developed in this work must be able to be adjusted to achieve both lateral (grinding) and vertical (crunching) trajectories. The device should allow some flexibility in cycle time, the number of chewing cycles and occlusal time in order to be able to accurately reproduce human chewing

2.3 Conclusion

From the research on the human chewing cycle it has been determined that the human masticatory system is very complex. Therefore the parameters for the chewing device must closely match those of a human in order to reproduce food bolus preparation in the mouth. Therefore the chewing device is required to perform the following:

Trajectories

- The frontal trajectories for chewing different food types are to be approximated by the entry and exit angles at occlusion of lateral and vertical chewing motions describe by Ogawa *et al* (2001) and can be seen in Table 2. The chewing device must also be able to achieve intermediate angles.

Table 2 Frontal trajectory properties (adapted from Ogawa *et al* 2001)

	Lateral chewing	Vertical chewing
Closing angle (degree)	46.6	72.5
Opening angle (degree)	113.1	78
Total angle (degrees)	66.5	5.5
Vertical opening (mm)	14.6	15.1
Lateral displacement in opening (mm)	1.1	0.4
Lateral displacement in closing (mm)	4.0	3.1

- The trajectories in the sagittal plane can be approximated to a straight line. This line needs to be able to have a 30 degree adjustment from vertical to match the common sagittal trajectories found in humans.
- Perform the opening and closing phases of the chewing cycle in 0.65 of a second and perform the occlusal phase in 0.12 of a second.

Teeth

- Only the pre-molars and molars of one side of the jaw need to be included as mastication is only performed by these teeth and chewing only occurs on one side of the jaw at a time.
- Anatomically correct teeth must be used to chew the food. This is due to the fact that the teeth are complex in shape and it is unlikely that there function can be simulated without accurate representations of the occlusal surfaces.
- The location of the teeth in relation to other teeth must also be anatomically correct to ensure that they function correctly and that there is minimal wear on the teeth.

Other

- Be able to apply up to 150N of force during chewing.
- Reposition food between occlusal phases to ensure that the teeth are used in a fashion that is close to what a human does. This will help closely approximate the correct particle size distribution after mastication.

- Use a system to retain the food sample on the teeth and therefore simulate the retention function of the tongue and cheek.
- Use saliva to help break down the food samples and bind the food particles together to better simulate the human mastorcatory system.

3 Possible design approaches

3.1 Introduction

To achieve the specifications outlined in chapter two there are many possible robotic systems that can provide a solution. Some of these systems are as follows:

- Four-bar linkage
- Cam system
- Two-axis system
- Platform robot

3.2 The four-bar linkage

The four-bar linkage is a relatively simple mechanical mechanism and consists of four links or 'bars' as the name suggests. The links are the crank, coupler, follower and ground and they are connected as shown in Figure 3-1.

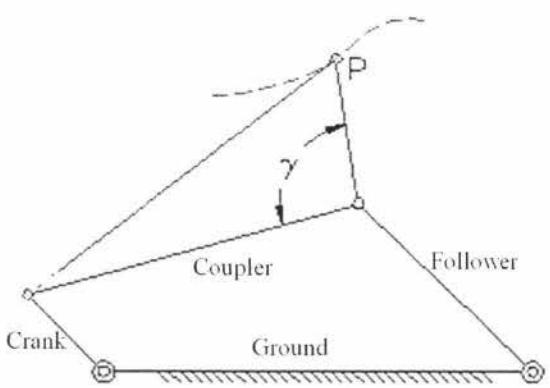

Figure 3-1 The four-bar linkage (adapted from Thompson 1999a)

The crank is the link that is driven and therefore produces the motion of the other links. The crank has the ability to rotate a complete 360 degrees. The ground link is a link that is fixed and does not move and has the task of locating the crank and follower a set distance apart. The follower connects to the ground and coupler. This link has to be large enough to stop itself from being able to make a complete turn when the crank is driven. This is necessary as if the follower was able to turn 360 degrees the trajectories of the coupler would be unpredictable and also could cause the mechanism to jam up

on itself. The coupler is connected to the crank and the follower and therefore has two floating points. This means that the trajectory of the coupler is influenced by the crank and follower. The point 'P' is used to achieve many different trajectories and is fixed in relation to the coupler. The trajectory of this point depends on the lengths of all the links as well as the position of the point 'P' in relation to the coupler. This system can provide can provide consistently repeatable trajectories but can only approximate the trajectories required. However this system is simple to control (Norton 2004).

3.3 Cam trajectory system

Cams can be used to achieve different trajectories very easily. A cam system involves a cam that is rotated on a shaft, and a cam follower that moves on the profile of the cam. This can be seen in Figure 3-2.

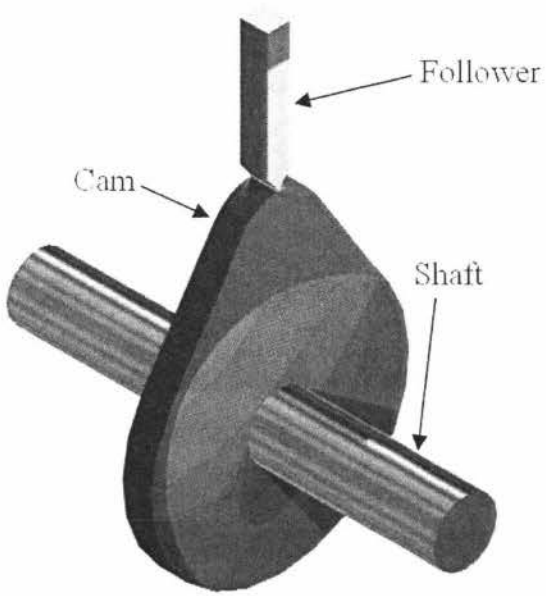

Figure 3-2 The cam follower system (adapted from University of Limerick)

Systems like this are commonly found in combustion engines like your everyday car. In this system the cam is used to open a valve to let a fuel/air mixture into the combustion chamber or let exhaust gasses out. The valves move in a linear one-dimensional motion where the motion is specified by the cam profile. However to achieve an approximate chewing motion a trajectory is required in at least two-dimensions. This then means that two cams would be required to actuate a follower making the system more complex. Also if more than one trajectory is required for more than one chewing

motion different cams would be required. This then means that the machine would either have to be disassembled to insert new cams or the cam system would have to dynamically change cams. A system that dynamically changes cams can be found in Honda VTEC combustion engines in many Honda cars. This system has two different cam profiles for each valve, one for low revs and one for high revs. The cam profile that is used by the follower changes on command. This system has two cam followers that follow the two different cams. One of these followers moves freely and does not effect the movement of the valves. This can be seen in Figure 3-3.

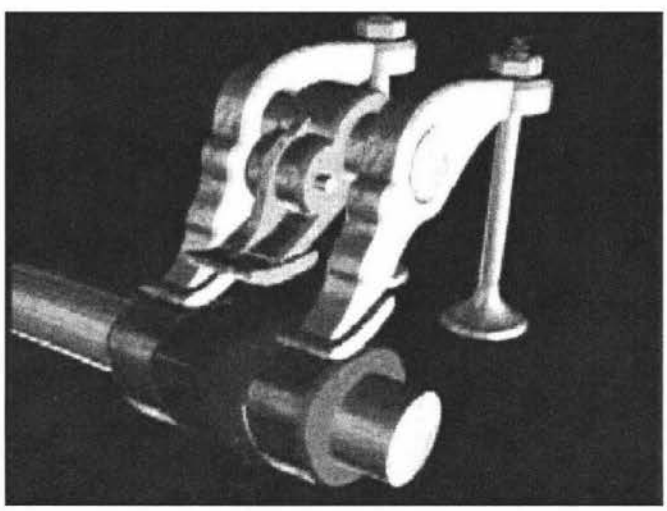

Figure 3-3 VTEC system at low revs (taken from Honda marine)

To activate the other cam profile the cam followers are locked together by a pin and then the valves are actuated by the larger cam. This can be seen in Figure 3-4.

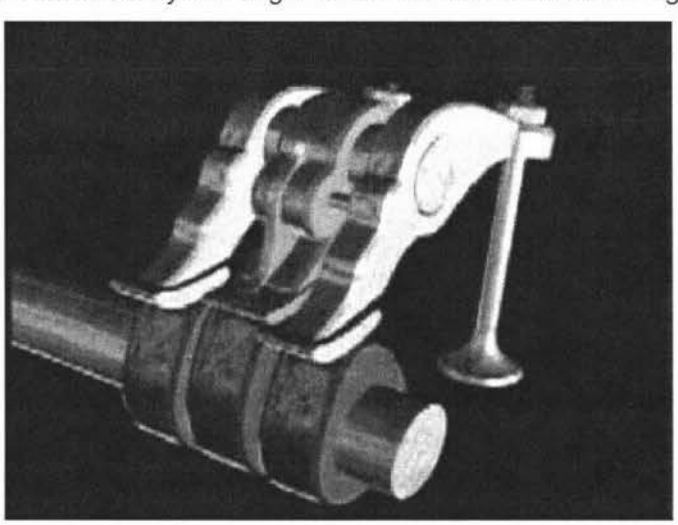

Figure 3-4 VTEC system at high revs (taken from Honda marine)

However a system such as this gets complicated very quickly if adapted for a two-dimensional trajectory system. It also only allows a few set trajectories and can not produce intermediate trajectories.

3.4 Two-axis trajectory system

Two-axis trajectory systems are widely used in systems such as scanners, printers and microscope tables. This system involves using two actuators positioned perpendicular to each other to move an actuating point. A system like this is mechanically simple and is also simple from a manufacturing point of view. This is due to the fact that the actuators can be purchased leaving only the mounting systems that need to be constructed. However the two actuators need to move at the same time. This then means that the control system to control the actuators is relatively complex. But due to the fact that this system uses a controller to make the actuators perform the desired trajectory means that the chewing trajectory can be changed by reprogramming the controller rather than making a new mechanism. It also means that the chewing trajectory can be dynamically changed from chewing cycle to chewing cycle. This however would require complex trajectory planning.

3.5 Platform robot

Platform robotic systems are usually found in complex systems such as flight simulators. They offer up to six degrees of freedom which means that they can move along and rotate around all of three dimensions. This allows them to move to any desired point in the defined workspace. The design of a platform robot centres around two parallel plates. One of theses plates is fixed while the other one is actuated and is shown in Figure 3-5. The two plates are connected by six actuators and by driving the actuators in different combinations, different motions are achieved.

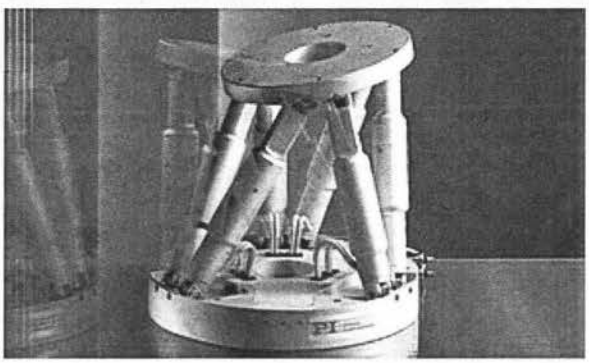

Figure 3-5 A hexapod platform robot (taken from Physic Instrumente 1996-2005)

This system would ideally suit a robot that simulates the human chewing behaviour. This is due to the fact that the human jaw can be thought of a two parallel plates where the mandible corresponds to the actuated plate and the skull corresponds to the fixed plate. A hexapod system such as this is also simple from a manufacturing stand point as only the two plates need to be constructed if the actuators are purchased. Although this would be an ideal solution the control of the system is very complex. This is due to the fact that there are six actuators that are required to move at the same time. Therefore trajectory planning becomes very difficult.

3.6 Robotic system evaluation

The robotic systems mentioned all have the ability to produce trajectories for chewing. Each of the systems has advantages and disadvantages and can be seen in
Table 3.

Table 3 Evaluation of the different possible robotic systems

System	Advantages	Disadvantages
Four-bar linkage	• Mechanically simple principle • Simple to control	• Can only approximate desired trajectories
Cam system	• Can accurately produce desired trajectories • Simple to control	• Can not perform a large range of trajectories • Mechanically complex when multiple cams are used
Two-axis system	• Simple to manufacture • Can accurately produce desired trajectories • Can dynamically change trajectories	• Relatively difficult to control
Platform robot	• Simple to manufacture • Can accurately produce any desired three-dimensional trajectory • Can dynamically change trajectories	• Difficult to control

As a prototype device is required in a relatively short time frame, a simple robotic system must be used. Therefore the four-bar linkage system was chosen. This will closely approximate the chewing trajectories and can be made robust due to its simple mechanical design without the need for complex control systems.

4 Four-bar linkage mechanism design

4.1 Introduction

The design of the four-bar linkage must facilitate the chewing of a variety of different foods. Due to the fact that humans chew foods with different properties differently, the four-bar linkage must be able to be adjusted to achieve the required motions for these food types.

4.2 Specifications

For the device to achieve an appropriate chewing motion of the human masticatory cycle, it must achieve the following parameters:

- It must apply up to a maximum force of 150 Newtons to the food sample.
- It must achieve a range of set trajectories in the frontal plane with the occlusion entry and exit angles being very close to the desired angles. These angles can be seen in section 2.3.
- The time taken for the opening, closing and occlusion phases must be very close to that of the human chewing cycle. These times can be seen in Table 2.

4.3 Linkage design

4.3.1 Constraints

The four-bar linkage is limited by the fact that it is difficult to design it to perform a desired trajectory. It will however constantly perform a set trajectory making it highly repeatable. As the four-bar linkage can only perform one set trajectory in its standard form means that it is limited in its adaptability. Some adaptability can be added by designing links that adjustable length. This is difficult to implement on all links except the ground link. The reason for this is that all the links move apart from the ground link. Therefore in this case where some adaptability is required to reproduce a range of trajectories, the ground link must incorporate some adjustability to approximate different chewing trajectories for different food types.

4.3.2 Design approaches

There are two common design approaches to ensure that the trajectory that the mechanism achieves is close to that desired. They are:

- The four-bar atlas approach, and
- The genetic algorithm approach

The four-bar atlas approach involves selecting a trajectory that is close to the desired trajectory from an atlas that has many different trajectories plotted in it. The link lengths and the position of the trajectory generating point in relation to the coupler are the determined by the use of a look-up table that specifies the parameters to the desired trajectory.

The genetic algorithm approach involves writing a genetic algorithm that takes the desired trajectory and makes a trajectory that closely matches it by changing the parameters of the linkage. This is a numeric solution that evaluates the trajectory produced by a set of linkage parameters. It then changes the linkage parameters and evaluates the new trajectory. This is done for many iterations and returns the parameters of the linkage that produces the trajectory with the least amount of error (Charbonneau *et al*, 2004).

Due to the fact that the genetic algorithm method requires a genetic algorithm program to be developed, it is rather time consuming and is not ideally suited for this application where only one set of link parameters is required to be found. It would however be very useful if different four-bar linkage parameters needed to be found on a number of different occasions. Therefore the four-bar atlas was chosen to be used, as it can provide the specifications for the four-bar linkage from a look-up table where the trajectories can be firstly visually evaluated to get a set of preliminary link specifications. From here further trajectory analysis can be used to determine the most suitable trajectory and therefore the most suitable link specifications.

Once the link lengths have been determined for the four-bar linkage, additional analysis needs to be done to ensure that it will function correctly. This analysis includes ensuring that the linkage stays well away from dead positions by ensuring suitable maximum and minimum transmission angles.

Limit and dead positions of a four-bar linkage occur when the crank and coupler form a straight line. This is due to the fact that the coupler transfers the force applied from either the crank or the follower in the direction of the coupler. As the crank and coupler form a straight line twice per cycle there are either two limit or two dead positions per cycle. These can be seen in Figure 4-1. A dead position is when the follower can not make the crank rotate when a torque is applied to it; therefore it has no mechanical advantage. A limit position on the other hand is where the crank can be used to apply an infinite mechanical advantage to the follower. Dead positions also occur if the follower and coupler form a straight line when driven by the crank. This means that the sum of the lengths of the coupler and the follower must be larger than the sum of the ground and crank lengths.

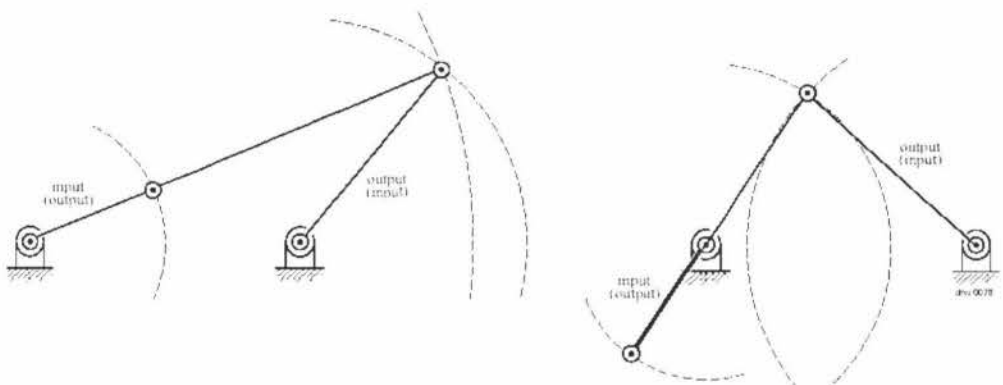

Figure 4-1 Limit and dead configurations of a four-bar linkage (taken from Stanisic)

The transmission angle is the angle between the follower and coupler. This angle varies as the mechanism is driven and serves as an indicator of how well the linkage can transmit torque from the crank to the follower. The maximum transmission angle μ_{max} and the minimum transmission angle μ_{min} can be seen in Figure 4-2. The general rule for the transmission angle is to never allow it to be less than 30 degrees or greater than 150 degrees (Erdman *et al*, 2001). If the minimum transmission angle was zero degrees or the maximum transmission angle was 180 degrees the mechanism would then have the coupler and the crank forming a straight line and would therefore be in a dead position. In practice this could cause the mechanism to fold over on itself as the coupler has two possible directions in which to travel. This means that the coupler could change its operating side resulting in irregular operation.

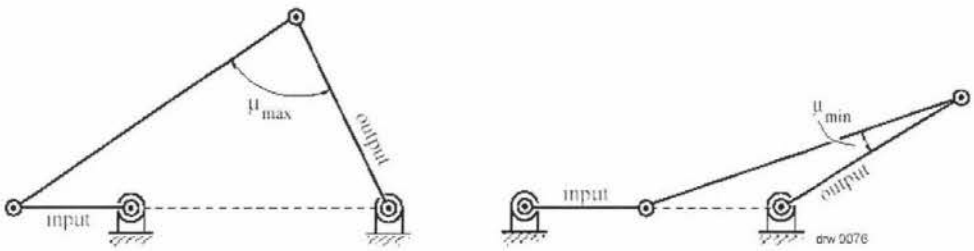

Figure 4-2 The maximum and minimum transmission angles (taken from Stanisic)

4.3.3 The four-bar design

The four-bar linkage was designed using the traditional four-bar atlas approach rather than genetic algorithms which had been used during a preliminary stage of this research [Charbonneau *et al*, 2004]. This was due to the fact that the results from this genetic algorithm were not as good as expected and it was more time efficient to use a four-bar atlas to look up a desired trajectory and link specifications rather than redesigning the genetic algorithm program.

The Cedarville engineering four-bar web atlas (Thompson 1999b) was used to find a number of suitable trajectories that had entry and exit angles that closely matched a lateral chewing cycle described in section 2.3. Trajectories where searched for by adjusting the parameters of a four-bar linkage shown in Figure 4-3 where link 'a' is the crank, link 'b' is the coupler, link 'c' is the follower and link 'd' is the ground. The point 'P' is the trajectory generating point that is located at and angle of 'γ' from the coupler length 'b' and a distance 'BP' from point 'B'.

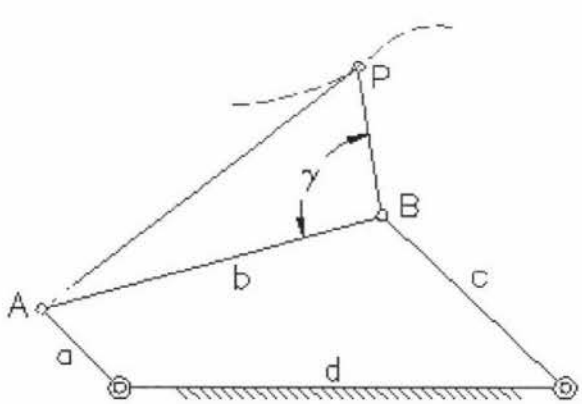

Figure 4-3 The four-bar linkage parameters (taken from Thompson 1999a)

When a trajectory was found that looked close to matching the desired occlusal angles of a lateral chewing motion it was marked down as a possible solution. However vertical chewing motions are also required when the ground link length is changed. Therefore the derivatives of these possible solutions where examined by changing the ground link length and observing how the trajectory responded. The link parameters that made trajectories that seemed close to both vertical and lateral chewing trajectories were noted. Some sample trajectories can be seen in Figure 4-4 and Figure 4-5. Figure 4-4 shows the final choice of the lateral chewing trajectory. The link parameters are shown at the top and the figure while the 'BP' length is read off the graph from the zero point to the point that falls on the desired trajectory (3 in this case). Figure 4-5 shows a derivative of the chosen lateral trajectory. It can be seen that the ground link length 'd' has been reduced from 5 to 4 to achieve a vertical chewing trajectory.

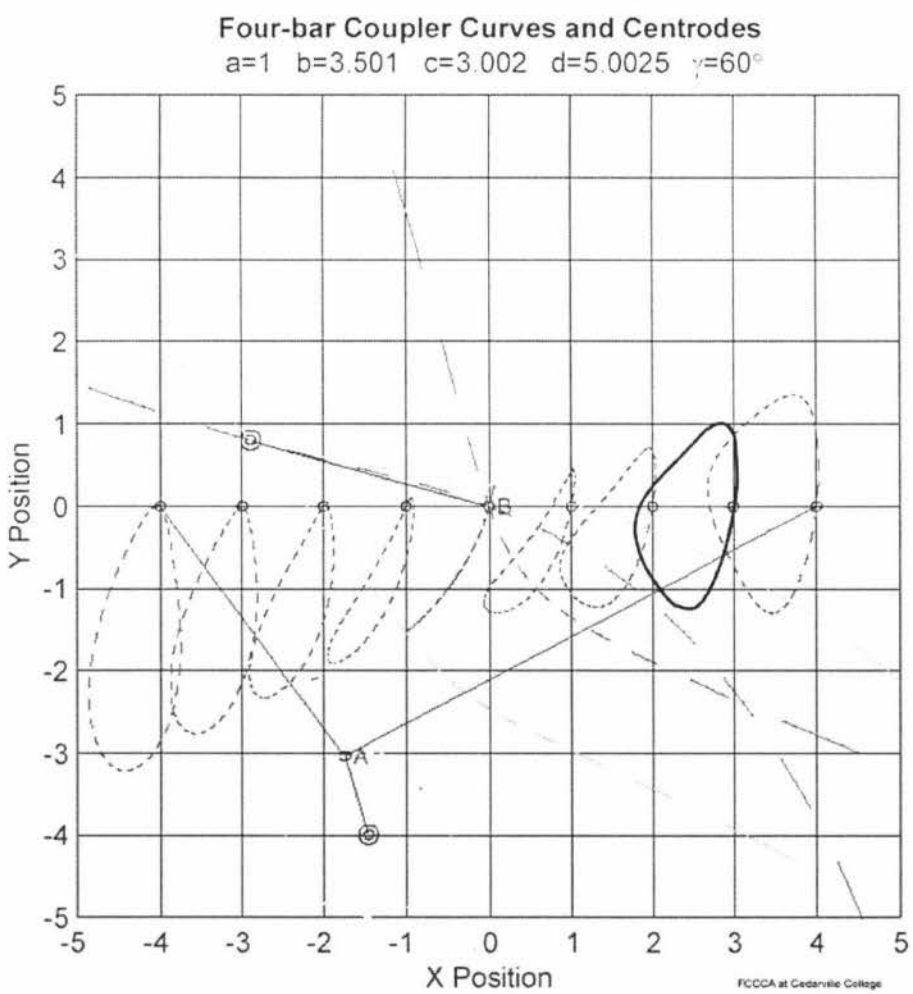

Figure 4-4 Candidate trajectories of the four-bar linkage (adapted from Thompson 1999b)

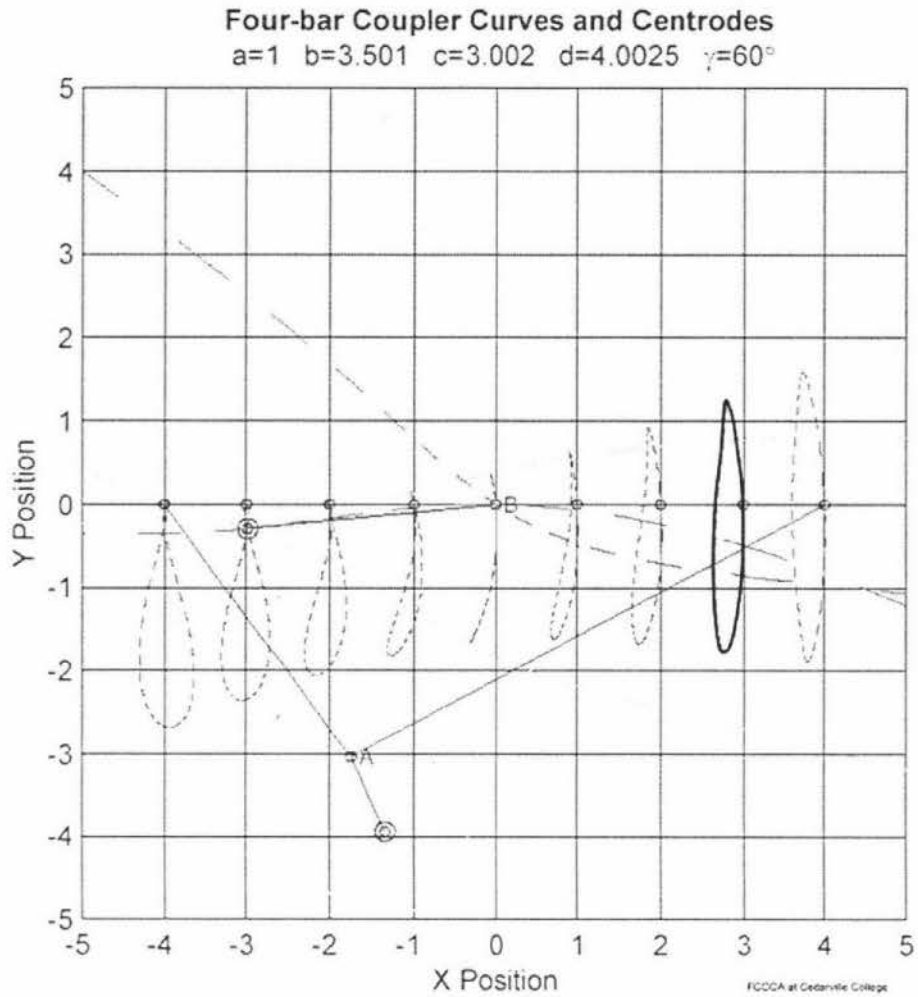

Figure 4-5 Candidate trajectories when the ground length is reduced (adapted from Thompson 1999b)

These trajectories were then examined further to determine the exact occlusal angle. It was determined that the trajectories shown in Figure 4-4 and Figure 4-5 were in fact the best solution that were found. The final values can be seen below. However these values are only ratios and the links can be any length as long as the ratios are obeyed.

The final ratios of the four-bar linkage are:

Crank (link 'a') = 1

Follower (link 'c') = 3

Ground (link 'd') = 3.8 – 5 to achieve horizontal and vertical chewing motions

Coupler (link 'b') = 3.5

Coupler (distance 'BP') = 3

Coupler (angle 'γ') =60 degrees

A simple model was constructed in SolidWorks to evaluate different link lengths as seen in Figure 4-6. The factor that limits how small the linkage can be made is the crank as it has the smallest dimensions and has to be able to incorporate shafts strong enough to securely connect the individual links of the linkage. For this reason it was decided to make the crank length 10mm. This also allows the linkage to be as compact as possible. The entire mechanism also had to be rotated 65 degrees to orientate the trajectory produced by the four bar linkage. This was required so that the teeth could be mounted vertically.

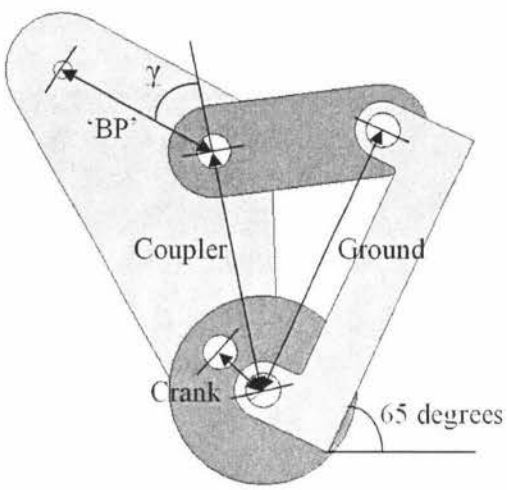

Figure 4-6 Simple model to evaluate different link lengths

The final four-bar linkage parameters were:
Crank (link 'a') = 10mm
Follower (link 'c') = 30mm
Ground (link 'd') = 38mm – 50mm
Coupler (link 'b') = 35mm
Coupler (distance 'BP') = 30mm
Coupler (angle 'γ') =60 degrees

These sets of results were then evaluated by comparing the entry and exit angles at occlusion with the data obtained in chapter two that shows lateral and vertical chewing motion. It can be seen from the data in Table 4 that using the four-bar linkage mechanism proposed, the vertical opening distances as well as the lateral

displacements are larger than those observed in the experimental data reported by Ogawa *et al* (2004). This is acceptable as these aspects of the chewing trajectory do not impact on the food breakdown process as long as they are sufficient to clear the food between chewing cycles. The motor can be speed up during this part of the cycle to ensure representative masticatory behaviour can be simulated. The chosen design is optimised to achieve a close match with the lateral chewing trajectory while still achieving reasonable trajectories for the vertical chewing process.

Table 4 Comparison between the designed four-bar linkage and the experimental data (adapted from Ogawa *et al*, 2004)

	Lateral chewing		**Vertical chewing**	
	From data	*Four-bar*	*From data*	*Four-bar*
Closing angle (degree)	46.6	45	72.5	99
Opening angle (degree)	113.1	112	78	105
Total angle (degrees)	66.5	67	5.5	6
Vertical opening (mm)	14.6	23	15.1	34
Lateral displacement in opening (mm)	1.1	3	0.4	3
Lateral displacement in closing (mm)	4.0	9	3.1	0

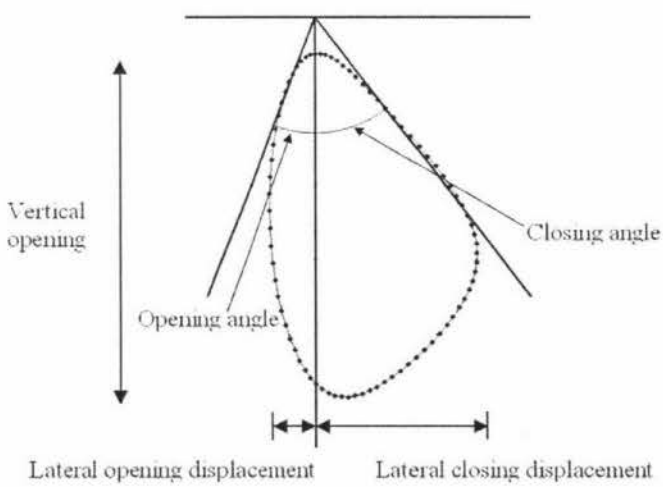

Figure 4-7 Definition of parameters in Table 4

Some sample trajectories that the four-bar linkage can perform can be seen in Figure 4-8. It shows different trajectories when adjusting the ground-link. It also shows that other parameters change when the ground link dimension is adjusted. It can be seen that the occlusal position moves as well as the vertical opening distance increasing as the ground link dimension decreases. This is due to the nature of the four-bar linkage and can not be helped. This however means that the chewing device needs some way of adjusting the occlusal position of the teeth.

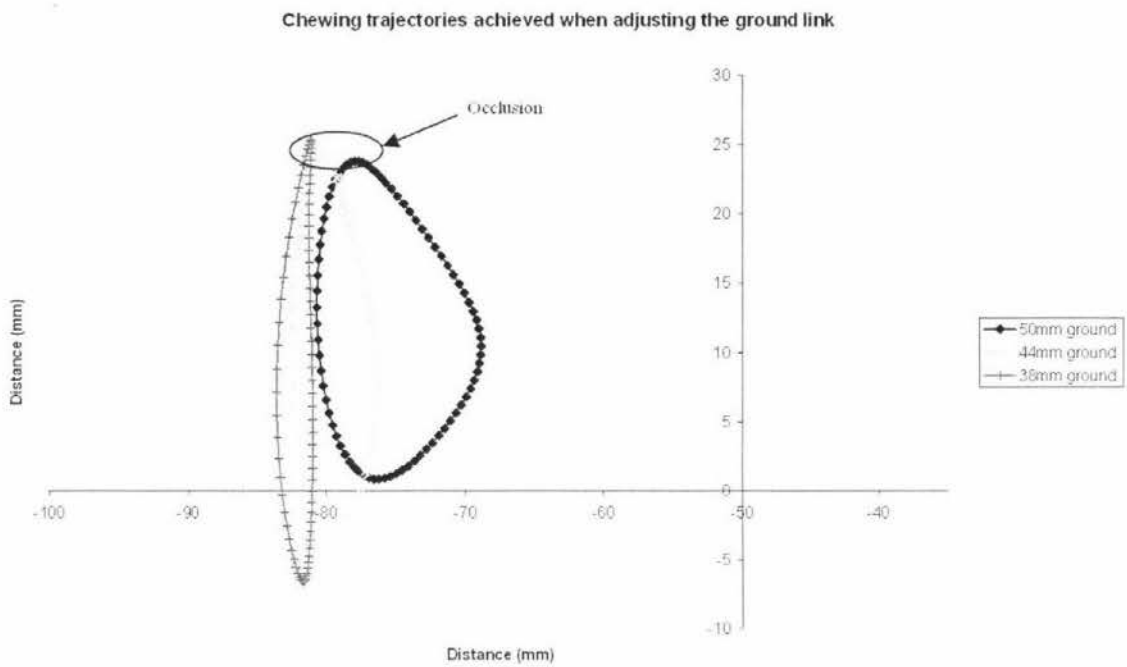

Figure 4-8 Sample trajectories that the four-bar linkage can achieve

The vertical and horizontal trajectories can be viewed as a function of the crank angle as shown in Figure 4-9 and Figure 4-10. Figure 4-9 shows that the actuating point on the coupler reaches maximum displacement at approximately 150 degrees when the ground link is 50mm. While Figure 4-10 shows that there is a maximum horizontal movement of approximately 11mm when the ground link is 50mm. This gives a good indication of how the mechanism responds in both the vertical and horizontal directions when the crank is driven.

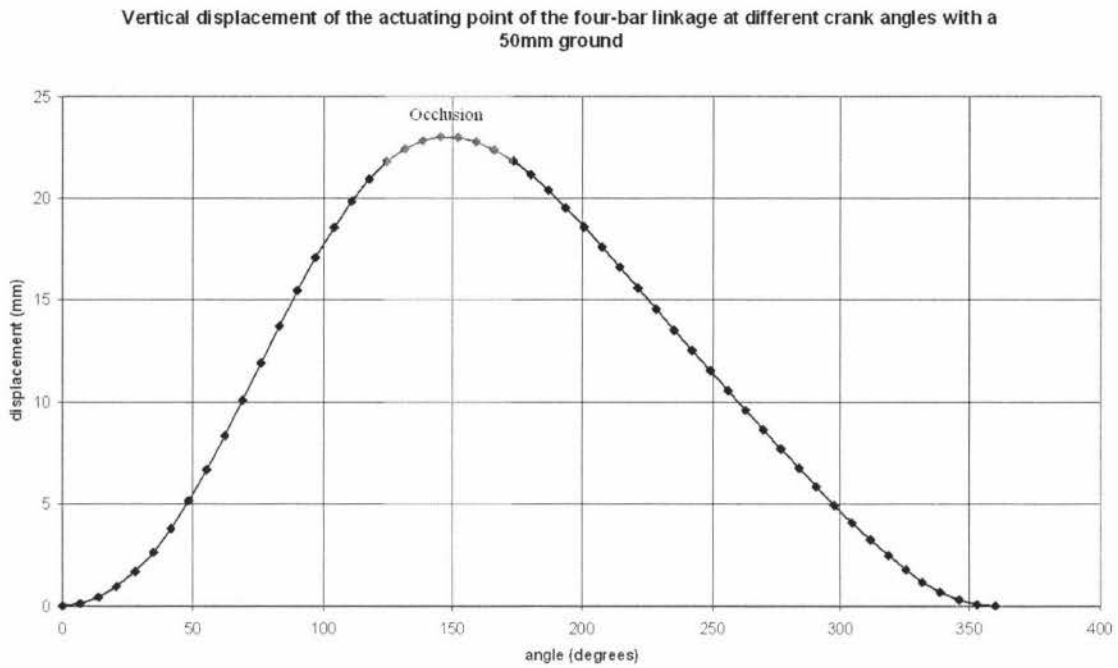

Figure 4-9 Vertical trajectory as a function of crank angle with a 50mm ground

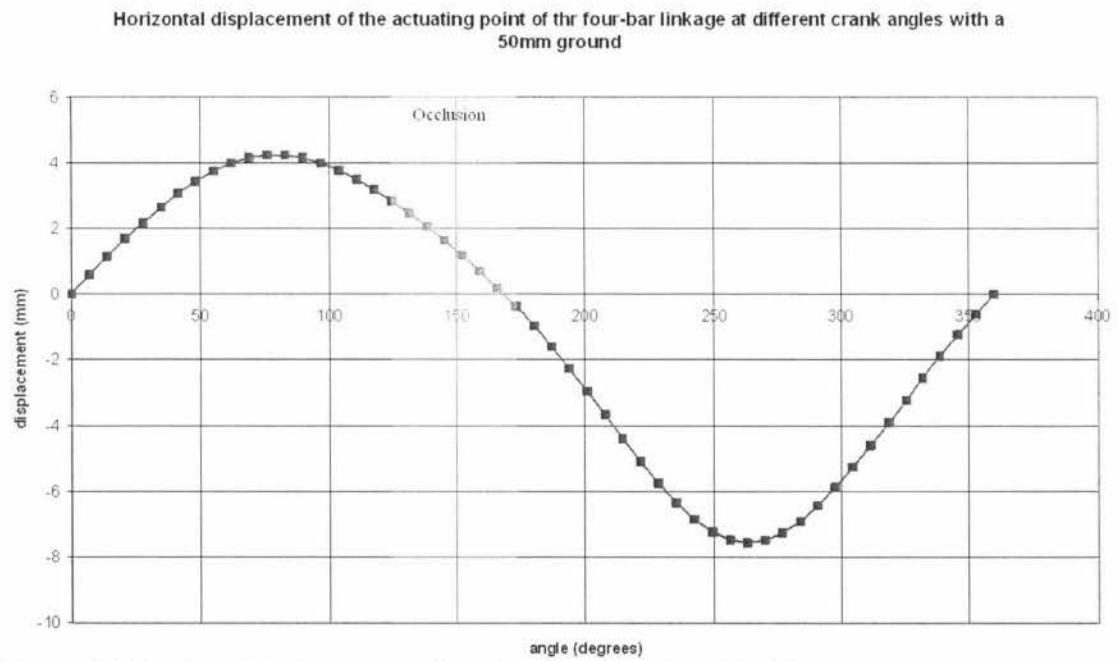

Figure 4-10 Horizontal trajectory as a function of crank angle with a 50mm ground

The transmission angles of the mechanism where then checked to ensure that they where not less than 30 degrees or greater than 150 degrees. This is due to the fact that the linkage will not be efficient if the transmission angles are outside of this range. Some example transmission angles for the maximum and minimum ground lengths can be seen in Figure 4-11and Figure 4-12.

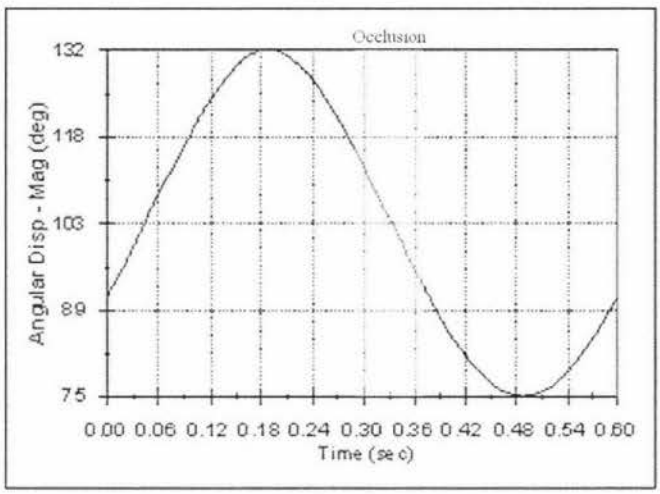

Figure 4-11 Transmission angle when ground length is 50mm

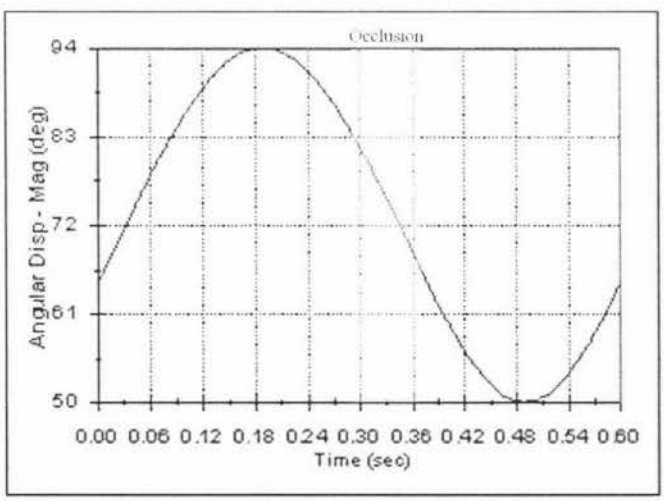

Figure 4-12 Transmission angle when ground length is 38mm

These figures show that the transmission angle stays well within the 30 and 150 degree range. The occlusal position of the teeth on these plots occurs at time 0.34s. At this time the transmission angles can be seen to be between approximately 72 and 95 degrees. Therefore the linkage is very close to 90 degrees where the linkage is most efficient. It also stays well away from dead positions (0° and 180°).

4.4 Mechanical design

4.4.1 The basic mechanical design

Once the link lengths of the four-bar linkage had been determined, the design of the mechanical device could commence. The basic designs of the crank, coupler and follower were relatively straight forward with only the pivot points of the links needing to match the lengths determined. The design of the ground link was more complicated however. This is due to the fact that the ground link had to be designed to have a 12mm adjustment that effectively changed the link length from 38mm to 50mm and any value in-between. The simplest way to do this proved to be by using a design that involved using a threaded rod to move a block when the rod is turned. This mechanism was selected and constructed because a similar system to do this could not be easily purchased. The design of the ground link can be seen in Figure 4-13.

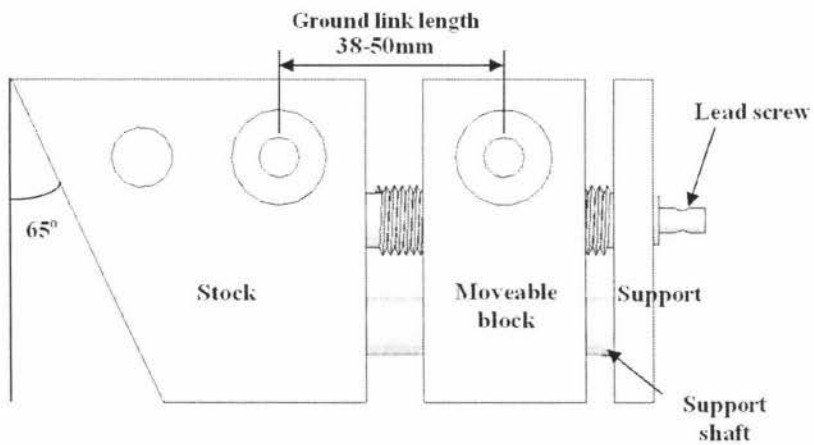

Figure 4-13 The ground link

This shows the design of the ground link that allows the moveable block to move back and forth when the threaded shaft is turned. It also shows that there is another rod that the movable block slides on. This was to remove the rotation that the moveable block has applied to it when the threaded shaft is turned.

The crank, coupler and follower could now be added to this ground link. The basic mechanical design can be seen in Figure 4-14. This shows how the links are positioned relative to each other.

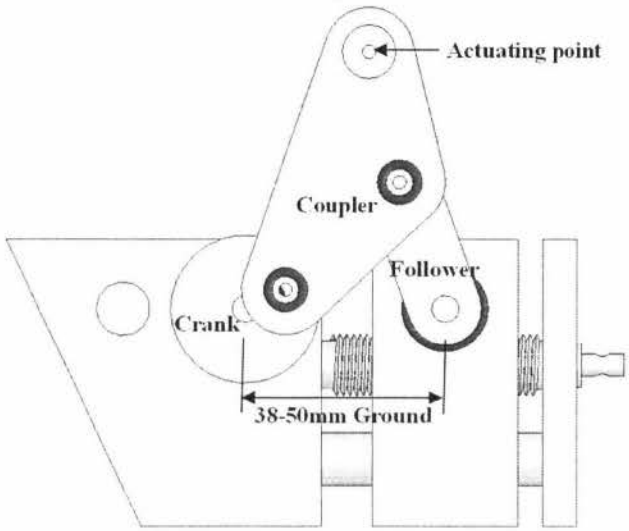

Figure 4-14 The basic design of the four-bar linkage

It can be seen that the links will slide over each other when the crank is rotated. This means that materials for each link needed to provided a bushing effect. This is due to the fact that if the links were made all out of the same material the links would wear in a way that would cause the mechanism to jam up. Therefore the materials chosen were aluminium and stainless steel. The ground link blocks and the coupler were chosen to be made out of aluminium while the crank and follower were made out of stainless steel. This means that each link is bushed by sliding on a different material. This bushing system was chosen over a thrust bearing system due to its simplicity. However all the rotating components in this design are supported by radial bearings and the movable block is supported by linear bushes. These bearings were chosen based on the calculated force applied at each joint as well as the space available in each component. The joint forces used to size the bearings can be seen in section 4.4.5.The locations of these bearings can be seen in the assembly drawing shown in Figure 4-15.

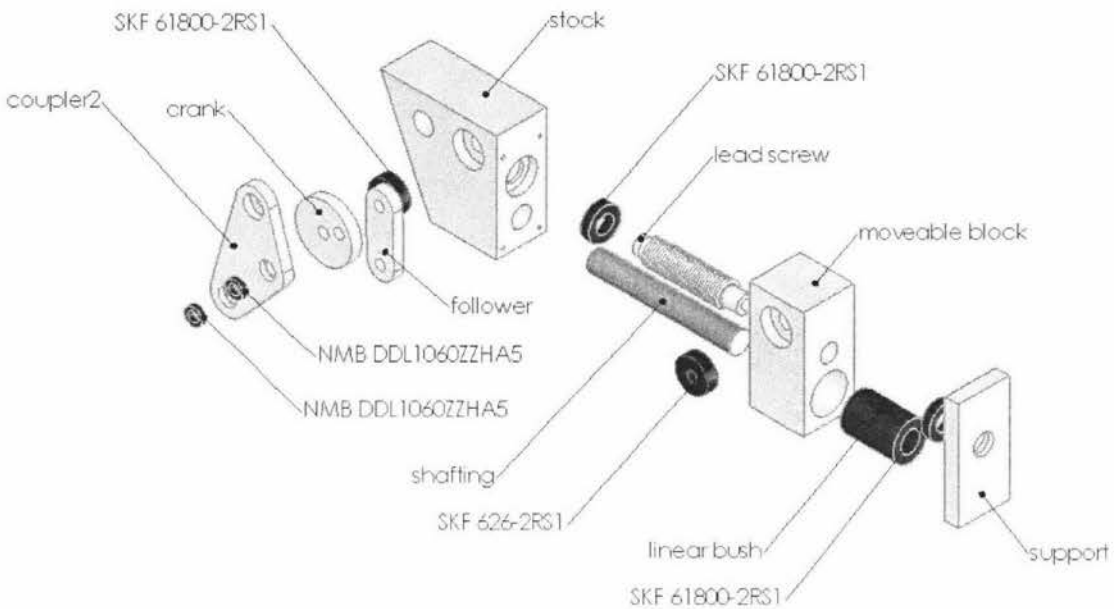

Figure 4-15 The assembly of the four-bar linkage

4.4.2 The six-bar linkage design

The four-bar linkage was designed to produce similar trajectories in the frontal plane to that of a human. A system is also needed to produce the correct trajectories in the sagittal plane. This system needed to not affect the trajectories that the four-bar linkage produced and create a linear approximation to human chewing trajectories in the sagittal plane. Therefore the simplest way of doing this was to add another two links to the four-bar linkage, thus making it a six-bar linkage. This can be seen in Figure 4-16.

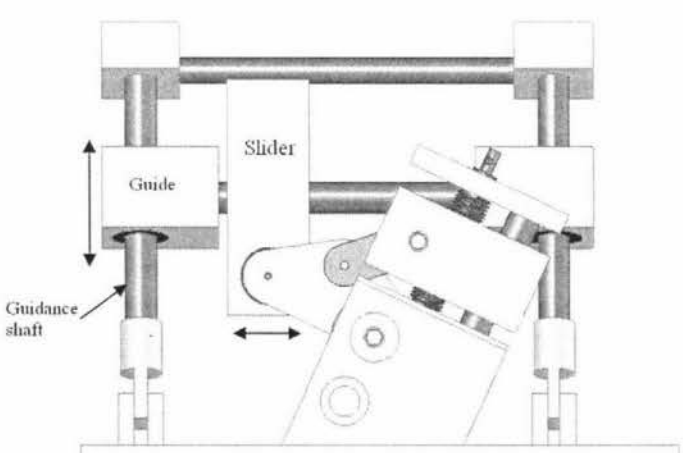

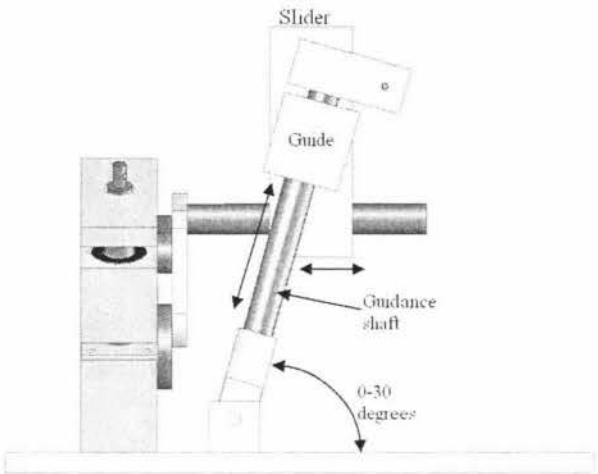

Figure 4-16 The six-bar linkage

It can be seen that the additional two links are only able to move in a linear motion in the directions shown. This then enables a linear approximation to human chewing trajectories in the sagittal plane to be achieved. The link that sets the trajectory in the saggatial plane was made to be adjustable between 0 and 30 degrees so that the chewing device could better match a greater variety of different chewing trajectories. However a cantilever design like this is not very balanced and would lead to very large forces being applied to all the joints and links. To reduce the forces that are applied to all the joints and links a second four-bar linkage was placed on the other side as seen in Figure 4-16. As both four-bar linkages are to produce the exact same trajectories at the same time, they have to be coupled together. Therefore the pivot points on the links were coupled together by steel shafts. This allows the links to rotate in synchronisation and also strengthens the design by not allowing the links to buckle inwards. However both four-bar linkages have to still be driven from their cranks. Due to the motion of the four-bar linkage, a shaft can not directly link both of the cranks without interfering with the four-bar linkages. This problem was overcome by driving both the cranks from spur gears that are driven from a driveshaft that runs below the cranks that allows the four-bar linkages to function without interference. This can be seen in Figure 4-17.

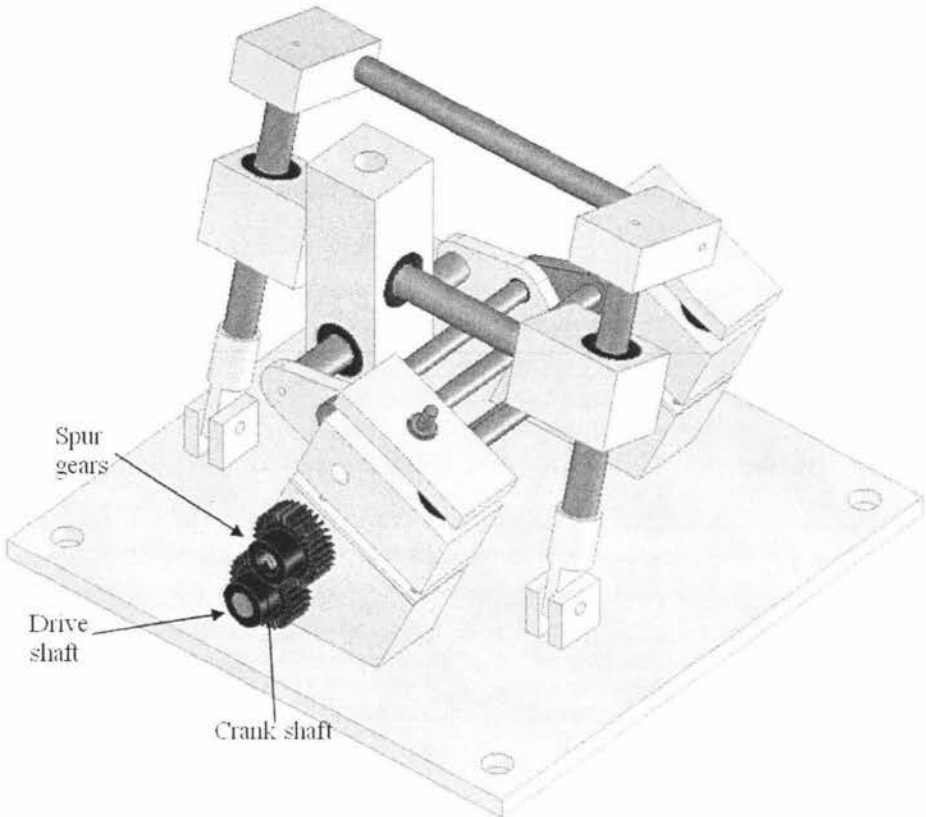

Figure 4-17 The final six bar linkage design

4.4.3 Stress analysis

The six bar linkage system was then simulated in the COSMOS Works software package to test if the mechanism can withstand the forces that are going to be applied. The device is required to applied 150N at the actuator, therefore a 150N static force was applied to the slider in the occlusal position and the stress was analysed over the mechanism. However this is not exactly how the force is applied in the real system. This is due to the fact that the real system is a dynamic system because the linkage is moving. Therefore the stress analysis should be done dynamically rather than statically. However COSMOS Works does not allow for dynamic stress analysis so the stress was approximated by applying the 150N chewing force at the maximum occlusal position. This is the position where the teeth are the closest to each other and therefore the position where the maximum force is applied to a food sample assuming that the food sample behaves like a spring. The assembly without the floating components of the mechanism was used for the stress analysis and was comprised of only the to four-bar

linkages, the rods that connect the two linkages and the slider. This was due to the fact that COSMOS Works recognises the sliding joints as fixed joints. The stress analysis showed that there is no excessively large stress on the mechanism, with the largest amount of stress being concentrated where the linear bush of the actuating block slides on the actuating shaft of the four-bar linkage. This can be seen in Figure 4-18. This is due to the fact that the linear bush makes a relatively sharp edge with the actuating shaft of the four-bar linkage. This can not easily be avoided as the linear bushes that were purchased products.

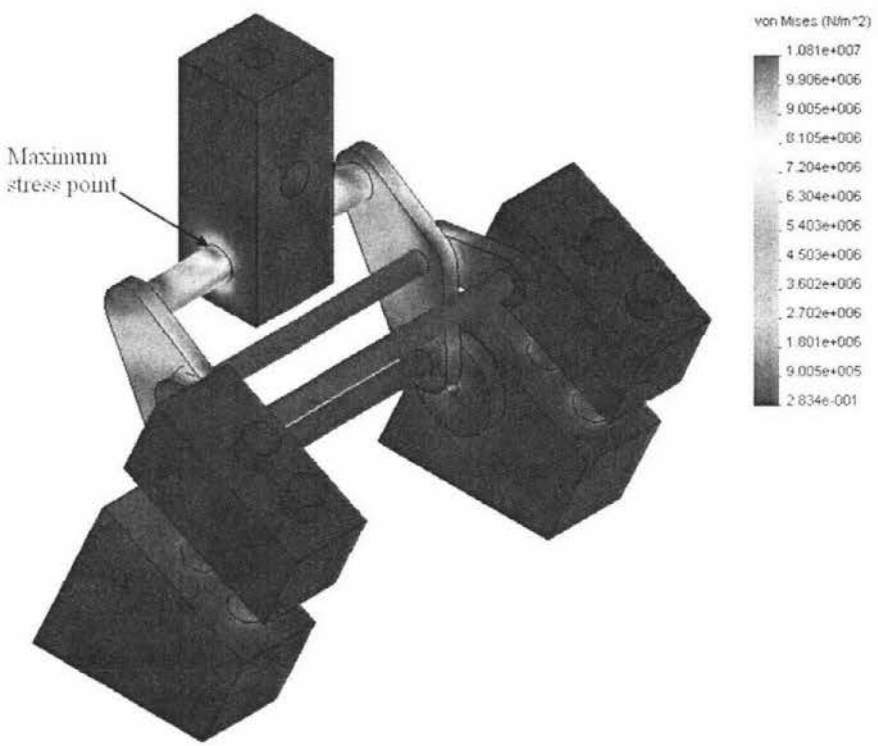

Figure 4-18 The stress analysis of the four-bar linkage

The deformation of the different components was then analysed to examine the buckling that occurs when the 150N load is applied. The simulation shows that the maximum deformation of the actuating shaft is 0.004mm where the linear bush meets the shaft that it slides on under maximum load. This can be considered negligible as this amount of buckling in the shaft will not cause the linear bush to jam. The simulation also shows that the maximum deflection of any component is 0.005mm which is in the actuating block. These results can be seen in Figure 4-19.

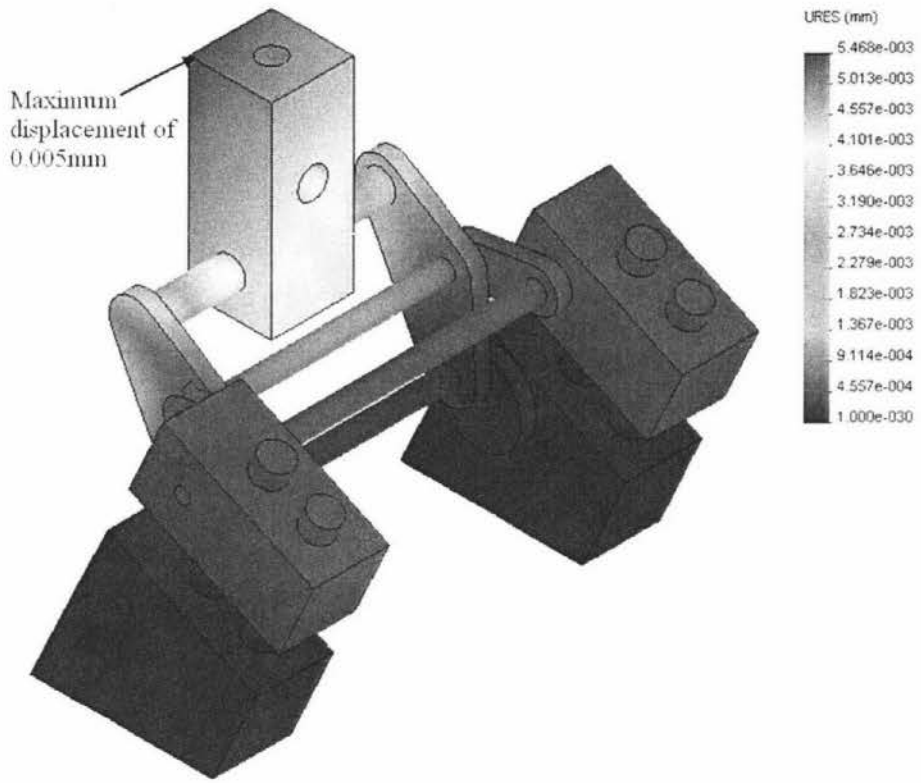

Figure 4-19 The deflection analysis of the four-bar linkage

4.4.4 Six-bar linkage kinematics

The kinematics of the linkage was evaluated by looking at the angles, displacements, velocities and accelerations of each link in the linkage. These parameters were examined to get a general idea of how each component was moving. More importantly it was done to ensure that each component moved in a smooth fashion so that no high forces are applied to the components and also that the values are realistic. The points in which these measurements were taken from can be seen in Figure 4-20.

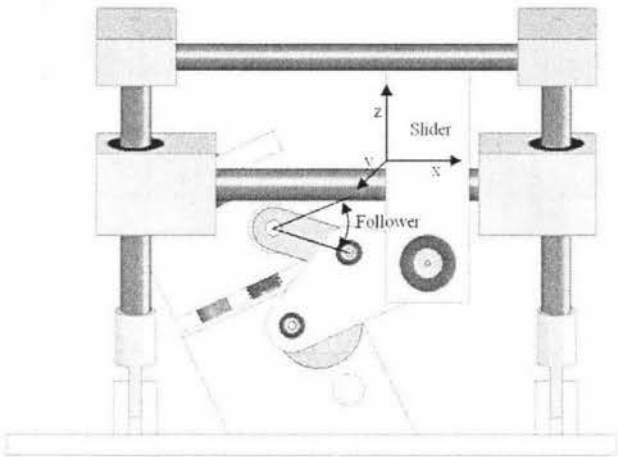

Figure 4-20 The co-ordinate system for the kinematics

Due to the nature of the four-bar linkage, the linkage can not be driven in reverse. This means that the crank will not rotate a complete 360 degrees when the coupler is actuated. Therefore the kinematic evaluation was done by setting the crank to rotate at a constant velocity so that the kinematics of the other links could be determined.

The crank was rotated at a constant angular velocity of 600 degrees per second with the ground link length set at 45mm and the sagittal trajectory set at 25 degrees for the following analysis.

Follower

The angular kinematics of the follower can be seen below. Figure 4-21 shows that the follower moves a total of 33 degrees with the 45mm ground length. Figure 4-22 shows that the maximum angular velocity is 215 degrees per second which can be thought of as 36rpm. Figure 4-23 shows that the maximum angular acceleration is 2920 degrees per second squared. Both of the peaks on this plot occur when the follower changes direction. This acceleration plot also shows that the acceleration profile of the follower is fairly smooth. This means that no large forces are instantly applied to the follower which would limit its life.

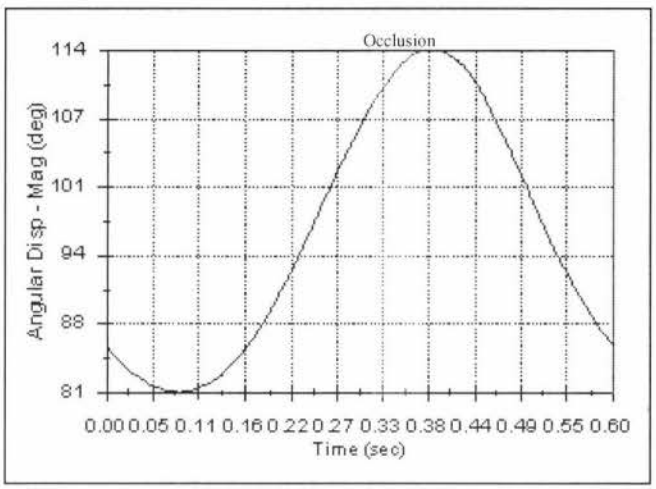

Figure 4-21 The angular displacement of the follower

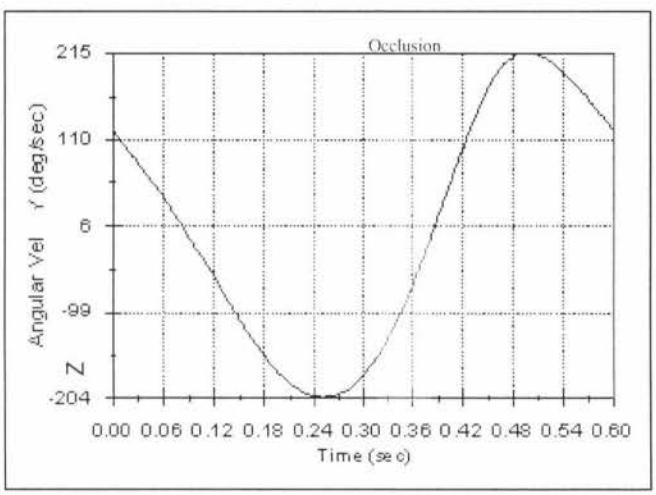

Figure 4-22 The angular velocity of the follower

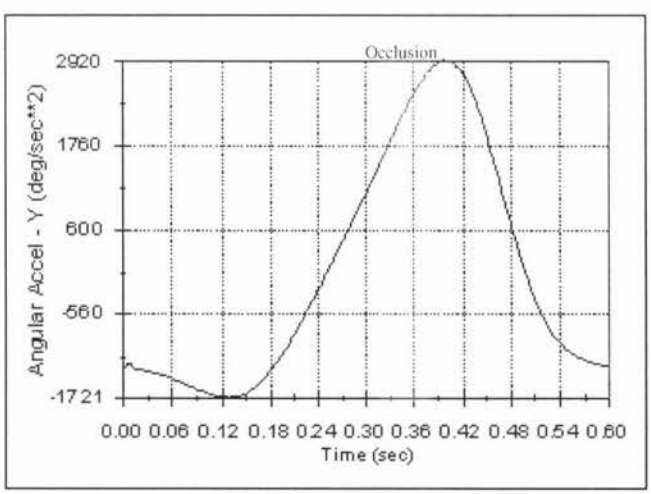

Figure 4-23 The angular acceleration of the follower

Slider

The linear kinematics for the slider in the 'X, Y and Z' directions can be seen below. The linear displacements of the slider are shown in Figure 4-24, Figure 4-25 and Figure 4-26. Figure 4-24 shows that the maximum travel in the 'X' direction is 7mm this corresponds to the horizontal opening of the mouth. Figure 4-26 shows that the maximum vertical opening of the mouth is 26mm. While Figure 4-25 shows that the maximum travel of the slider in the 'Y' direction is also 7mm for the setup used.

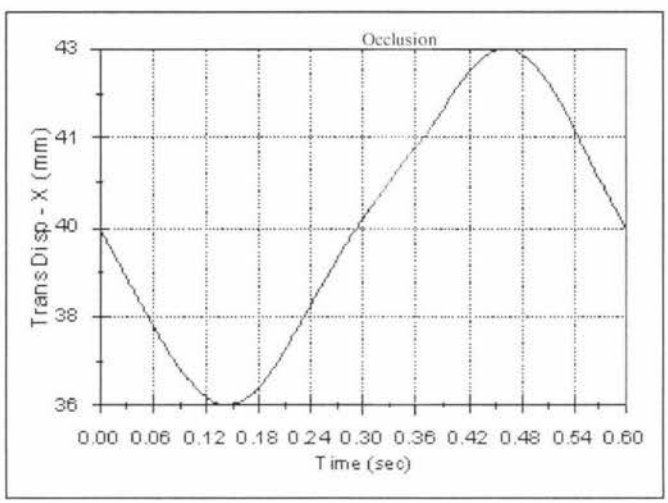

Figure 4-24 The linear displacement of the slider in the 'X' direction

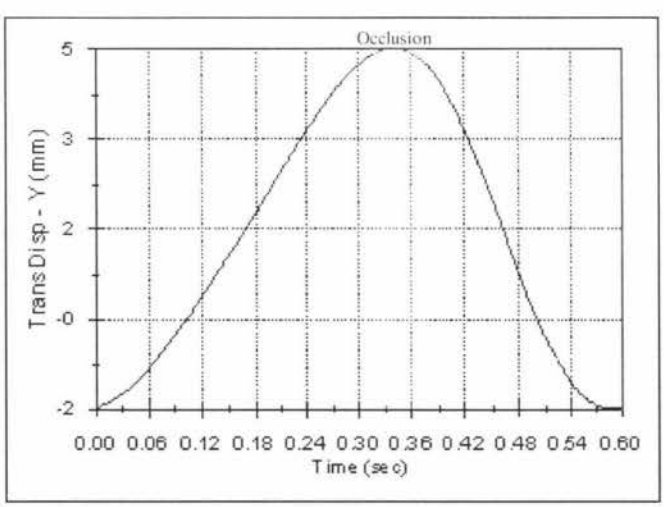

Figure 4-25 The linear displacement of the slider in the 'Y' direction

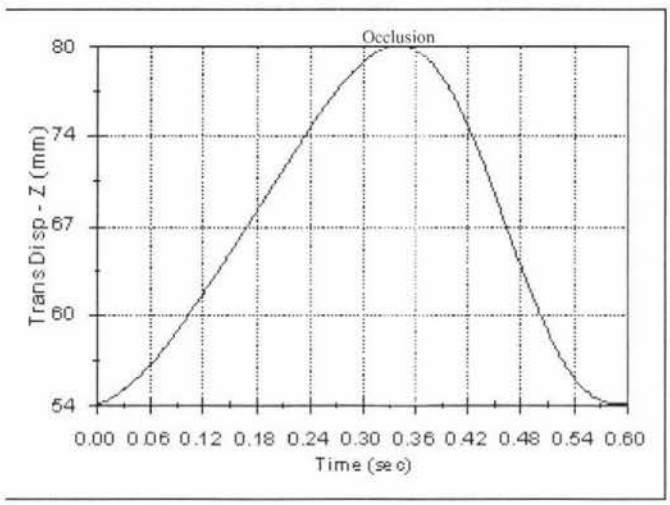

Figure 4-26 The linear displacement of the slider in the 'Z' direction

The velocities of the slider in the 'X, Y and Z' directions can be seen in Figure 4-27, Figure 4-28 and Figure 4-29. Figure 4-27 shows that the maximum velocity in the 'X' direction is 32mm/s. Figure 4-28 shows that the maximum velocity in the 'Y' direction is 50mm/s. While Figure 4-29 shows that the maximum velocity in the 'Z' direction is 181mm/s.

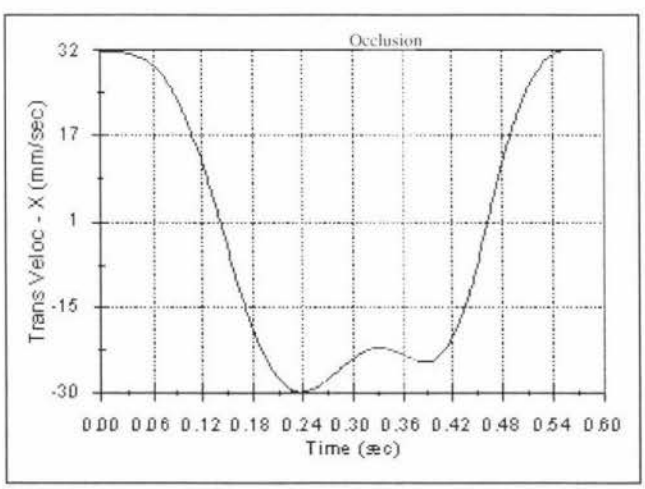

Figure 4-27 The velocity of the slider in the 'X' direction

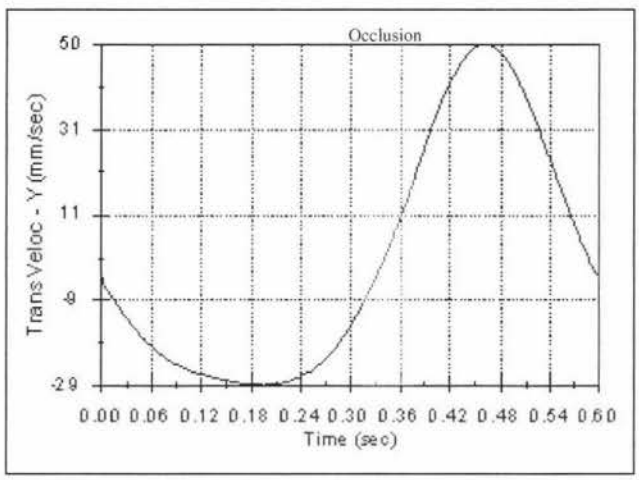

Figure 4-28 The velocity of the slider in the 'Y' direction

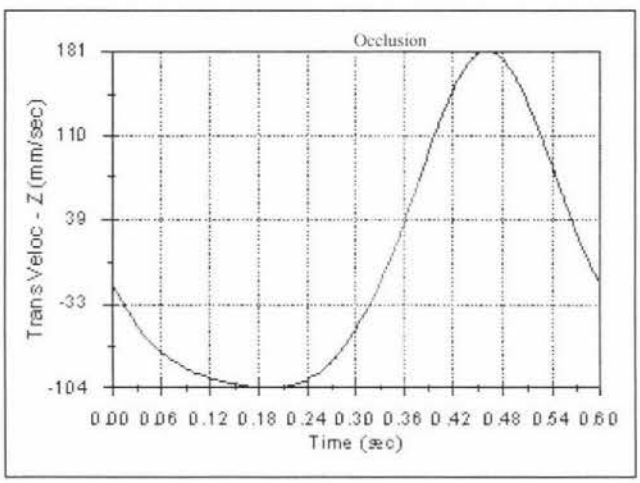

Figure 4-29 The velocity of the slider in the 'Z' direction

The accelerations in the 'X, Y and Z' directions can be seen in Figure 4-30, Figure 4-31 and Figure 4-32. Figure 4-30 shows that the maximum acceleration of the slider in the 'X' direction is 620mm/s^2. Figure 4-31 shows that the maximum acceleration in the 'Y' direction is 550mm/s^2. While Figure 4-32 shows that the maximum acceleration in the 'Z' direction is 1978mm/s^2. All of these graphs show that there are smooth acceleration profiles of the slider so that no large forces are instantly applied to the slider.

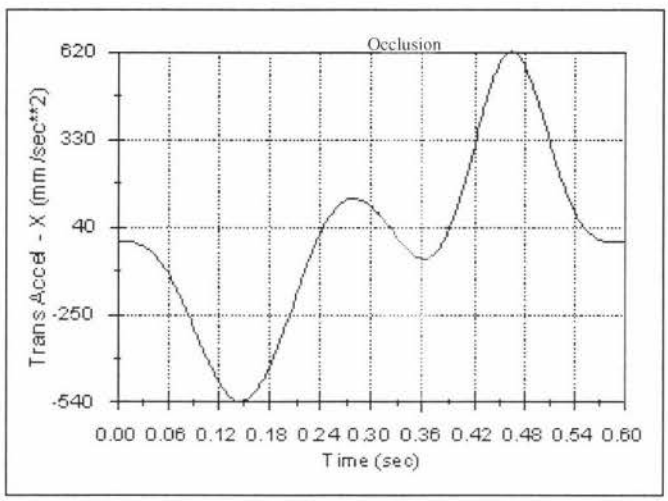

Figure 4-30 The acceleration of the slider in the 'X' direction

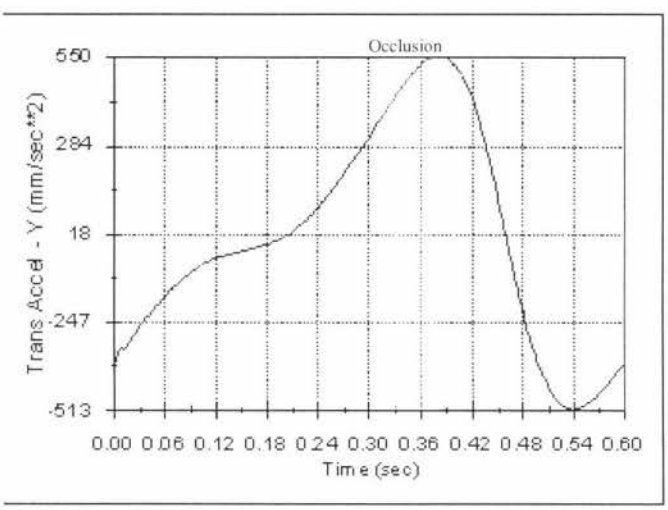

Figure 4-31 The acceleration of the slider in the 'Y' direction

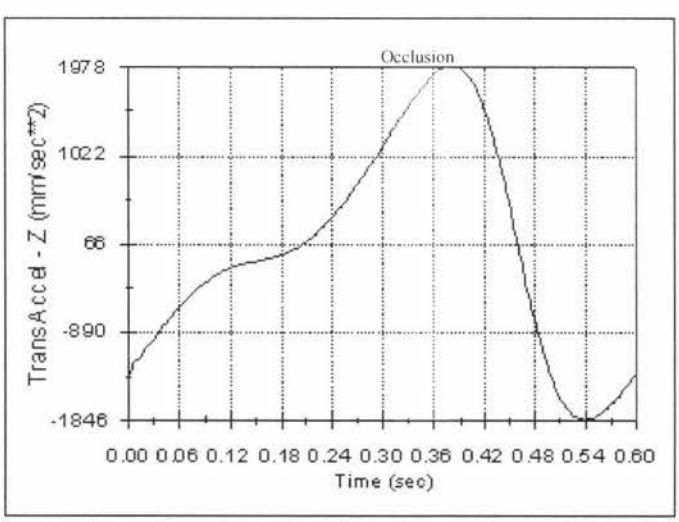

Figure 4-32 The acceleration of the slider in the 'Z' direction

The kinematic analysis of the six-bar linkage shows that there are no unrealistically large accelerations applied to the six-bar linkage components and therefore no large forces on the components. The kinematic analysis also shows that all the acceleration profiles are smooth and continuous which implies that there is no large forces are instantaneously applied to components of the six-bar linkage ensuring a longer life.

4.4.5 Six-bar linkage dynamics

The dynamics of the six-bar linkage were examined to see if any excessive forces or torques were applied to any of the joints. Once again the plots from this analysis were required to be smooth so that there is no instantaneous loading of the components, and are of realistic value. This analysis was also required to choose suitable bearings for the mechanism.

A static force of 150 Newtons was applied to the slider to simulate chewing. However this force was constantly applied to the slider over the entire chewing cycle. This was done as applying the force over only the occlusal period was not straight forward. The position where the teeth would be fully occluded in the following plots is at time 0.34s. The joints of main interest and their dynamics are shown below and defined in Figure 4-33.

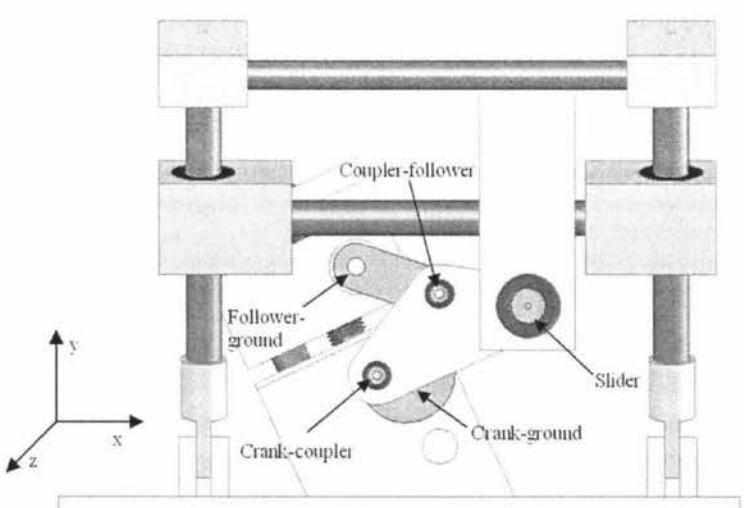

Figure 4-33 The joints of interest in the dynamic analysis

Figure 4-34 shows the torque that the crank needs to drive the mechanism at constant speed when a 150N force is applied to the slider. It can be seen that the peak toque does not occur when the teeth will be occluding. This is good as in the real system the linkage will not be applying this amount of force over the entire chewing cycle. It also shows that the linkage can efficiently transmit the torque applied to the crank in the occlusal position. This however was expected as the transmission angle analysis showed this.

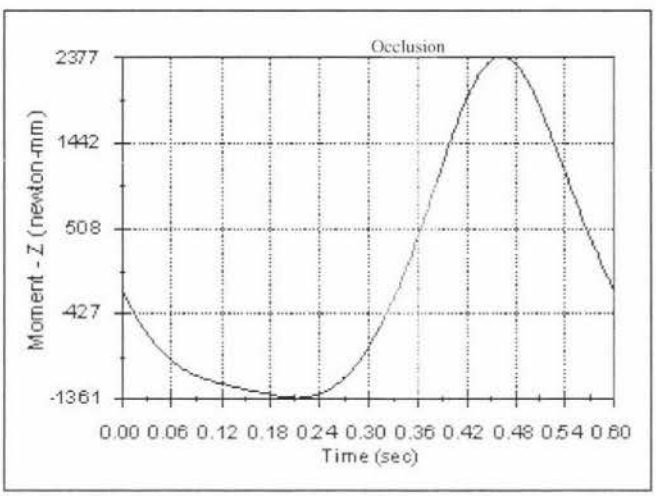

Figure 4-34 The crank torque of the six-bar linkage

Crank-coupler joint

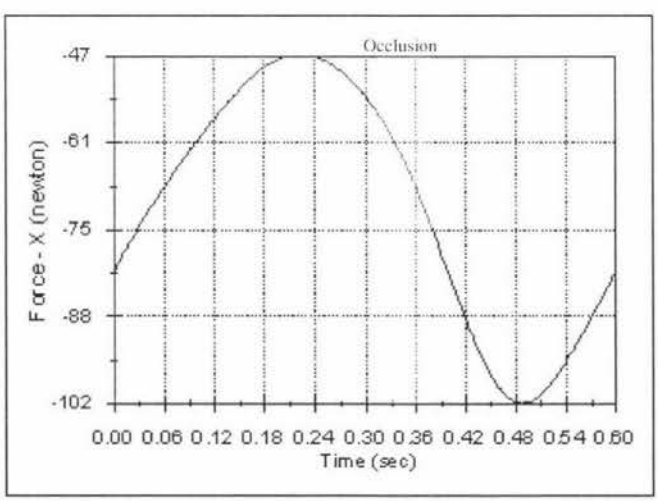

Figure 4-35 'X' direction force in crank-coupler joint

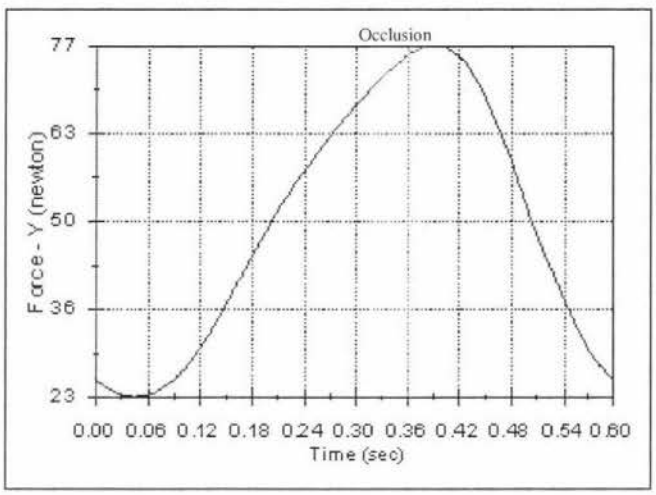

Figure 4-36 'Y' direction force in crank-coupler joint

Figure 4-35 and Figure 4-36 show the force components acting on the crank-coupler joints. Figure 4-35 shows that the force applied to the crank-coupler joint at the maximum occluding position in the 'X' direction is approximately 60N, while Figure 4-36 shows that the force applied to this joint in the 'Y' direction is approximately 70 N at the maximum occlusal position. Both of these plots show smooth force functions as required and also have realistic force applied to the joints. With this data NMB DDL1060ZZHA5 bearings were selected for the crank-coupler joint. They are rated for a maximum dynamic force of 460N and a maximum static force of 196N at 49,000 RPM. Therefore these bearings are suited to the application as they exceed the required specifications.

Follower-ground joint

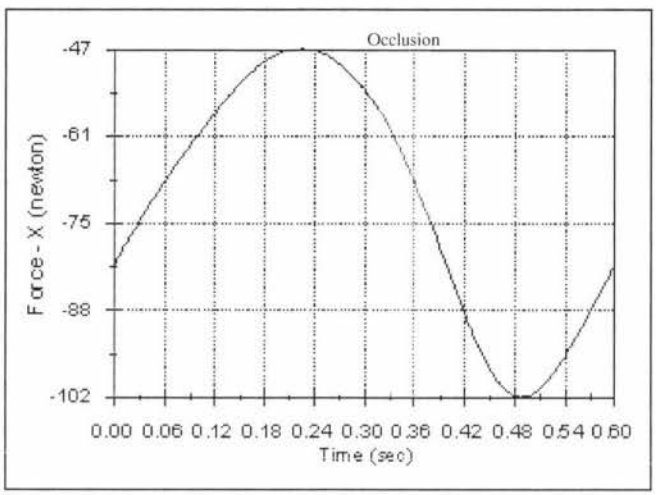

Figure 4-37'X' direction force in follower-ground joint

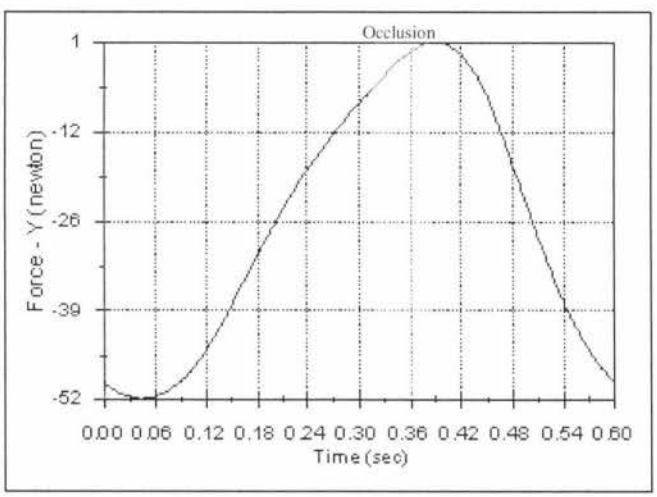

Figure 4-38 'Y' direction force in follower-ground joint

Figure 4-37 and Figure 4-38 show the force components acting on the follower-ground joints. Figure 4-37 shows that the force applied to the follower-ground joint at the maximum occluding position in the 'X' direction is approximately 60N, while Figure 4-38 shows that the force applied to this joint in the 'Y' direction is approximately 5N at the maximum occlusal position. These force functions are smooth and have realistic values as required. The bearings chosen for the follower-ground joints were the SKF 626-2RS1 bearings. They exceed the forces that are applied to follower-ground joint as they are rated at a maximum dynamic force of 1720N and a maximum static force of 620N at 36,000 RPM.

Follower-coupler joint

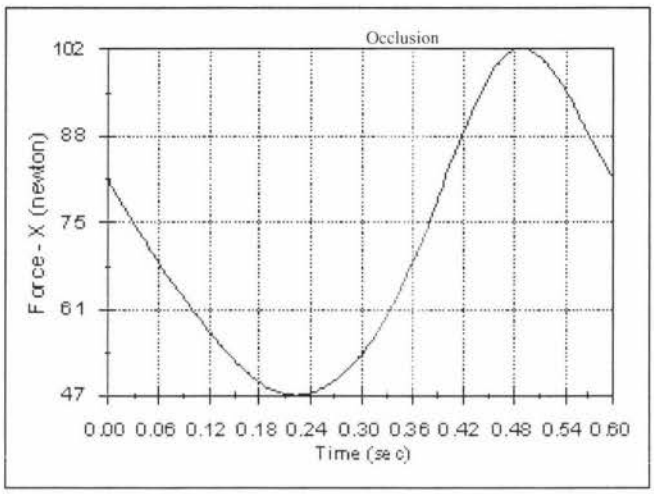

Figure 4-39'X' direction force in follower-coupler joint

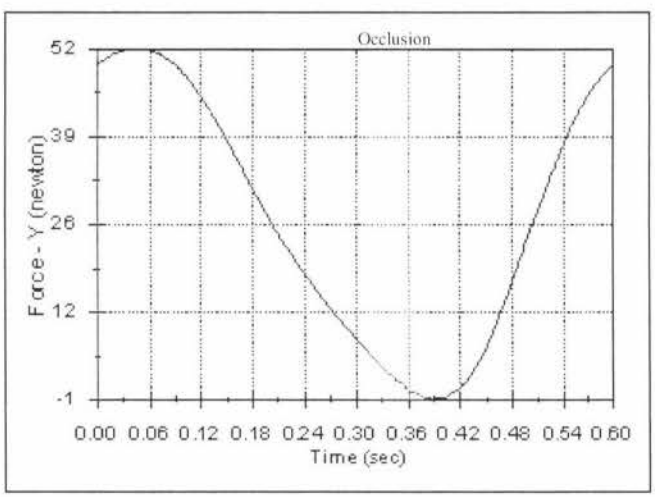

Figure 4-40 'Y' direction force in follower-coupler joint

Figure 4-39 and Figure 4-40 show the force components acting on the follower-coupler joints. Figure 4-39 shows that the force applied to the follower-coupler joint at the maximum occluding position in the 'X' direction is approximately 60N, while Figure 4-40 shows that the force applied to this joint in the 'Y' direction is approximately 5N at the maximum occlusal position. It can also be seen that the forces acting on this joint are same but in the opposite to those acting on the follower-ground joint. These force functions are again smooth and have realistic values. The NMB DDL1060ZZHA5 bearings were also selected for this joint as they exceed the required specifications.

Crank-ground

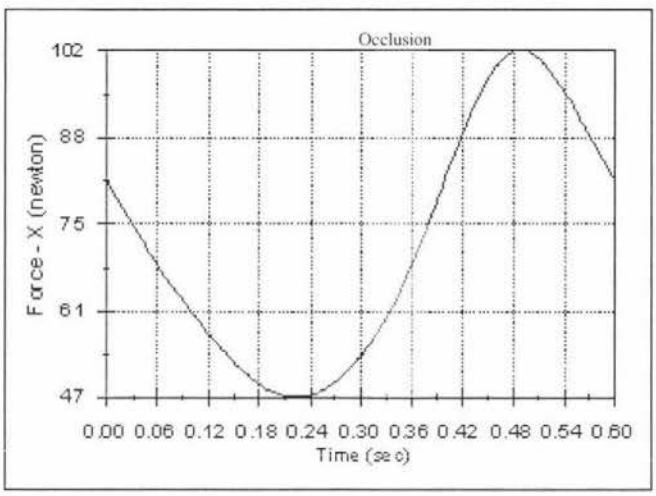

Figure 4-41 'X' direction force in crank-ground joint

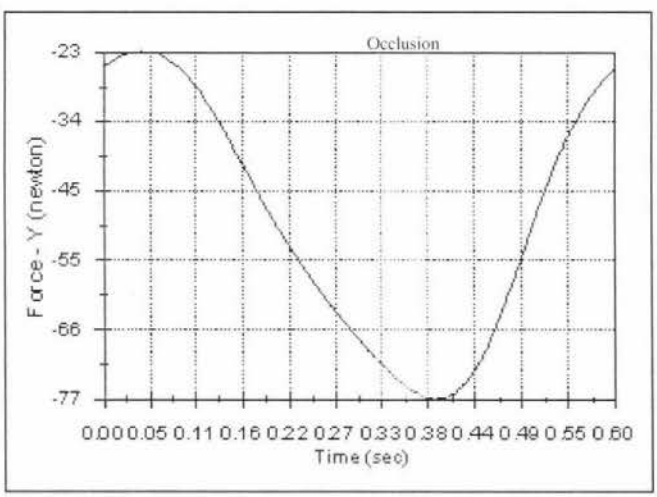

Figure 4-42 'Y' direction force in crank-ground joint

Figure 4-41 and Figure 4-42 show the force components acting on the crank-ground joints. Figure 4-41 shows that the force applied to the crank-ground joint at the maximum occluding position in the 'X' direction is approximately 60N, while Figure 4-42 shows that the force applied to this joint in the 'Y' direction is approximately 70N at the maximum occlusal position. It can also be seen that the forces acting on this joint are approximately the same to those acting on the crank-coupler joint but in the opposite. Once again these forces are smooth and of realistic value. The bearings chosen for these joints are the SKF 61800-2RS1 bearings. They allow for a maximum dynamic

force of 1380N and a maximum static force of 585N at 36,000 RPM which exceeds what is required.

This dynamic analysis showed that the force functions at the joints are smooth functions so that no large forces are instantaneously applied to any of the joints. It also shows that there are no unrealistically large forces that are applied to the joints which ensures that the mechanism will function as desired. The dynamic analysis also allowed for suitable bearings to be selected.

4.5 Motor selection

The motor that was selected to drive the mechanism had to be able to perform the following tasks:

- Be able to move the mechanism at the desired speed
- Be able to accelerate at the desired rate
- Have sufficient torque to move the mechanism and all the actuating components
- Be easily attached to the driveline of the six-bar linkage

As the motor needs to have its speed controlled by software the simplest motor to use was a DC motor. Due to the fact that this is an industrial project the motor must be low maintenance. Therefore a brushless DC motor was chosen as it has the advantage of not having any brushes that easily wear out, ensuring a long life. The brushless DC motors also have Hall Effect sensors in them that are used to determine when to switch the current in its coils. This means that these Hall Effect sensors can be used to determine the speed and therefore control it. However an optical encoder is used for more precise measurement and compatibility issues as discussed in chapter 6. To make better use of the motor a gearbox also needs to be selected. By using a gearbox the torque that can be applied is greatly increased but the speed is reduced. However a high torque, low speed system is in fact exactly what the chewing device requires.

The speed required from the motor was calculated using the data from the velocity profile described in chapter 6 which shows that the maximum speed that the crank has

to rotate at is 100rpm. Therefore the speed required of the output shaft of the gearbox must be a minimum of100rpm.

Once a crank speed was obtained, calculations of the torque that the motor require could begin. This was done in SolidWorks using COSMOS motion. The materials of the parts were specified so that the software could calculate correct inertia values. A constant force of 150N was then applied vertically to the actuating point to simulate chewing under maximum force conditions. The crank was then set to run at 300 degrees per second which is the occlusal speed of the crank described in chapter 5. A torque versus time plot was then produced as shown in Figure 4-43. This showed that the maximum torque that the crank requires to run the chewing device under maximum force maximum speed conditions is 2603Nmm or 2.6Nm which happens to occur at occlusion. Therefore the output of the geared motor must be able to produce a minimum torque of 2.6Nm at 300 degrees per second (78rpm) to achieve the desired force.

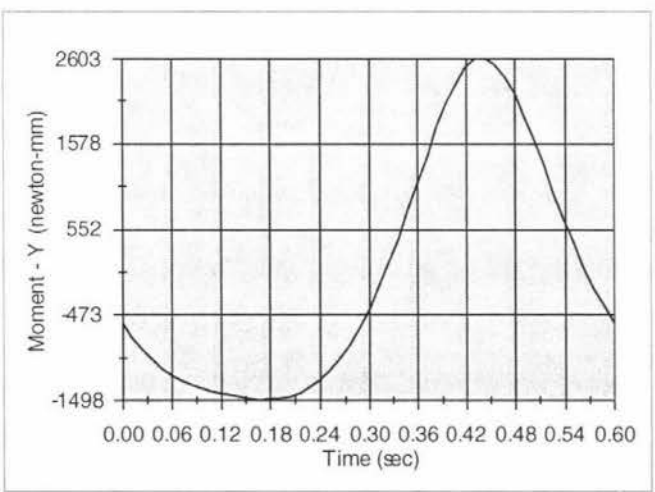

Figure 4-43 The torque required at the crank shaft

The motor also requires enough torque to accelerate the motor fast enough. From the trajectory planning described in chapter 6 it is known that the crank must be accelerated at 190 degrees per second squared to achieve the correct trajectory profile for the standard chewing profile. The angular acceleration can be estimated by knowing the torque applied at the crank and knowing the distance from the crank where the weight of the mechanism is concentrated as well as the weight force. The weight of the moving assembly of the six-bar linkage can be estimated at being at the actuating point on the

coupler as shown in Figure 4-44. This is due to the fact that another whole assembly needs to be added to this point to attach the teeth. This assembly will have a far greater weight than the components that make up the four-bar linkage meaning that these parts can be neglected for the acceleration estimates.

The occlusal position was used as the point to calculate the maximum acceleration that the crank can achieve as this is where the acceleration of the linkage is at a maximum. The weight of the assembly to attach the teeth was estimated to be 1.2Kg acting a horizontal distance of 45mm from the crank. This means that if the motor chosen has 2.6Nm of torque at the crank it can accelerate at 4.9 radians per second squared or 281 degrees per second squared. This is greater than the acceleration of 190 degrees per second squared required in the standard chewing case, but if the user changes the chewing parameters it may not be high enough. Therefore the motor and gearbox combination must be able to produce much more torque to be safe.

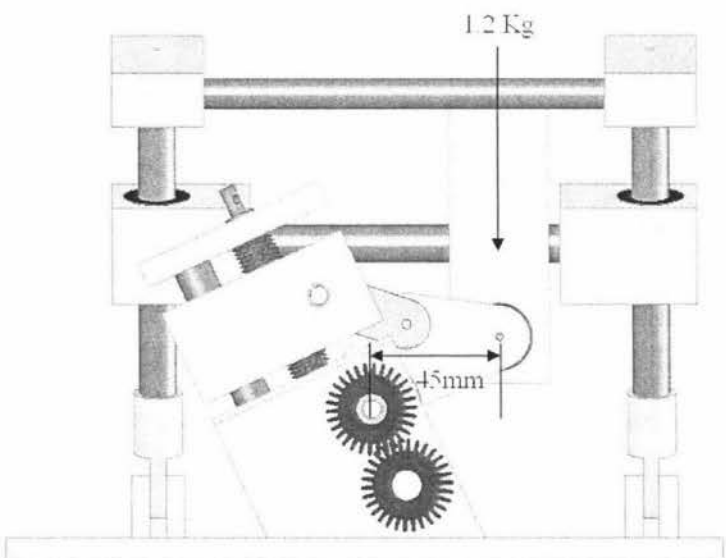

Figure 4-44 The weight concentration of the linkage

A brushless DC motor and gearbox combination was found from Maxon Motors that could deliver 6.0Nm of torque continuously and deliver 7.5Nm of torque for short periods. This motor can also revolve at 8000 rpm through the gear box and the output from the gearbox could be chosen as there were a number of different gearing options available. A gear reduction of 66:1 was chosen as this allows the drive shaft to rotate at a maximum rate of 121rpm which is above the rate required of 100rpm in the standard

chewing case. This motor and gearbox combination also had a dedicated control card that was available specifically designed to control this motor.

As the motor and gearbox are quite compact in design it made it much simpler to mount to drive the cranks. It was decided to drive the cranks of the mechanism by the use of a spur gear attached to the motor. This takes advantage of the fact that the two cranks of the six-bar linkage are coupled together by the use of spur gears. This means another can easily be added to allow the motor to drive the mechanism. The location of the motor and the how it drives the six-bar linkage can be seen in Figure 4-45.

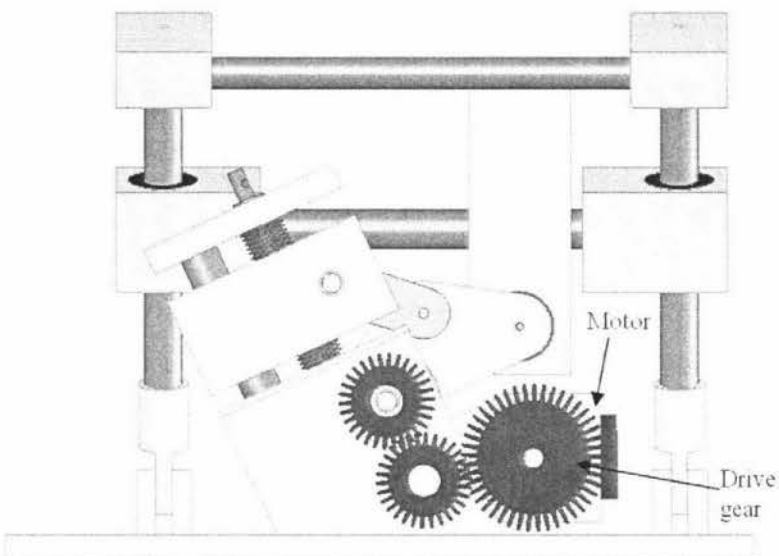

Figure 4-45 The location of the motor and the drive line

To make the motor fit in this location the spur gear used to drive the pinions attached to the cranks had to be large enough to ensure that the motor did not interfere with any other part. This however means that the speed of the crank is increased and the torque at the crank is reduced. The spur gear chosen to drive the pinion attached to the cranks has 44 teeth while the pinion has 28 teeth. The result of this changes the gear ratio to 42:1. This means that the torque was decreased by a ratio of 1.57 and the speed is increased by a ratio of 1.57. Therefore the torque at the crank is 3.82Nm and the speed is 190rpm assuming 100% efficiency.

This means that the motor and gearbox can exceed the required specifications as shown in Table 5.

Table 5 Comparison of required and achievable specifications

Parameter	Required	Estimated capability
Speed	100rpm	190rpm
Torque	2.6Nm	3.82Nm
Acceleration	190deg/s^2	414deg/s^2

4.6 Construction

Technical drawings of the components were then produced and given to the Massey University Institute of Technology and Engineering workshop where the components were made to specification and also assembled. The technical drawings produced can be seen in appendix B. Figure 4-46 shows the six-bar linkage that was constructed.

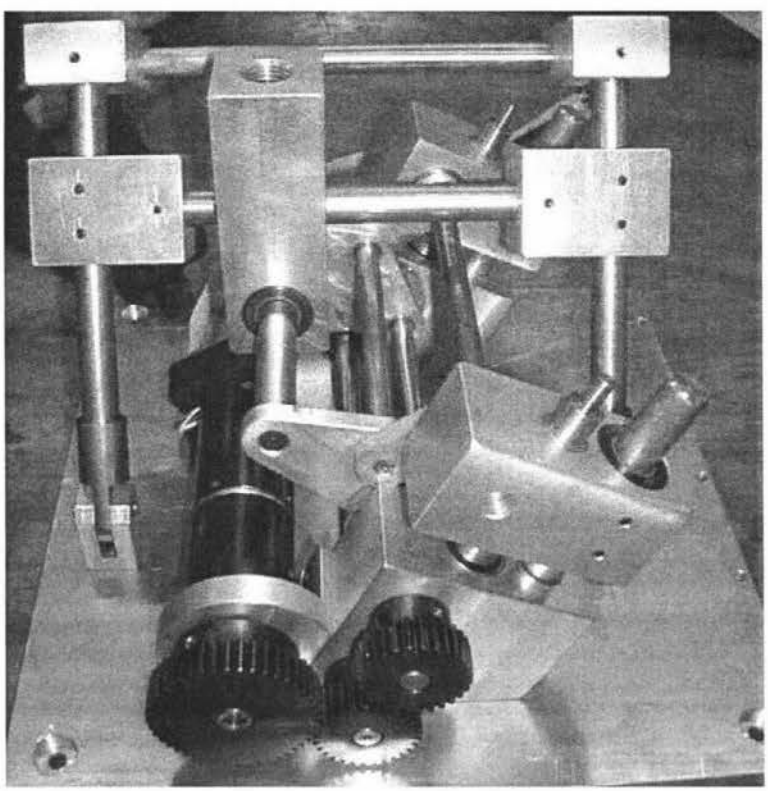

Figure 4-46 The six-bar linkage constructed

4.7 Results

Once the mechanism was constructed some basic testing of the six-bar linkage was done to see if the mechanism could in fact apply the desired force and also achieve the design trajectories.

4.7.1 Force measurement

The force testing was chosen to be done by the use of a load cell. This idea involves having the actuating point of the six-bar linkage pressing down on the load cell to measure the force applied. A load cell was chosen to perform the task of measuring the force as load cells use strain gauges to sense the force and therefore have a linear output. This is due to the fact that strain is equal to stress divided by Young's modulus as shown in Equation 4.1 and stress is equal to force divided by area as shown in Equation 4.2.

$$strain = \frac{stress}{Y} \tag{4.1}$$

$$stress = \frac{force}{area} \tag{4.2}$$

Therefore substituting 4.1 into 4.2 gives:

$$strain = \frac{force}{Y.area} \tag{4.3}$$

Equation 4.3 shows that strain is proportional to force which therefore makes the calibration of the load cell very simple. However the only load cell that was available was a 30N load cell. This meant that a lever system had to be constructed to divide down the force from the 0-150N range that the mechanism was designed to provide to the 0-30N range of the load cell. The measurement system can be seen in Figure 4-47. This was done by defining that a 150N force applied to the lever would result in a 20N force applied to the load cell. Therefore the lever system required a 7.5:1 divide down ratio. This lever system was chosen to have the dimensions shown in Figure 4-47 so that it could easily be attached to the chewing device.

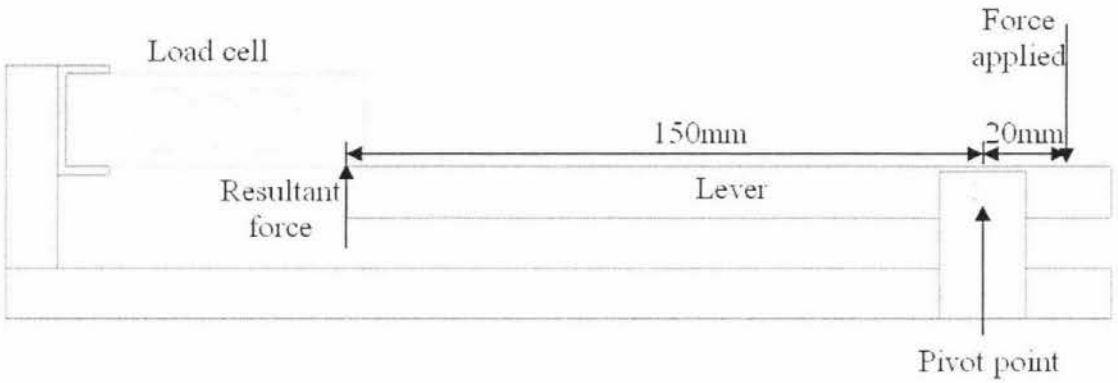

Figure 4-47 The force measuring device

The information that the load cell measures then had to be recorded so that it could be calibrated and also provide a measurement of the forces that are applied to it. This was done by the use of an analogue to digital converter that was interfaced to Labview. This allowed the data from the load cell to be displayed on a computer. Once this had been established the system could then be calibrated to display the results of the force that is applied to the lever. This was done by hanging a series of known weights off the point where the force was going to be applied. Once the calibration was complete the system was tested by again applying a series of known weights to the input of the lever system to see if the force shown on the computer matched the force applied to the lever.

This simple testing showed that the system was sufficient to test the six-bar linkage as it was accurate to approximately 5N. The force measuring system was then securely attached to the six-bar linkage so that it would press its actuating point down onto the lever in the appropriate position. The chewing device was then set to run continuously and the force of the linkage impacting on the lever was measured. This testing showed that the chewing device could in fact apply the desired 150N chewing force and would stall at approximately 260N. A screen shot of the force measuring program can be seen in Figure 4-48.

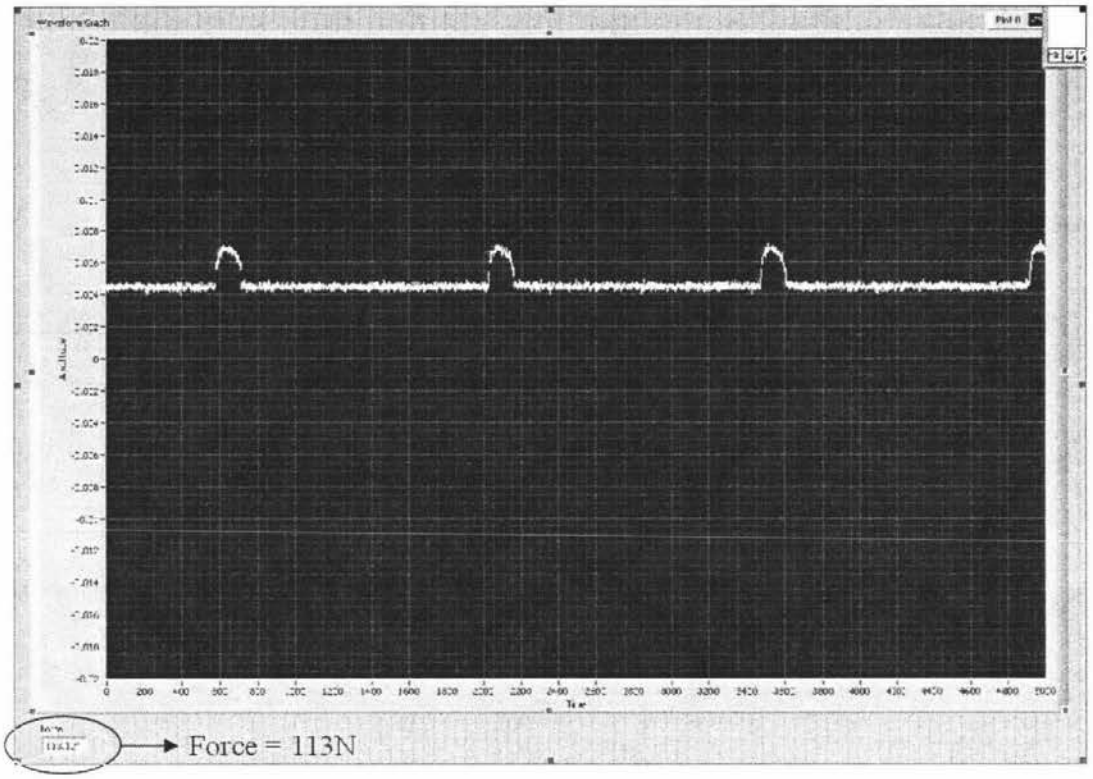

Figure 4-48 Sample of force measuring program

4.7.2 Trajectory measurement

The trajectory measurement was only required for the frontal plane. This is due to the fact that the sagittal trajectories are approximated by a straight line and it could easily be seen that it could perform these linear trajectories with the desired 0-30 degree adjustment. The simplest way to compare the trajectories that the device can perform and the designed trajectories was to use a modified pen to trace the trajectories achieved and overlay them. The pen used to trace the trajectories was modified so that the spring was used to push the nib out rather than retracting it. This was done so that the nib of the pen could make consistent contact with the card that it traced the path onto. The pen was securely attached to the slider of the six-bar linkage and the card was setup in a vertical fashion so that the nib was in contact with the card. This required the trajectory in the sagittal plane to be set at 0 degrees so that the slider only moved in two dimensions. The trajectories produced where scanned onto the computer and overlaid with the desired trajectories. It was observed that the trajectories produced by the chewing device were close to the desired trajectories. Some examples can be seen

in Figure 4-49. However the traced trajectories did not exactly match the desired trajectories. They slightly differ in the opening/closing phase of operation but this is not important as no chewing occurs in this phase of the chewing cycle. The entry and exit angles match very closely however. This means that representative chewing will be achieved.

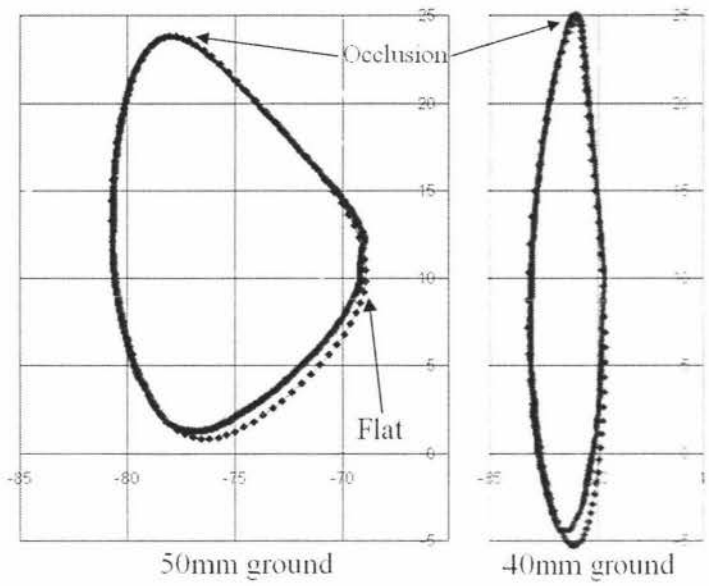

Figure 4-49 The overlay comparing the achieved trajectory and desired trajectories

Figure 4-49 also shows that there is a flat section where the direction changes. This is due to the fact that there is in fact some play in the six-bar linkage caused by the linear bushes.

4.8 Conclusions

The mechanical design of the six-bar linkage device that performs the actuation for the chewing motion was able to achieve the desired criteria of:

- Generating the correct occlusion entry and exit angles in the frontal plane.
- Create a linear approximation to the human chewing trajectories in the saggatial plane.
- Withstanding the forces that are applied during chewing.

The six-bar linkage closely follows the frontal trajectory of a lateral chewing motion and still approximates a vertical chewing motion. This can be seen in Table 4. The six-bar linkage can also achieve a 2D approximation of human chewing trajectories in the

sagittal plane. This is due to the fact that the linear guide shafts that set the trajectory in the sagittal plane have a 0 to 35 degree adjustment.

The mechanism also effectively transmits the torque of the motor through the six-bar linkage which converts the torque into the chewing force. This is due to the fact the transmission angle of the four-bar linkage is within the 30 to 150 degree range. It is also very efficient at the occlusion point of the chewing cycle where the food will be chewed. This is because the transmission angle at this location is centred around 90 degrees where the linkage has the greatest efficiency.

The dynamic analysis of the forces that act on the joints of the linkage shows that no excessive forces are applied. The analysis shows that the maximum force applied during the simulation to any joint was 102N in the horizontal direction and 77N in the vertical direction. However this analysis involved a 150N force being applied over the entire chewing cycle which is not how the real system operates. Using the data obtained from the dynamic analysis it was seen that the maximum force applied to a joint during occlusion was approximately 65N in the horizontal direction and 75N in the vertical direction. This however does not include any impact force analysis which may cause larger forces to be applied.

The stress analysis showed that there were no major deformations to any of the parts when exposed to the 150N chewing force. The maximum deformation of any part was only 0.005mm which is minimal and nothing to be concerned about and there was no major concentrations of high stress. This analysis however was done under static conditions where a 150N force was applied to the linkage when in the occlusal position as the software package did not allow for dynamic stress analysis. Therefore the stresses will be different when the mechanism is running.

These conclusions were reached after designing the mechanism and simulating it in software. This ensures that there is a good estimation of how the constructed device will function and therefore provides confidence in the mechanism.

5 Supporting design

5.1 Introduction

Auxiliary components were required for an operational chewing device. These components include:

- a system to limit the level of force applied to the food
- anatomically correct teeth
- a system to allow the teeth to be easily inserted and removed from the device for food loading and cleaning
- a system to set up the teeth so that they occlude correctly
- a system of retaining the food that has been chewed between cycles
- a system to reposition the food
- an enclosure to house all the systems

5.2 The force control

The force control in this project is needed to limit the amount of force that the chewing device can apply. This ensures that the motor does not easily stall and that excess stress is not applied to the six-bar linkage. As the teeth do not touch each other during chewing the force that is applied to the food is dependent on the properties of each food sample. This is due to Newton's third law which states that every action has an equal and opposite reaction. In the case of the chewing device this means that the maximum force that the device can apply to a food sample is equal to the maximum force the food sample can apply to the chewing device. The maximum forces that are applied during chewing range from 70 to 150N as stated in chapter 2. This means a force limiting system can be set at 150N to allow the chewing device to apply the maximum chewing force that a human can apply. This helps better simulate human chewing behaviour.

As a prototype system, it was decided that a spring and damper system could be used to limit the force. This concept works by having the spring and damper attached to either the upper or lower set of teeth. When the chewing device chews the food the spring and damper will compress when the force exceeds the 150N limit. However the

nature of the spring and damper system means that the damper will apply different amounts of force depending on the impact velocities at which the teeth hit the food. Therefore the damping has to be adjustable.

An adjustable shock absorber was chosen to perform the force limiting task and selected based mainly on the effective weight that is to be applied to the shock absorber. The effective weight applied to the shock absorber can be calculated by equations that can be found in the ACE Controls deceleration catalogue page 15. As there are many different equations for many different applications the chewing device system can be adapted to the vertical free fall equation. This is because the 150N impact force can be thought of as a 15Kg weight resting vertically on top of the shock absorber.

As the equations in the ACE Controls catalogue are specified in imperial units the values that were known were changed to the correct units as specified by the equations. These conversions can be seen below.

W= weight= 150N= 33.7lbs
V= impact velocity= maximum occlusal velocity= 44mm/s= 0.1444ft/s
F= propelling force at the shock= W
s= stroke of shock= occlusal distance= 0.5mm= 0.0197 inch

These values were then substituted into equations 5.1 – 5.4 to establish the values to find the effective weight.

$$E_1 = 0.2W.V^2 \qquad (5.1)$$

$$E_2 = F.s \qquad (5.2)$$

$$E_3 = E_1 + E_2 \qquad (5.3)$$

$$W_e = \frac{E_3}{0.2V^2} \text{ (Effective weight)} \qquad (5.4)$$

After substitution

W_e= 193lbs= 87kg

As the effective weight is 87kg the shock absorber chosen was the ACE MA150-MB which has an effective weight range of between 0.9kg and 90kg. This shock absorber also has a rod rest time of 0.4 of a second which meets the required criteria of being fully returned in time for the next cycle as the average cycle time is 0.75 of a second. The shock absorber also has an energy capacity of 17Nm which is well above the 6.5Nm of torque that the motor can apply. The weight of the shock absorber is also extremely minimal as it only weighs 60 grams which reduces the inertia of the actuating assembly allowing the motor to respond quickly.

The shock absorber was chosen to be mounted onto the slider of the six-bar linkage due to the fact that it can easily be attached to it. This is because the outside of the shock absorber is threaded and can screw into the slider block. This can be seen in Figure 5-1.

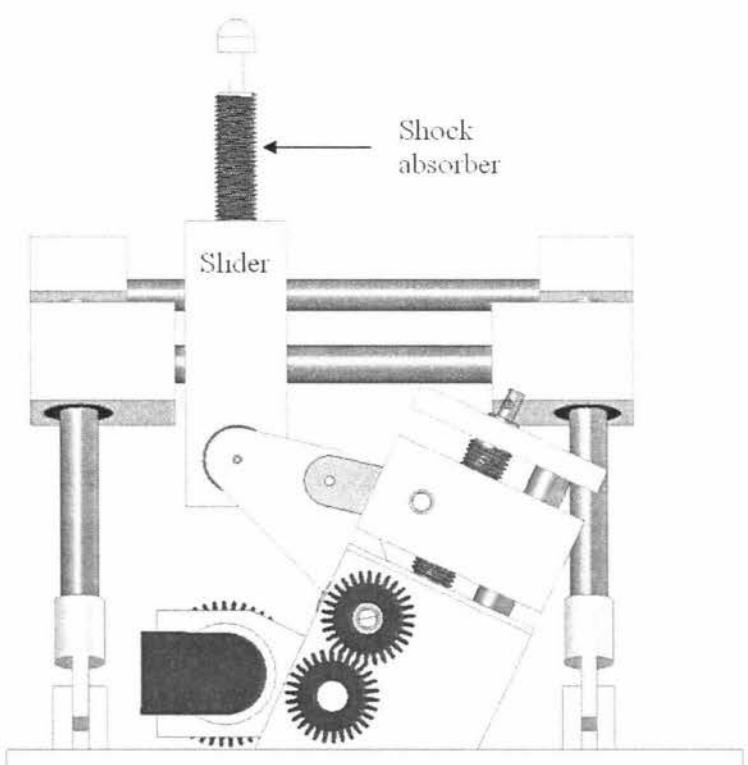

Figure 5-1 The location of the shock absorber

Some basic testing was done to evaluate the shock absorber and see how it functioned. The spring constant and damping co-efficient were measured to get an idea of how the shock absorber would affect the dynamics of the mechanism. These measurements were performed on a TA2 texture analyser that allows for force, displacement, velocity and time measurements when specifying a desired linear motion. To measure the spring constant the machine was set to compress the shock absorber by applying a constant force of 3N. The displacement was then measured when the 3N force could not compress the shock absorber any more. The displacement recorded after a few runs was recorded as 7.479mm. Using Hookes law shown in Equation 5.1 the spring constant was determined to be 408Nm^{-1}.

$$F = k.y \quad \text{(Hookes law)} \tag{5.1}$$

The result shows that the spring constant does not dramatically affect the force that is applied during chewing. This is due to the fact that the maximum displacement of the shock absorber is 17mm and at this maximum displacement a force of only 6.9N is applied by the spring and can be considered negligible when applying forces in the order of 150N. Therefore the damping co-efficient is going to have the greatest affect on the forces that the mechanism can apply. The damping co-efficient was also measured with the same machine but this time the machine was set to compress the shock absorber at a constant velocity for a 13mm distance and measure the reaction forces. Due to the fact that machine is designed for the testing of food properties it can not move at great speed. The maximum speed used for testing the shock absorber was 10mm/s which is well below the 55mm/s vertical occlusal velocity that the chewing device can achieve (shown in Figure 5-2). However the damping co-efficient could be calculated at this speed as the damping co-efficient is proportional to the velocity. Figure 5-3 shows the response of the shock absorber when compressed at different velocities. This shows that the force applied increases quite quickly over the first couple of millimetres and the changes so that the force only increases slightly over the rest of the cycle. The latter is expected as the force applied from the damper is constant when compressed at a constant speed and the increase in force is due to the reaction force of the spring. The damping co-efficient was then found using the data in Figure 5-3 using Equation 5.2.

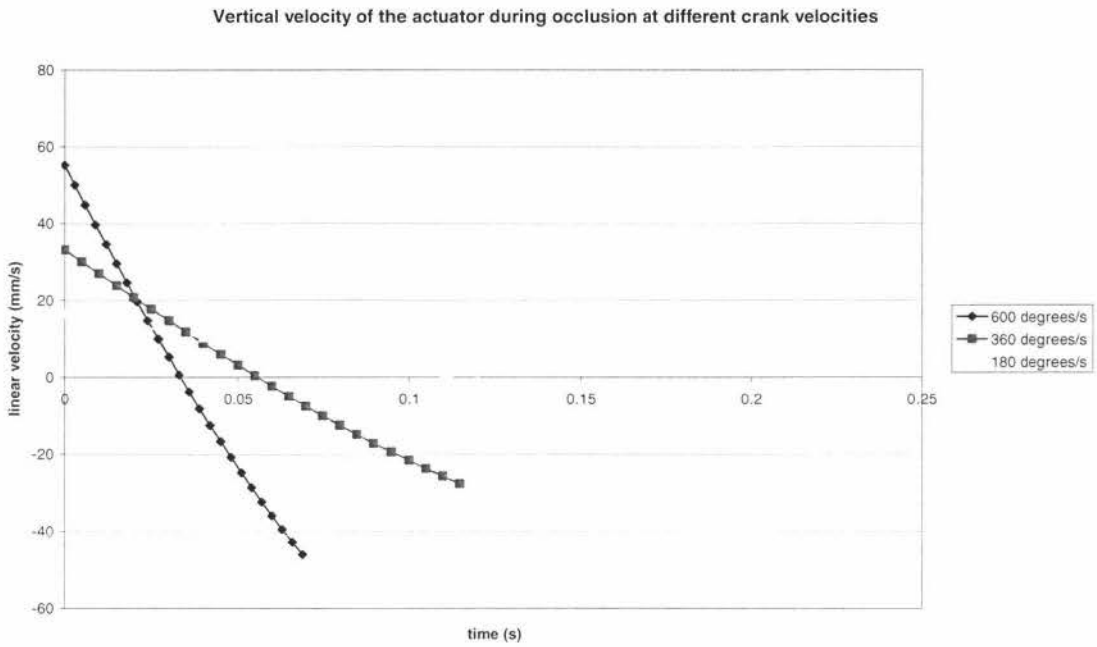

Figure 5-2 The vertical velocity of the actuator

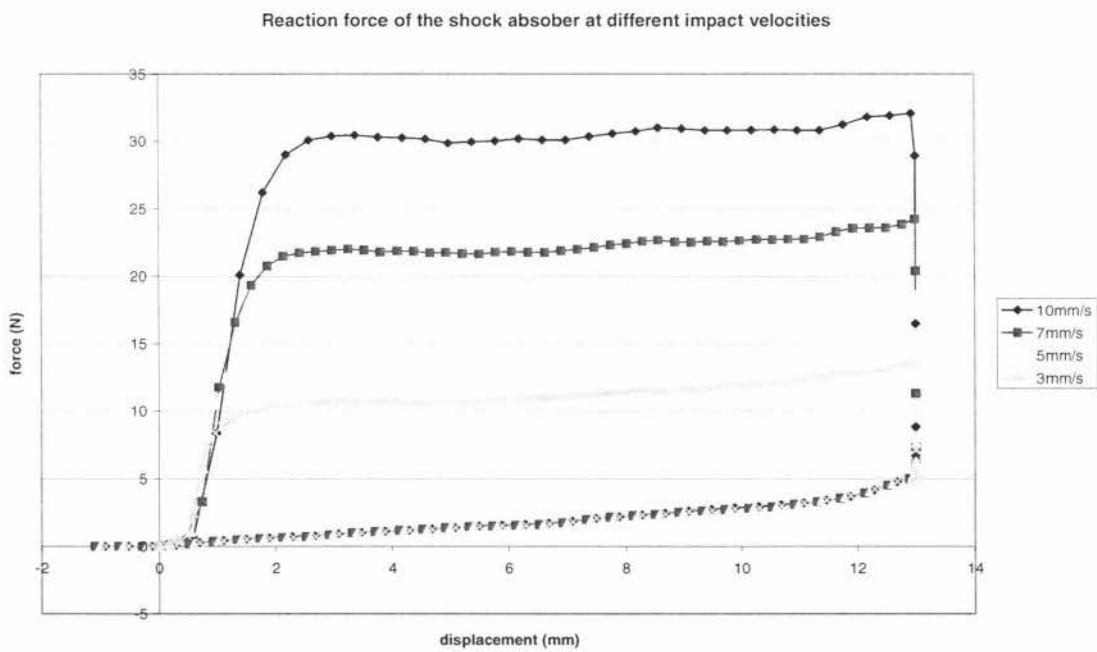

Figure 5-3 The response of the shock absorber when compressed at different velocities

$$F = R.\frac{dy}{dt} + k.y \qquad (5.2)$$

Substituting:

$F = 30N$

$\frac{dy}{dt} = 10mm/s$

$k = 408Nm^{-1}$

$y = 6mm$

Giving:

$R \approx 2760Ns/m$ (damping co-efficient)

Therefore:

$$F = 2760\frac{dy}{dt} + 408y \qquad (5.3)$$

However this model only works for quite large displacements of the shock absorber so that the force falls on the line of secondary section of Figure 5-3. The real system will also have a mass of approximately 600 grams that is attached to the shock absorber to hold the teeth. This mass will be moved when the shock absorber is compressed. The equation for a mass-damper-spring system is also widely known and can be seen in Equation 5.4.

$$F = M.\frac{d^2y}{dt^2} + R.\frac{dy}{dt} + k.y \qquad (5.4)$$

This equation shows that the force component applied by the mass is equal to the mass multiplied by the acceleration. The maximum acceleration during occlusion at the maximum occlusal speed is approximately 1700mm/s^2 as shown in Figure 5-4. This means that the 0.6Kg mass accelerated at 1700mm/s^2 applies 1.02N of force. This implies that the damping co-efficient should have the greatest affect on the system. The size of the food sample being chewed will also affect the force that can be applied. This is due to the fact that if the food sample is higher the shock absorber impacts at a

higher velocity due to the nature of the six-bar linkage and therefore causes a higher force. This however assumes that the food sample is an immoveable object. If it was not an immovable object then the force is dependent on the properties of the food as to whether the food will compress before the shock absorber. This has been previously described.

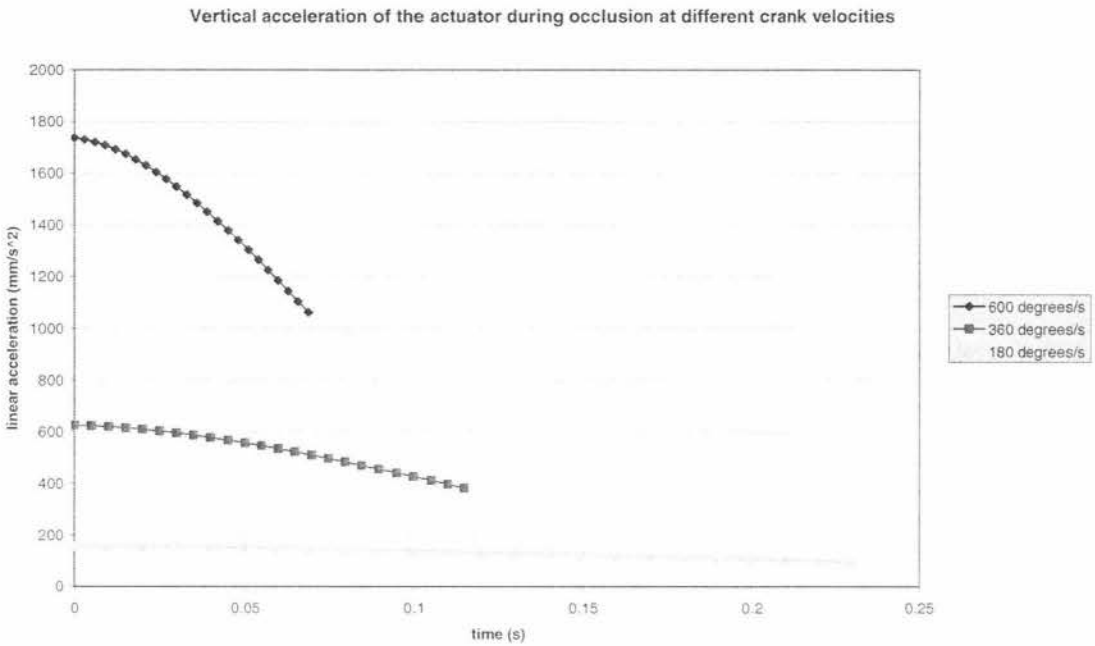

Figure 5-4 The vertical acceleration of the actuator

The mass-damper-spring model shown in Equation 5.3 has been used to estimate the force response of the shock absorber in the chewing device. This can be seen in Figure 5-5. It can be seen that the damper has the greatest affect on the system as the force closely follows the velocity profile shown in Figure 5-2. This however is expected from the values previously determined. Figure 5-5 shows that the initial force is high and tapers off due to the fact that the velocity is decreasing. Therefore it would be a good idea to investigate a shock absorber that has the highest force applied by the spring so that the maximum force is applied at the maximum intercuspal position. However the current shock absorber is adequate for the current stage of development.

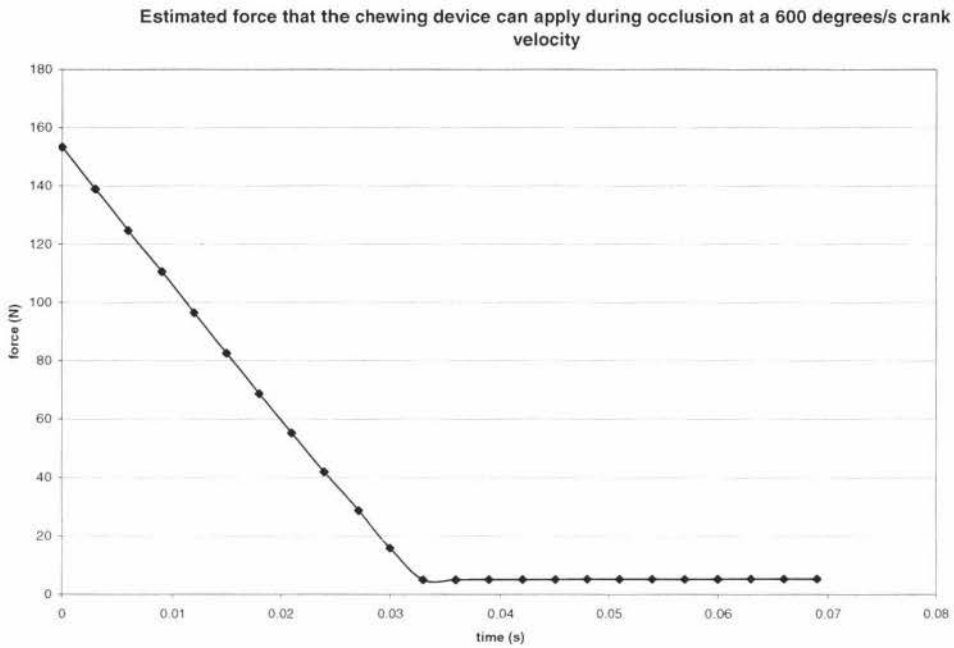

Figure 5-5 The force response of the shock absorber

5.3 The chewing device enclosure

The chewing device enclosure is the housing that holds all the sub systems together. The device was originally chosen to be of an inverted design. This was due to the fact that the original idea of the retaining the food involved the use of a bowl with teeth embedded in it to retain the food. This uses gravity to ensure that the food is guided back on to the teeth by the profile of the bowl. The human masticatory system involves moving the lower set of teeth while the top set of teeth remains fixed. But it is not important what set of teeth moves as long as there is the correct relative motion. Therefore the upper set of teeth was chosen to be actuated in the chewing device. This meant that the lower teeth would have to be located in the bowl to allow the use of gravity, hence the inverted design.

Due to the fact that chewing device needed to be inverted, the six-bar linkage needed to be located above the teeth. This meant that the majority of the weight is to be located near the top of the device. Therefore the enclosure needed to be designed so that it is stable by having the overall height of the device as low as possible.

As the dimensions of the six-bar linkage mechanism and the clearance allowed for the teeth cannot be made smaller, means that only the position of the power supply and control card can be chosen to effect the centre of gravity. The two main options for the location of the power supply and control card were having them located on top or below the device. They were chosen to be placed above the six-bar linkage mechanism due to the fact that they weigh less than the six-bar linkage. This makes the device have a lower centre of gravity than having them placed below the device.

The device also needed an adjustable table to allow the height adjustment of the teeth. This is due to the fact that the height where the teeth occlude changes when the ground link of the four-bar linkage is adjusted. This was chosen to be achieved by the use of a screw thread device that moves a platform up and down with the aid of linear bushes to remove the rotational movement. Two lead screws were used to move the table up and down. This allows the table to be supported in two positions making it more stable. These lead screws are kept in time with each other by the use of a toothed belt and matching pulleys. The belt is kept tensioned by the use of a third pulley. Linear bushes were used in the four corners of the table that slide on shafts. This stops the table from twisting when force is applied to the table. These shafts are also used as to position all the parts in the correct orientation and height. The lead screws are driven via a handle that when turned drives a set of bevel gears that connects both the lead screws and the handle. The enclosure also has a case positioned on top to enclose the power supply and motor control card. This can be seen in Figure 5-6.

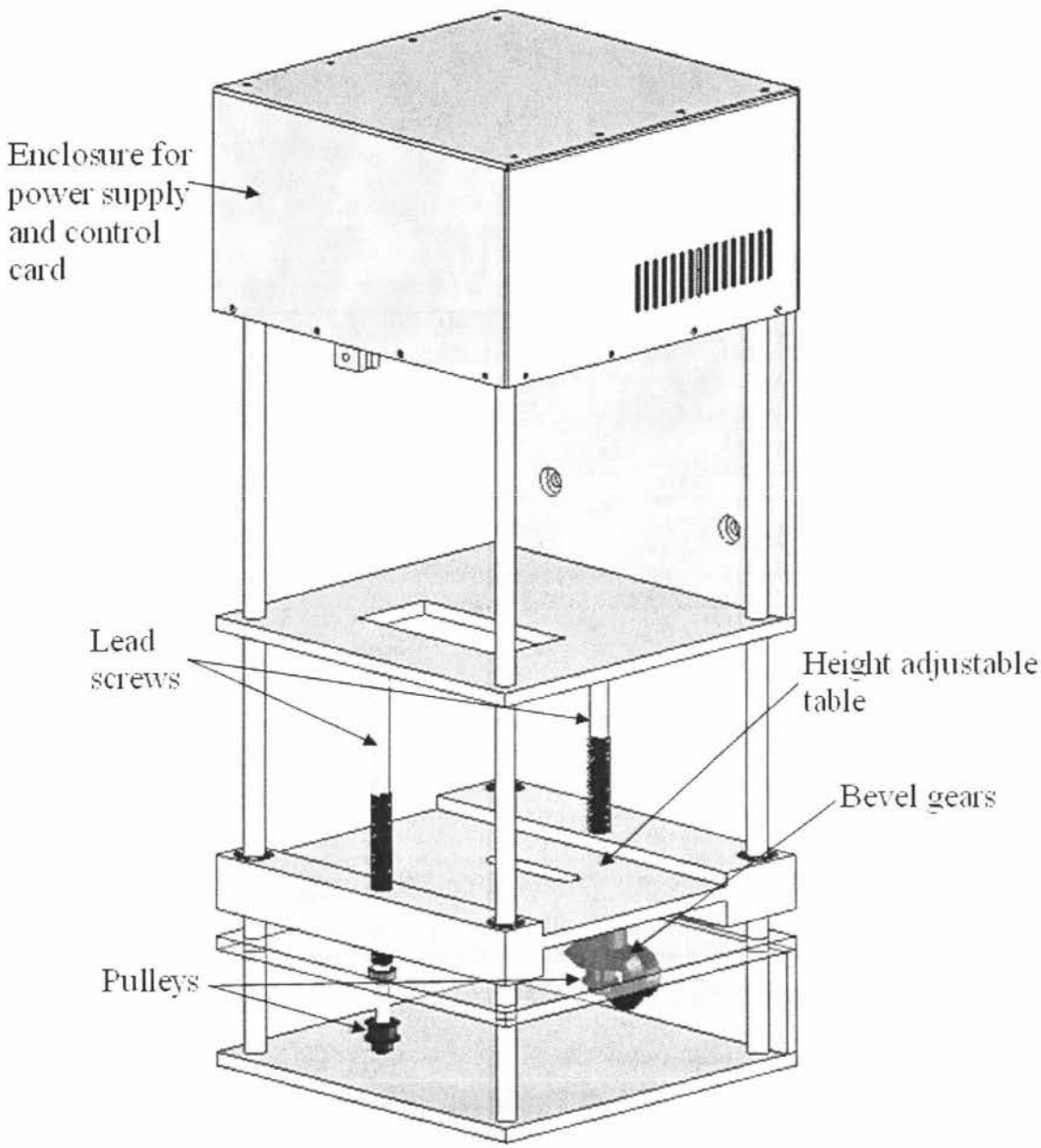

Figure 5-6 The enclosure of the chewing device

5.4 The teeth locking mechanisms

The mechanisms to hold the teeth in position were designed so that the operator could easily remove the teeth for cleaning and gathering the food sample that has been chewed. As the teeth can have different occlusal positions depending on the setting of the ground link of the four-bar linkage, the teeth have to be positioned every time the

settings are changed. This meant a way of quickly adjusting the occlusal position of the teeth was required.

Only one set of teeth needed to be adjusted to match the other set. Therefore the teeth that are attached to the six-bar linkage can have a fixed position while the bottom teeth can have an adjustable position. The bottom teeth were made adjustable as there is more space on the plate that the bottom teeth mount to. This means that the locking mechanism can be incorporated into the system much more easily and excess weight from the locking mechanism is not being added to the actuating assembly of the six-bar linkage.

5.4.1 The lower teeth locking mechanism

The positioning and locking system of lower set of teeth is a simple system that allows the operator to slide in the teeth into the locking mechanism, position them correctly and then lock it in place. This is done by using the system shown in Figure 5-7.

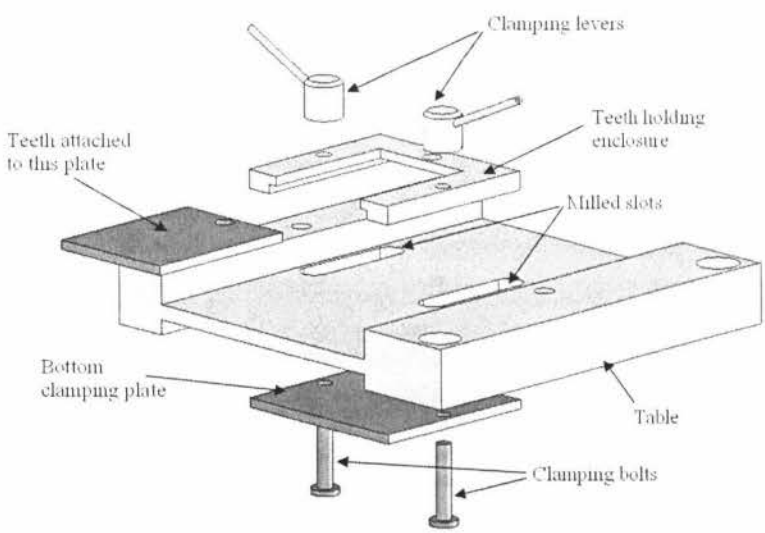

Figure 5-7 Exploded view of lower teeth locking mechanism

This shows that the plate that has the teeth attached to it slides into an enclosure. The enclosure can then be locked in place by two clamping levers that tighten themselves on bolts which in turn clamp the top enclosure and bottom plates together. This system allows the lower teeth locking mechanism to be positioned in the entire operating range by having slots milled in the table that it sits on. These slots accommodate the clamping

bolts and allow them to move the desired amount. Once this enclosure is clamped into place, the plate with the teeth on it can be slid into position. The teeth plate is held in place by the flanges of the locking enclosure as well as a locating pin. This allows the teeth to be removed and inserted easily without re-aligning the upper and lower teeth every time a food sample is inserted.

5.4.2 The upper teeth locking mechanism

The positioning of the upper teeth set is less complicated than the lower teeth set. This is due to the fact that the upper teeth set can have a fixed location. But the device that holds the teeth has to be attached to the shock absorber. To make this device so that there are no clearance issues it was designed to screw onto the shock absorber. While the teeth have an enclosure that the teeth slide into which get locked in position by a locating pin. The upper teeth locking mechanism can be seen in Figure 5-8.

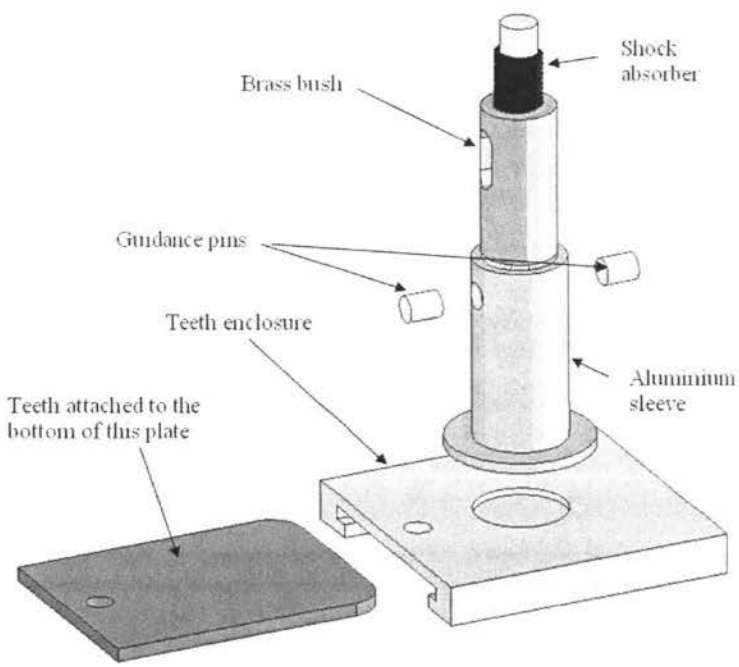

Figure 5-8 The upper teeth locking mechanism

This shows that a brass bush screws onto the shock absorber which has an aluminium sleeve that slides over the top of it. The rotational movement is removed by having slots milled into the brass bush and holes in the aluminium sleeve that a couple of pins screw through and slide in the slots in the bush. This also stops the sleeve from falling off the bush. The sleeve has a flange at the bottom of it to use to bolt the teeth locking

mechanism on to it. This is located by a hole that is milled in the teeth locking mechanism that the sleeve slots into. The teeth locking mechanism is a simple billet of aluminium that has a groove milled into it. This allows a stainless steel plate with the teeth attached to it to slide into position. This plate and therefore the teeth are locked by the use of a locating pin. The location of the six-bar linkage and the teeth locking mechanisms can be seen in Figure 5-9.

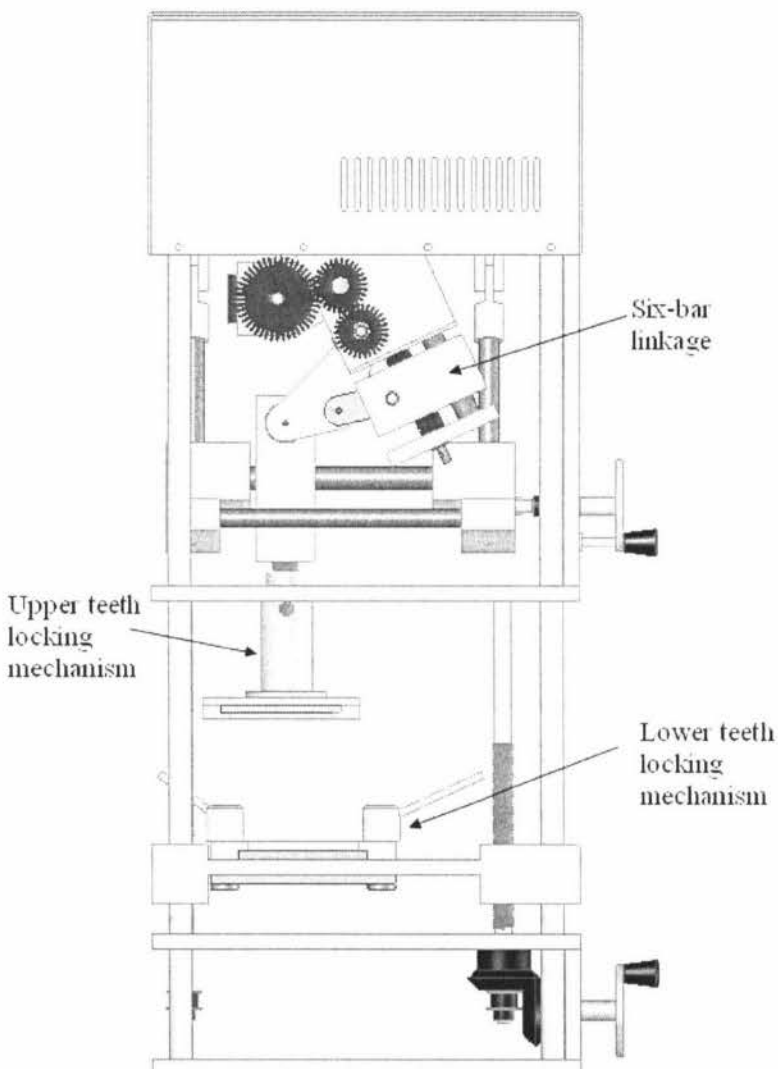

Figure 5-9 The enclosure showing the location of the six-bar linkage and the teeth locking mechanisms

5.5 Teeth, food retention and repositioning

5.5.1 The teeth

In the human mastication system only the pre-molars and molars are used for mastication, therefore these are the only teeth that need to be included in the chewing device. Mastication also only occurs on one side of the mouth at a time, therefore only one set of pre-molars and molars need to be included in the chewing device. As anatomically correct teeth need to be used it was decided to use some from a dentistry study model (Nissin dental model D85-TRM.300). These teeth are made out of a hard durable plastic but they will wear out faster than ceramic coated plastic teeth which are used in dentistry. The straight plastic teeth were chosen due to the fact that this is a prototype and can be replaced in the future if the chewing device is successful. The study model used plastic moulds of the top and bottom of the mouth to locate the teeth in the correct positions. However there were doubts about whether the plastic moulds were strong enough to handle the 150N maximum chewing forces that the chewing device can apply. Therefore these moulds were reconstructed out of epoxy resin. This was done by taking a mould of the upper and lower mouth of the study model out of plaster and using it to make the epoxy resin moulds. The plaster moulds were originally taken as a one piece mould where the study models upper and lower mouths moulds were submerged in plaster. However the plaster moulds could not be removed from the study model with out destroying the part of the moulds that corresponded to the locating holes for the teeth. Therefore the plaster mould was taken as a two piece mould. This involved taking plaster moulds of the locating holes for the teeth and ensuring that they could be remove intact. They were then placed back into the teeth locating holes and submerged in plaster to mould the mouth. The plaster moulds for the upper and lower jaws can be seen in Figure 5-10. This plaster mould was then submerged in epoxy resin to create the resin mould of the upper and lower mouth sections. The teeth were then inserted into place and glued in. The final resin mould of the upper jaw with the teeth in place can be seen in Figure 5-11.

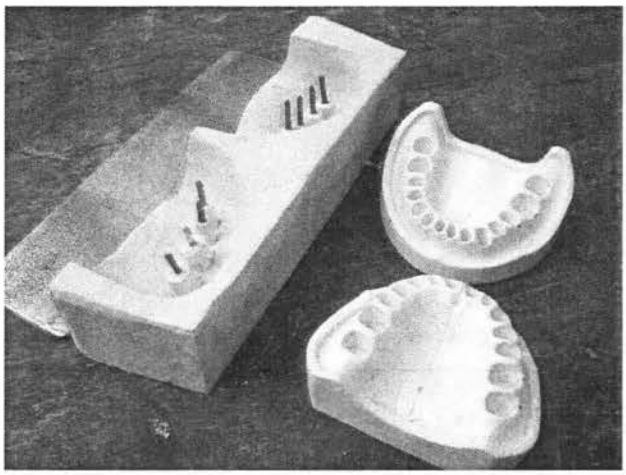

Figure 5-10 The plaster moulds of the upper and lower jaws

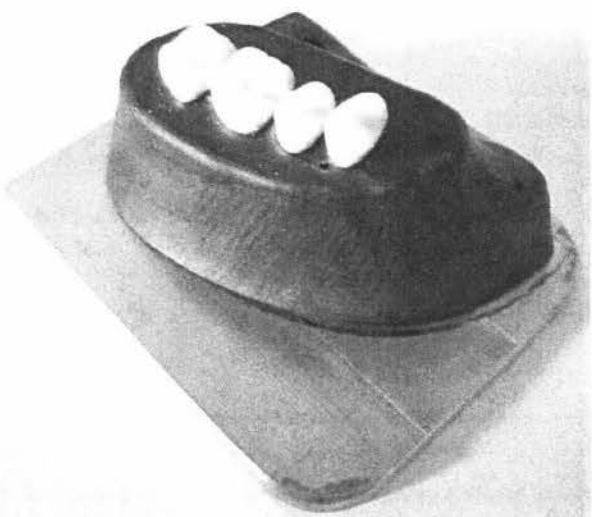

Figure 5-11 The final resin mould of the upper jaw with the teeth in place

5.5.2 The food retention system

The system to retain the food sample and keep it located on the teeth is a rather simple design. It uses silicon flaps around the lower set of teeth to retain the food as shown in Figure 5-12. This simulates the retention function of the tongue and cheek. The silicon material used is food safe so that it does not affect the food sample. Although this system retains the food sample with only a minimal amount of particles falling out of the enclosure, a lot of the food sample gets stuck on the top set of teeth.

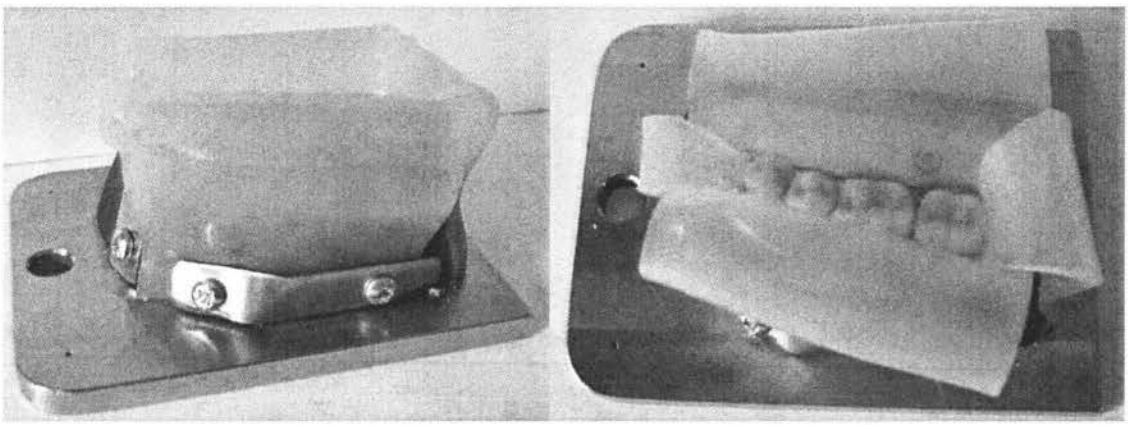

Figure 5-12 The food retention system

5.5.3 The food repositioning system

In the human masticatory system the tongue and cheek keep the food retained in the mouth and positioned on the teeth. They also reposition the food particles between the occlusal phases of each chewing cycle so that the larger particles get broken up by the pre-molars and the smaller particles get ground down by the molars. This repositioning function that the tongue performs is very complex and difficult to simulate by the use of an automated system. Therefore the repositioning function was chosen to be performed by the human operator for the time being. This will be done by running the device for a set amount of cycles with the food sample on the pre-molars, stopping it and positioning the food on the molars and then running it again. This repositioning function that the tongue and cheek perform however is very important in the human mastication system. This is due to the fact that it places the food particles on the correct teeth at the beginning of every chewing cycle which ensures that every particle is sufficiently broken down. This will not be achievable by the human operator and therefore can be the focus of future work.

5.6 Construction

All of the mechanical design for the chewing device and all of its components had now been developed and can be seen in Figure 5-13 to Figure 5-17. Technical drawings (as seen in appendix B) of all of the supporting designs and there component were then made and given to the Massey University Institute of Technology and Engineering workshop. The workshop constructed the components to specification and assembled

the chewing device which can be seen in Figure 5-18. The chewing device was now ready to be controlled.

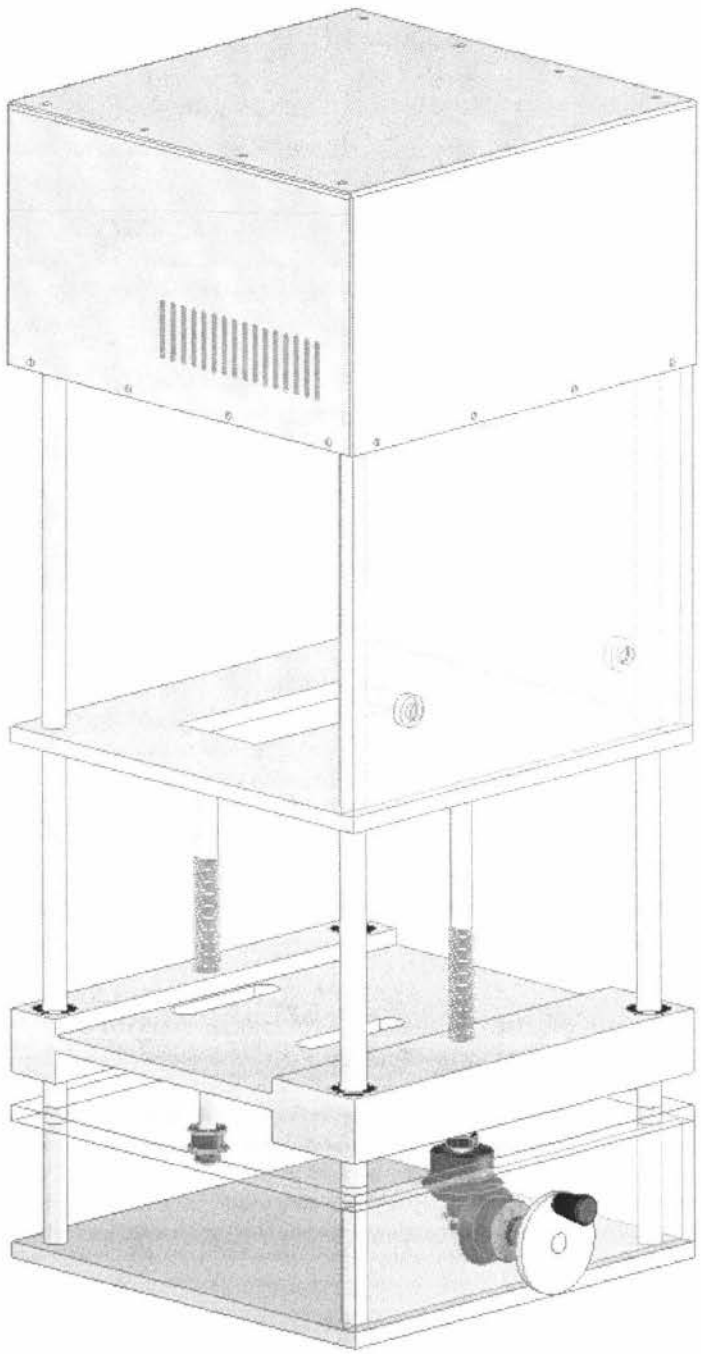

Figure 5-13 The chewing device enclosure

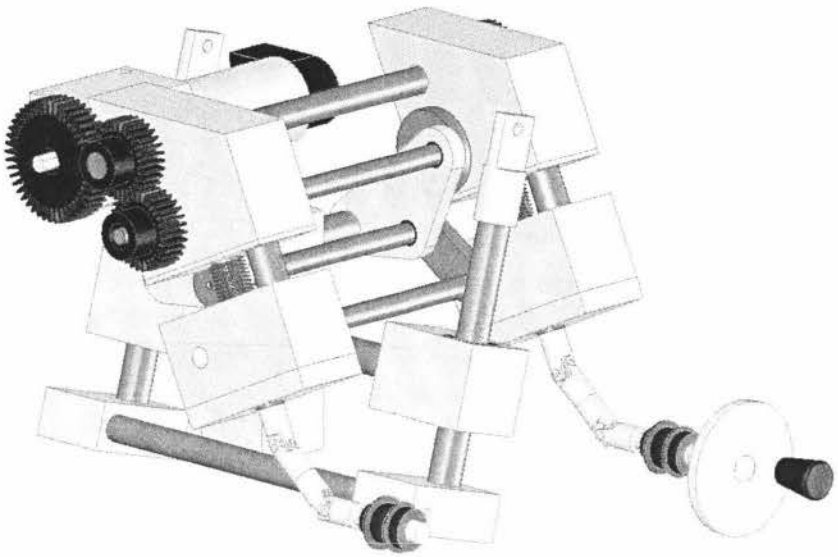

Figure 5-14 The six-bar linkage

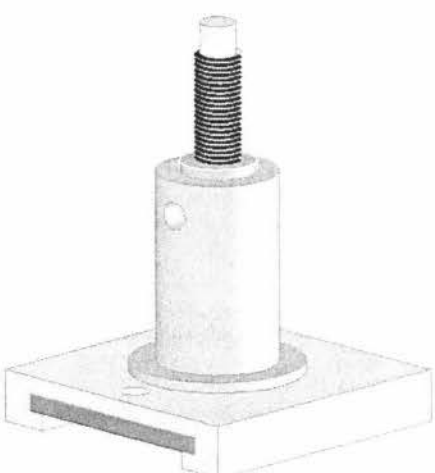

Figure 5-15 The upper teeth locking mechanism

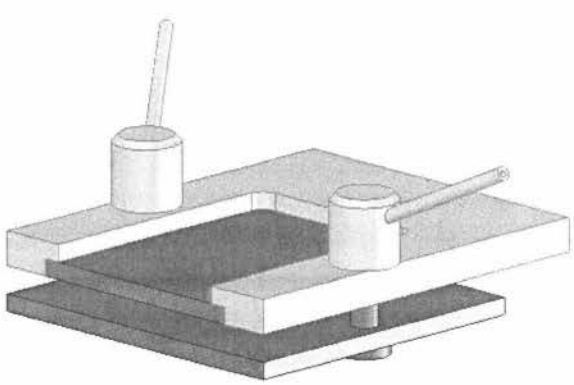

Figure 5-16 The lower teeth locking mechanism

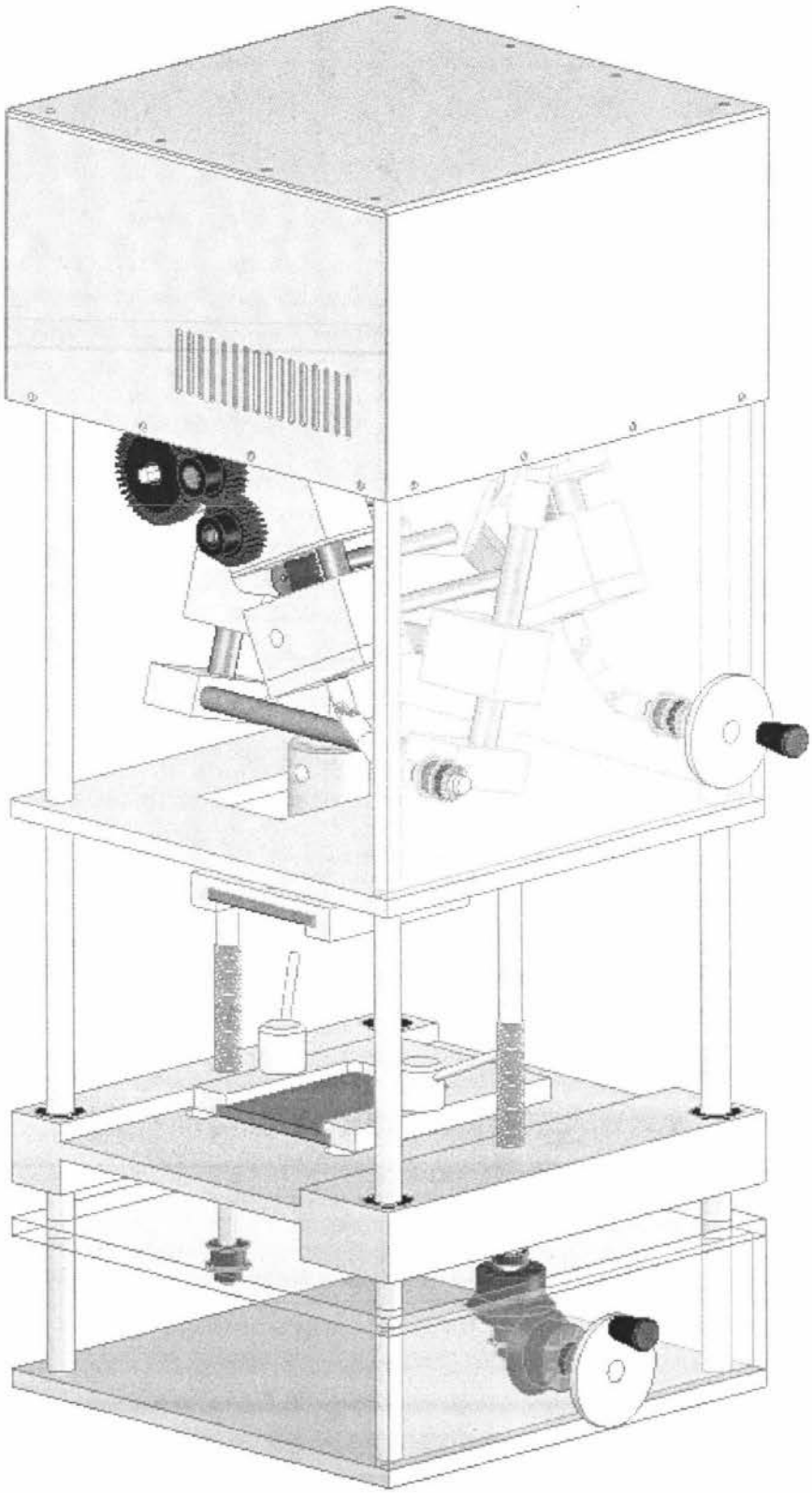

Figure 5-17 The final assembled SolidWorks model of the chewing device

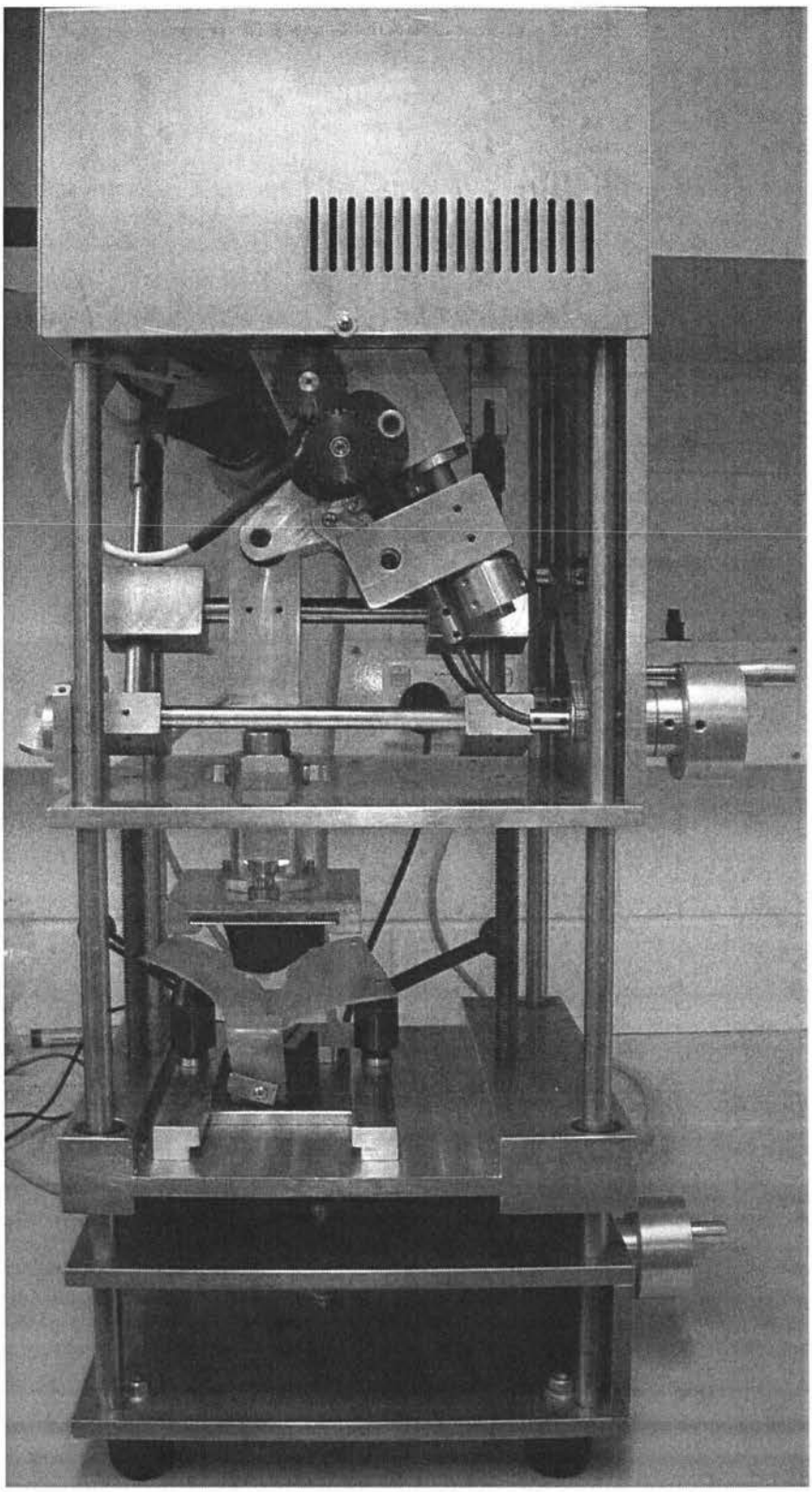

Figure 5-18 The constructed chewing device

5.7 Conclusions

The six–bar linkage was extended to include anatomical teeth, easy teeth attachment mechanisms and made adjustable. The assembly incorporated a simple food retention mechanism which allowed practical food chewing simulations to be performed. The food repositioning capability of the tongue and cheeks were not included because of the complexity that would be required for such a system. Instead it is intended that manual repositioning would be performed by the operator regularly though the chewing cycle.

The design of the enclosure that houses the mechanical sub systems could have in fact been constructed so that the six-bar linkage was located on the bottom. This would mean that the lower set of teeth would be actuated. This is due to the fact that the food particles do not move around as much as thought. Therefore the food retention mechanism would have to be attached to the actuated set of teeth. However the inverted design does have the help of gravity to applied higher forces more easily.

The teeth used for the chewing device are anatomically correct but they are not as hard as teeth. Therefore this may cause them to wear out quickly. They are also not positioned exactly in relation to each other. This is due to the fact that the mould made to hold the individual teeth was taken from a study model that's complex shape could not be easily replicated. However the teeth do occlude well enough for effective chewing.

The mechanisms used to locate and lock the teeth into position work very well. They allow the teeth to be lined up and the lower enclosure to be locked into position. The teeth can then be removed by removing the locating pins and sliding the teeth out. This allows for the teeth to be removed and inserted without needing to set up the teeth so that they occlude correctly every time.

The shock absorber used can provide forces that are approximately the same as in the human mastication system. However as the shock absorber used has a large damping co-efficient, the maximum force that is applied occurs upon impact as the shock absorber is moving at a greater velocity at this point compared to any other point during occlusion. Therefore it would be a good idea to have a shock absorber that is based on the spring, so that the force depends on the compression of the shock rather than the

velocity. This would then applied the maximum force at the maximum intercuspal position rather than at impact.

The food retention system ensures that the food is positioned on the teeth while chewing. But it makes the teeth difficult to clean as the retention system can not be easily removed. It also makes it difficult to set the lower teeth so that they occlude with the upper teeth correctly. This is due to the fact that the teeth can not be easily seen as they are covered by the silicon flaps of the food retention system. This all means that it would be a good idea to revise the food retention system so that it can easily be removed to allow for the positioning of the lower teeth and also the cleaning of the teeth.

There is currently no automated solution to reposition the food particles onto the correct teeth. This will have to be done by the operator by moving the food particles onto the correct teeth. This does however rely on the operator's judgment and therefore may cause different results from sample to sample. It also means that the chewing device is not as efficient as the human masticatory system, as the food particles are not placed on the correct teeth at the beginning of every cycle. This could be the focus of future work.

6 Control

6.1 Introduction

Because the chewing cycle time and occlusal time vary between people and foods being chewed, the motor in the device required control. This control was implemented in National Instruments 'Labview' programming language to allow flexibility in subsequent prototypes.

Labview is a programming language developed by National Instruments and like any programming language it has advantages in certain aspects and disadvantage in others. Labview is a high level graphical programming language rather than a text based one. This means that the programmes written in Labview tend not to run as fast as programs written in a lower level language. However it has the advantage of being easy to programme with as the code can be debugged by looking at icons and pictures rather than having to read through text. For the application of controlling the chewing device Labview is suitable as it will only be used as a supervisory controller as the control of the motor will have to be done by a dedicated controller in the form of a micro-controller or suitable control card. This is due to the fact that Windows is not a real-time operating system. This means that if the motor control was done directly from the computer, the motor may not do what it is expected to. This is because Windows may go and perform another action while the motor needs to be controlled.

6.2 Computer/motor interface

6.2.1 The control card

A dedicated control card was chosen rather than the other options as it is an 'off the shelf' solution. This meant that it would be reliable and it also saved time by not having to write software for it.

As the device was to be controlled from a Labview program it made sense to choose a control card that could easily interfaced with Labview. Originally a Galil motion control system was to be used as there was access to one to develop the system. This also

can be interfaced with Labview simply. After investigating a few different options it was decided to select a Maxon control card which was more cost effective for a standalone device being developed. The Maxon DES 50/5 control card was a perfect choice for the chewing device because it was designed to control the Maxon EC 32 motor the chewing deviceutilises. This also comes with Labview programming examples and is inexpensive compared to other similar systems.

The DES 50/5 control card instructions stated that the card requires an encoder with a line driver to run. Therefore an encoder was to be purchased. After searching many different suppliers it was found that the encoder that is recommended for the motor was either available with the mounting plate and no line driver, or with the line driver and no mounting plate. So an encoder with a mounting plate and no line driver was ordered as well as a line driver chip to construct a line driver circuit. Before the line driver circuit was constructed the encoder was mounted onto the motor and tested without the line driver circuit. The idea behind this was that line drivers are used to eliminate noise when transmitting signals over large distances, and as we are only transmitting over a short distance it may not be required. Line drivers work by sending the desired signal as well as the inverse of this signal and are then decoded at the final destination to check if there is any error. In this case there are three channels coming off the encoder so these three signal lines were wired into the control card. Then the card was then plugged into the computer and the control program that the control card came with was started up. It was found that the motor did not move. This means that the control card expects the signals from the encoder as well as the inverted signals. Therefore a line driver was required. This however was pretty much expected and is why a line driver chip was ordered the same time as the encoder.

6.2.2 The line driver circuit

The line driver circuit was based around the DS26LS31CM surface mount line driver chip. This is the line driver chip that the control card is expecting to get a signal from, so there are no compatibility issues. The only other addition to this chip is a decoupling capacitor to provide a more smooth power supply and some connectors. This can be seen in Figure 6-1.

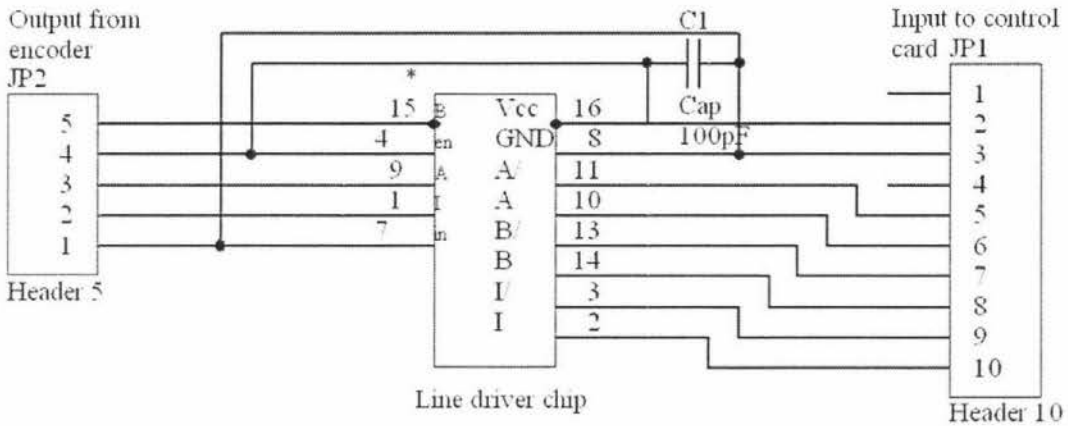

Figure 6-1 The line driver circuit showing the line driver chip in the centre and the connectors on either side.

The circuit board was designed to be as small as the Massey University facilities would allow. This was to make the circuit board fit inside the encoder housing where it would normally be positioned if the encoder included a line driver. The circuit board layout can be seen in Figure 6-2.

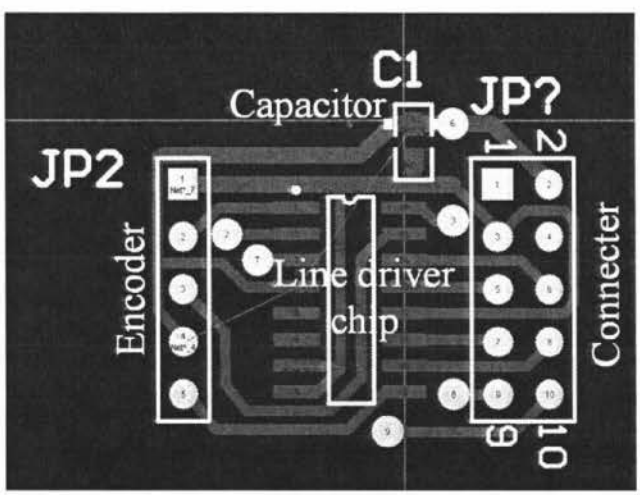

Figure 6-2 The circuit board design (Board dimensions 22x15mm)

6.2.3 Computer I/O

The communication between the control card and the computer based software was done via a RS-232 serial interface. Therefore the computer based software had to be made to access the appropriate transmit and receive registers. This proved to be a very simple task as there was an example program written in Labview provided with the

control card that was used as a template for the final software package. This example program had all the communications programming done including initialisation and error handling. This meant that only the code for the operation of the control card had to be changed to include all the necessary functions for the chewing device.

6.3 The software functions

For the chewing device to function in a way that the human operation would be satisfied with, it was important to try to include all the functions that would be necessary for simple operation. The functions that were included in the chewing device are as follows:

- ***Set to lower position*** – this function sets the chewing device to the occlusal position so that the teeth can be aligned when setting up the device.
- ***Set to top position*** – this function sets the chewing device to the position where the teeth are maximum distance apart so that a food sample can be placed in it. This can be thought of as the mouth being open.
- ***Start chewing*** – this will be used to make the device chew by making the device follow a velocity profile that matches that of a human chewing velocity profile. The number of chews will also be able to be set for repeatability.
- ***Single cycle*** – this function will be used as a quick select 'one chew' button and will only perform one chewing cycle.
- ***Low speed manual control*** – the user will be able to use this control to make the chewing device move at a slow speed to check the occlusion once the teeth have first been set up.
- ***Master stop*** – this will be used as a safety feature that allows the user to stop it at any time during any function.

The software functions can be seen on the graphical user interface shown in Figure 6-3.

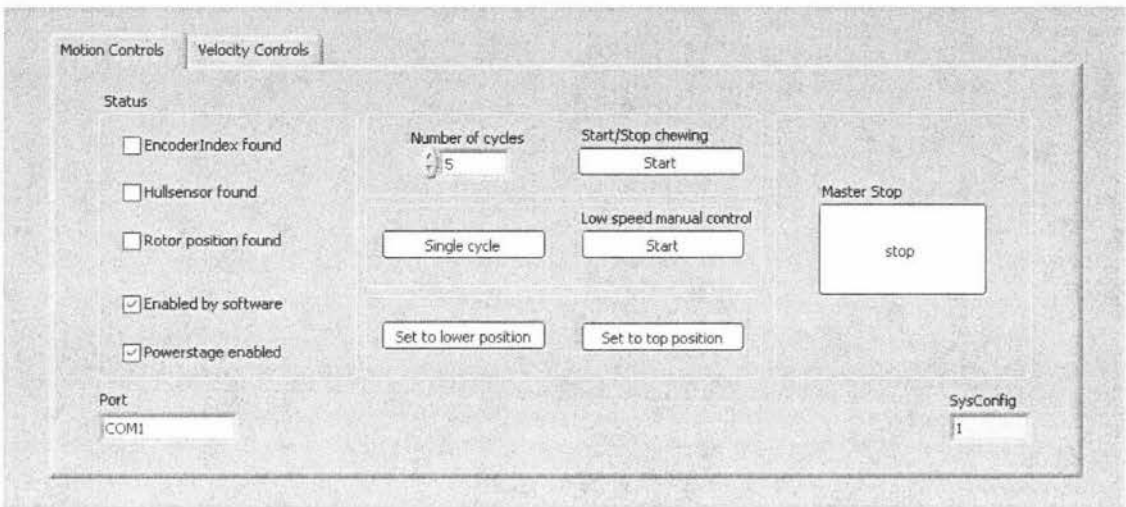

Figure 6-3 The software functions on the GUI

6.3.1 Set to lower position

To be able to set the chewing device to the lower position where the teeth occlude, a reference point on the crank that corresponds to the lower position needs to be known. It was originally thought that the position could be determined by the encoder on the motor. This idea would have involved counting the pulses of the encoder to do this. However there would have to be a known start position. But the pulses that the encoder provides to control card to determine the speed were not able to be accessed from the control card. Only the speed of the motor in RPM could be measured, therefore the positioning of the motor had to be done another way. As only the lower and top positions need to be detected, this was done by using Hall Effect sensors and a small magnet mounted on one of the gears. This system is a very robust way of detecting the two required positions compared to counting the encoder pulses and also much more simple. The pulses that the Hall Effect sensors provide are easily detected due to the fact that the gear that the magnet is mounted on is only turning relatively slow at a maximum speed of 100 rpm. This corresponds to one pulse every 0.6 of a second on each sensor.

The Hall Effect sensors then had to be mounted somehow. The simplest way of doing this was to make a circuit board in the shape of a ring that includes all the supporting circuitry that can have the gear positioned inside of it. To keep the design as small as possible surface mount resistors and capacitors were used. The circuit consisted of two Hall Effect sensors with a resistor connecting the output of the sensor to the five Volt

VCC rail, a couple of decoupling capacitors and a couple of connectors for the power and signals. The resistors are required in these locations due to the fact that Hall Effect sensors being used are of the open collector design. The circuit design can be seen in Figure 6-4.

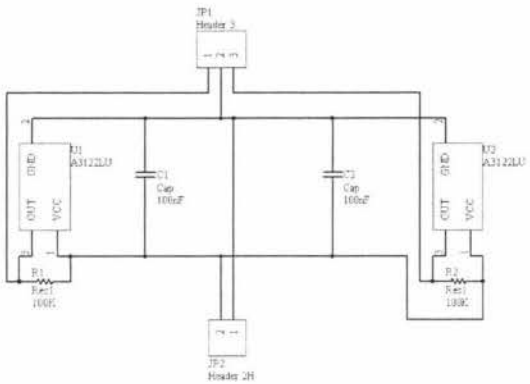

Figure 6-4 The Hall Effect sensing circuit

The circuit board was chosen to be a dual layer board to make it tidy as there are no jumper wires. The design of the circuit board can be seen below where the blue inside circle is a copper track that is connected to ground and the outside one is connected to +5 Volts. The red lines are tracks for the output signals of the sensors which are on the top layer of the board as seen in Figure 6-5.

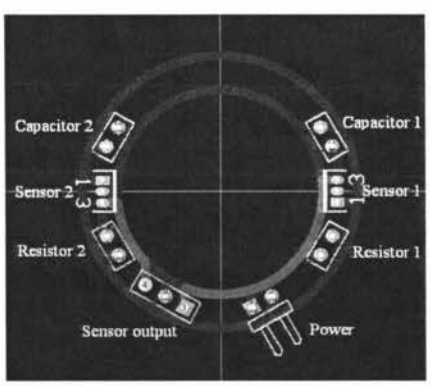

Figure 6-5 The Hall Effect circuit board

The output from this sensing board provides a +5 Volt output when the magnet on the gear is not positioned at the sensor locations and a 0 Volt output on one of the output lines when the magnet is positioned over the corresponding sensor. This information then has to be passed on to the control program on the computer. Since the RS-232 serial interface is already been used by the control card, the next most obvious port to

use is the parallel port. This then meant that a Labview program had to be developed to read the position information provided by the Hall Effect sensing board. An example program of how to do this was found in the Labview example directory. This code was examined and modified to better suit what was required. An example of how this was done in the software can be seen in Figure 6-6.

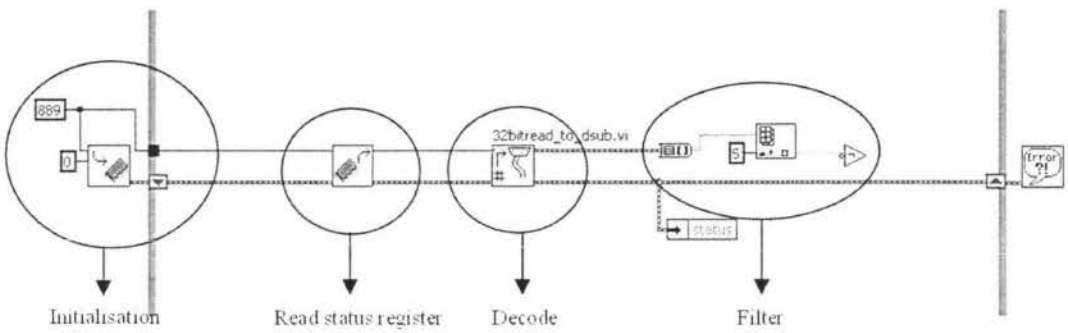

Figure 6-6 Example of accessing the parallel port in Labview

The first part of this code initialises the parallel port by writing '0' into the status register which has the address 889 in decimal. The status register is then read and decoded so that the input corresponds with the pin numbering on the I/O connector. This is necessary as the data stored in memory is arranged differently to how it is entered through the I/O connector. The data is then filtered to look at the specified pin that the Hall Effect sensor is plugged into. In this case the pin that the sensor is plugged into corresponds to number five. The status of the Hall Effect sensor is then inverted due to the fact that 0 Volts corresponds with the sensor being turned on which makes it easier to think about. There is also an error detector so that the program can be stopped if an error occurs. The signal from the Hall Effect sensor can now be detected in software and can be used to turn things on and off for example.

Once the system was fully operational the Hall Effect sensing board was fixed in place and the magnet was positioned so that it is located over a sensor when the chewing device is in the lowest occlusal position. The system could then rotate until a signal from the 'lower-position' Hall Effect sensor is detected and then stop.

6.3.2 Set to top position

The 'set to top position' function was written at the same time as the 'set to lower position' function. The only difference is in the software when in the filtering phase. The software in this case looks at the sensor corresponding to the top position which is plugged into a different pin on the parallel port I/O connector. Therefore the device stops when it is at the 'top' position.

6.3.3 Start chewing

The 'start chewing' function was the most complicated of the functions that had to be developed. It involved making the chewing device perform the number of chewing cycles specified by the user and follow a velocity profile. The velocity profile that the chewing device must follow did not need to be exactly the same as that of a human in all cases. It only needed to perform occlusion the same as a human and get back to the occlusal position in the same time as what a human does. This is due to the fact that the four-bar linkage system is designed to closely match the occlusion of a human. It does not matter what trajectory it has in the opening and closing phases as no chewing occurs here.

The operation of the 'start chewing' function works by firstly moving the actuator at the occlusal velocity until it reaches the 'lower position' which is in the middle point of occlusion. It then moves for a specified amount of time to reach the position where occlusion ends as seen in Figure 6-7 A. The chewing device then speeds up from occlusal velocity to a maximum velocity and back down to occlusal velocity in a specified time as seen in Figure 6-7 B. This allows the correct angle of the motor to be turned to return it to the start position. Therefore the chewing devices actuator returns back to the position where occlusion first occurs in the correct amount of time. This process is repeated for the number of times that the user specifies. The chewing devices actuator then returns to the 'top position' so the food sample can be removed as seen in Figure 6-7 C.

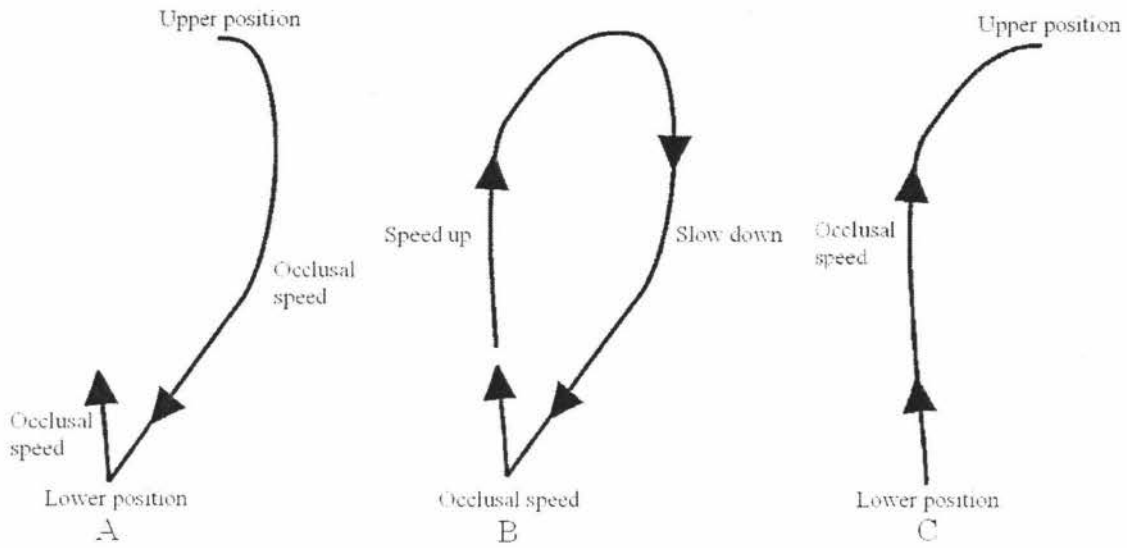

Figure 6-7 The general velocity profile of the chewing device

The velocity profile was calculated using a cubic trajectory planning technique (Craig, 1989). This requires the start angle, finish angle, start velocity, finish velocity and time taken to be known. For these values to be determined first of all the occlusion point had to be specified on the trajectory plots that where generated by the SolidWorks model that has been shown throughout chapters 4 and 5. This was done by defining the occlusal phase as being 0.5mm from the maximum intercuspal position as stated by Ogawa (2001) and can be seen in Figure 6-8. Where the maximum intercuspal position is the position in the middle of the occlusal phase where the 'lower position' is located. From here it can be seen that there are eight points plotted on the graph in the occlusal phase. As each point corresponds to the crank shaft rotating 4.5 degrees the occlusal phase is represented by a 36 degree turn of the crankshaft. The time to complete this occlusal phase is taken at 0.12s as specified by Ogawa (2001). Now that an angle and a time are specified the occlusal velocity can be calculated.

36 degrees in 0.12 of a second	= 360 degrees every 1.2 seconds
	= 0.83 revolutions per second
	= 50rpm of the crank
Occlusal velocity	= 2100rpm (1:42 gear ratio)

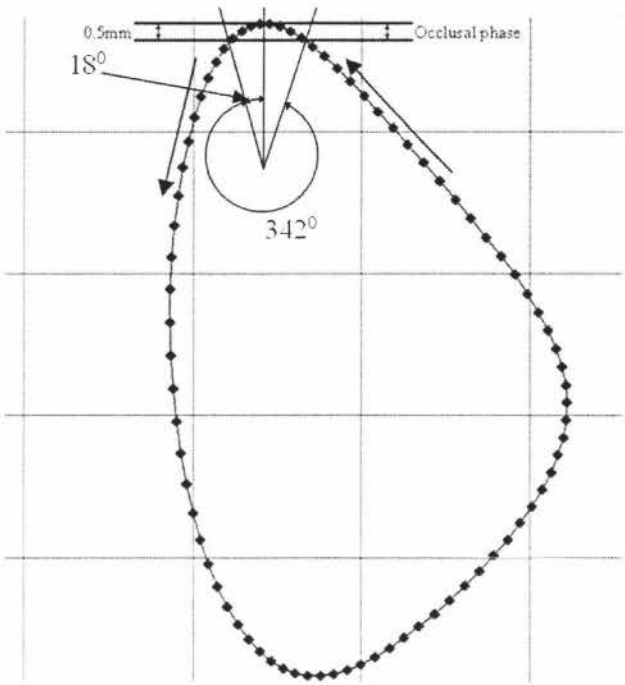

Figure 6-8 The occlusal phase definition

The start angle for the trajectory planning cubic was set at 18 degrees. This is because we want the motor to speed up when the occlusion phase ends, which in this case is 18 degrees from the maximum intercuspal position. The final angle is set at the point where occlusion begins again which in this case is 342 degrees. However these angles are measured from the crank shaft and have to be converted to angles relative to the motor. This is due to the fact that the motor is what is being controlled. As there is a 1:42 gear reduction between the motor and the crank the start angle is 756 degrees and the final angle is 14364 degrees. The time taken to get between these points is 0.65 of a second as stated by Ogawa (2001) which is the opening and closing times of the mouth combined. As the angles are measured in degrees and the times are measured in seconds the occlusal velocity has to be converted from a revolutions per minute value to a degrees per second value. Therefore the occlusal velocity is 12600 degrees per second. These values can then be substituted into the cubic trajectory planning formulas below taken from Craig (1989).

$$a_0 = \text{start angle} \tag{6.1}$$

$$a_1 = \text{start velocity} \tag{6.2}$$

$$a_2 = \frac{3}{\text{time}^2}(\text{final angle} - \text{start angle}) - \frac{2}{\text{time}}\text{start velocity} - \frac{1}{\text{time}}\text{final velocity} \tag{6.3}$$

$$a_3 = -\frac{2}{\text{time}^3}(\text{final angle} - \text{start angle}) + \frac{1}{\text{time}^2}(\text{final velocity} + \text{start velocity}) \quad (6.4)$$

This gives the results

$a_0 = 756$

$a_1 = 12600$

$a_2 = 38471$

$a_3 = -39457$

These are then substituted into the following (taken from Craig, 1989):

$$displacement(t) = a_0 + a_1 t + a_2 t^2 + a_3 t^3 \quad (6.5)$$

$$velocity(t) = a_1 + 2a_2 t + 3a_3 t^2 \quad (6.6)$$

$$acceleration(t) = 2a_2 + 6a_3 t \quad (6.7)$$

Giving:

$$displacement(t) = 756 + 12600t + 38471t^2 - 39457t^3 \quad (6.8)$$

$$velocity(t) = 12600 + 76942t - 118371t^2 \quad (6.9)$$

$$acceleration(t) = 76942 - 236742t \quad (6.10)$$

These equations can then be plotted over the range of 0 to 0.65 second to produce the following plots seen in Figure 6-9, Figure 6-10 and Figure 6-11.

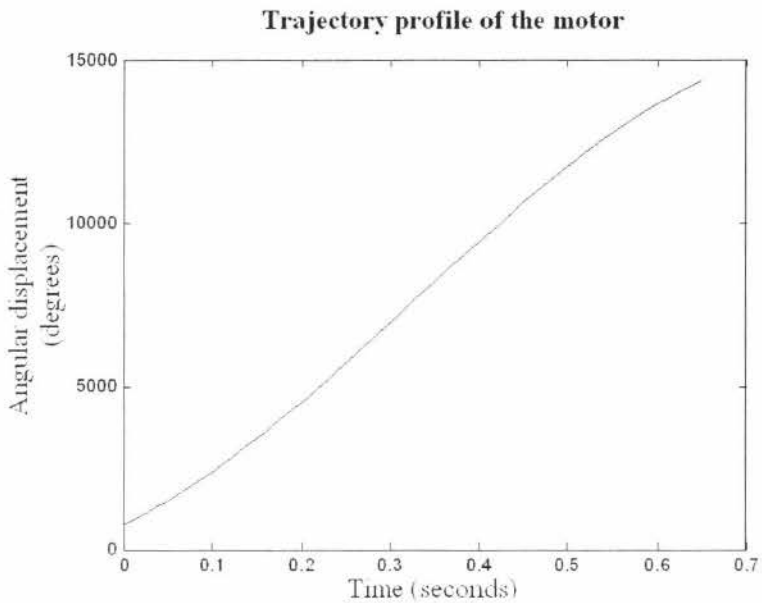

Figure 6-9 The trajectory profile

This plot of the trajectory profile shows that the motor moves from 756 degrees to 14364 degrees in 0.65 of a second which is what is required.

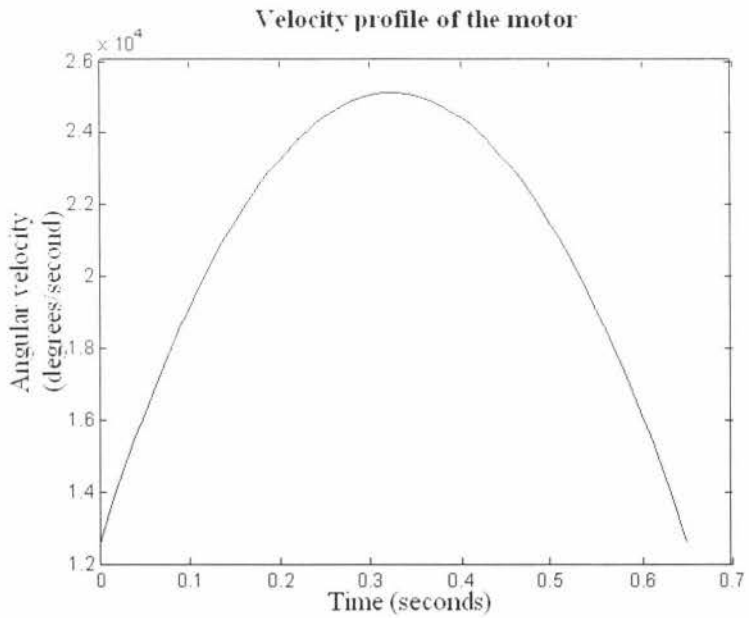

Figure 6-10 The velocity profile

This plot of the velocity profile shows that the velocity is sped up and then back down in a symmetric fashion. It shows that the velocity starts at the desired 12600 degrees per second and also ends at this velocity. The maximum velocity can be seen to be at 0.325 of a second into the velocity profile. This corresponds to a maximum velocity of

25103 degrees per second which equals 4184 rpm of the motor. This is below the maximum speed of the motor which is 8000 rpm through the gear box. After this the motor is driven at the occlusal speed for 0.12 of a second which then make the cycle time 0.77 seconds.

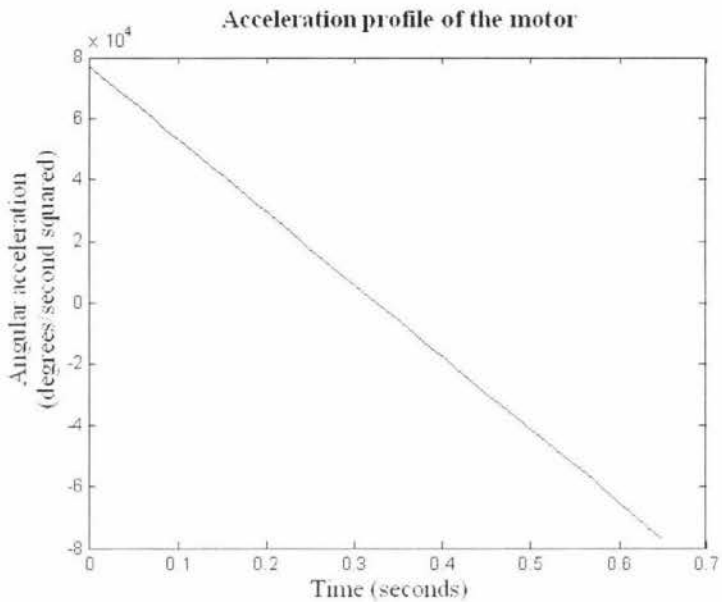

Figure 6-11 The acceleration profile

The graph shows that there is a maximum acceleration of 80000 degrees per second squared. This corresponds to an acceleration of 190 degrees per second squared at the crank which is below the maximum acceleration that can be achieved.

These plots show that the chewing device can achieve the desired motion. Therefore the velocity profile can be included into the software.

The operator of the chewing device may wish to chew foods differently. Therefore the device has to allow different velocity profiles. Therefore controls were added to allow the user to change the velocity profile by changing the parameters for the velocity profile equation. These control parameters include:

- ***Occlusal time*** – This specifies the time that the occlusal phase is to take.
- ***Opening/closing time*** – This specifies the time that it takes to return to the start of the occlusal phase.

- ***Occlusal angle*** – This specifies the point where the user wants the occlusion to begin and also the duration of occlusion. This is done by taking the value that the user enters and placing the point where occlusion begins at being half this value before the maximum intercuspal position. The point where occlusion finishes is half the value that the user enters after the maximum intercuspal position. This can be seen in Figure 6-12.

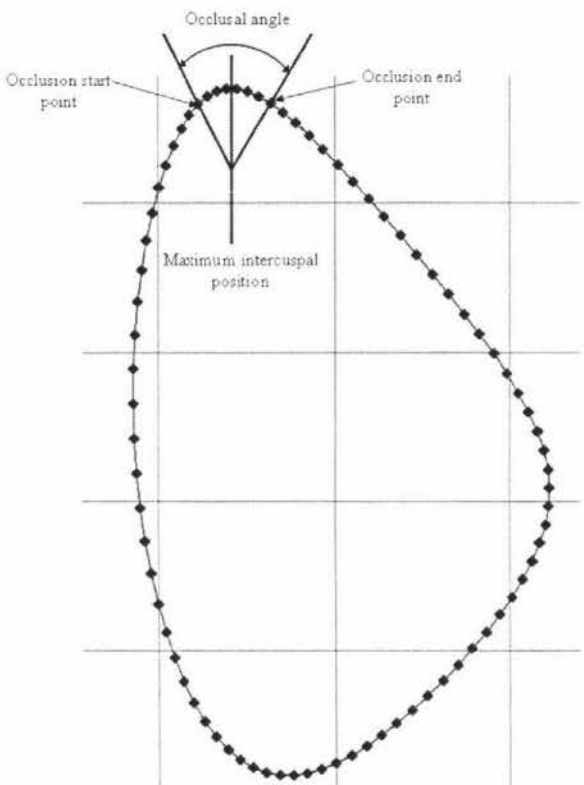

Figure 6-12 The occlusal angle

These controls are then linked to the velocity profile equation in the software. This is done by using the 'occlusal time', 'opening/closing time' and 'occlusal angle' inputs to configure the a_1, a_2 and a_3 parameters of the velocity profile equation. This can be seen in the following equations:

Start velocity

$$\dot{\theta}_0 = \frac{42 * \text{occlusal angle}}{\text{occlusal time}} \qquad (6.11)$$

Final velocity

$$\dot{\theta}_f = \dot{\theta}_0 = \frac{42 * \text{occlusal angle}}{\text{occlusal time}} \tag{6.12}$$

Start angle

$$\theta_0 = 21 * \text{occlusal angle} \tag{6.13}$$

Final angle

$$\theta_f = 15120 - 21 * \text{occlusal angle} \tag{6.14}$$

These function are then substituted into the a_1, a_2 and a_3 parameters

$$a_1 = \dot{\theta}_0 \tag{6.15}$$

$$a_2 = \frac{3}{\text{open/close time}^2}(\theta_f - \theta_0) - \frac{2}{\text{open/close time}}\dot{\theta}_0 - \frac{1}{\text{open/close time}}\dot{\theta}_f \tag{6.16}$$

$$a_3 = -\frac{2}{\text{open/close time}^3}(\theta_f - \theta_0) + \frac{1}{\text{open/close time}^2}\left(\dot{\theta}_f + \dot{\theta}_0\right) \tag{6.17}$$

Then theses parameters are then substituted into the velocity profile equation taken from Craig (1989).

$$velocity(t) = a_1 + 2a_2 t + 3a_3 t^2 \tag{6.18}$$

This equation then has time values substituted into it every 0.01 of a second. The resulting velocity value is then sent to the control card to speed the motor either up or down. The velocity control menu used in the software can be seen in Figure 6-13.

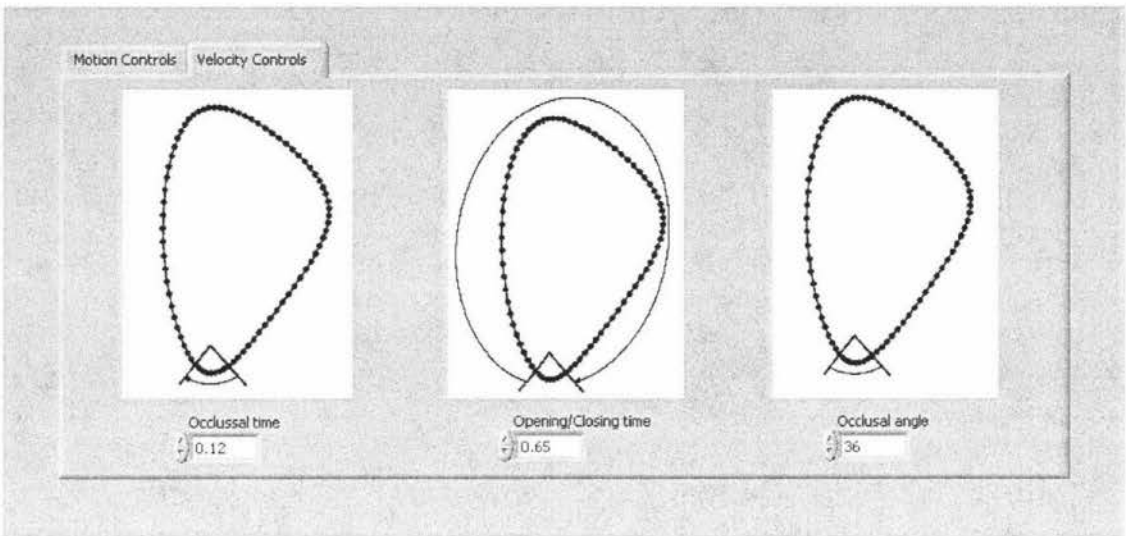

Figure 6-13 The velocity control menu

6.3.4 Single cycle

The 'single cycle' function is to perform only one chewing cycle. This makes use of the Hall Effect sensors that let the software know when one chewing cycle has been completed. As occlusion only occurs once per chewing cycle the device can be run at the occlusal velocity for the whole cycle without needing to follow a specified velocity profile. This ensures that the occlusion of the teeth is at the correct velocity to better simulate the human chewing behaviour, it is also less complicated as it does not have to dynamically change the chewing velocity. The initial acceleration of the motor is taken care of by the control card so only the occlusal velocity has to be specified in this case. The final deceleration of the motor is also taken care of by the control card by putting the motor into a 'brake state' when the software tells it to stop. The basic code for this function can be seen in Figure 6-14.

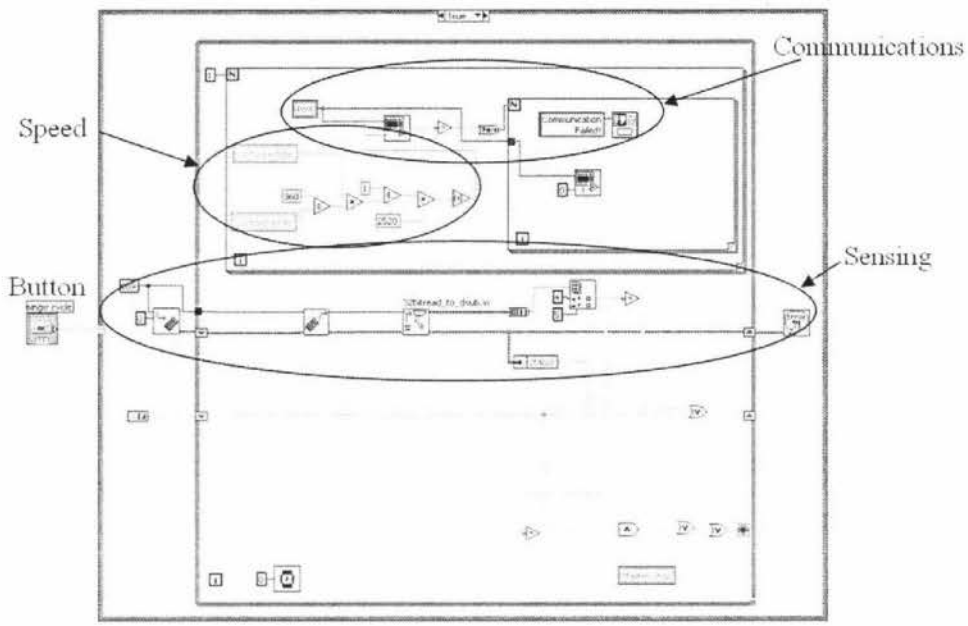

Figure 6-14 The 'single cycle' Labview code

The 'single cycle' function works by detecting when the 'single cycle' button has been pushed by the user. When it is pushed it firstly determines what speed the user wants the occlusion at by checking the 'occlusal time' and 'occlusal angle' parameters that can be specified in the velocity control menu and calculates the occlusal speed. This is then sent to the control card. The status of the Hall Effect sensors is then polled to check the location of the actuator of the chewing device. When the actuator has gone past the 'lower position' sensor it will then stop when it next reaches the 'top position'. There is also a function that detects whether there is active communication between the software and the control card and displays the message 'Communication Failed!' when there is not.

6.3.5 Low speed manual control

This function allows the user to manually control the chewing device at low speeds. This function does not use the Hall Effect sensors at all as it is not automated. Therefore the code for this function is very basic and can be seen in Figure 6-15.

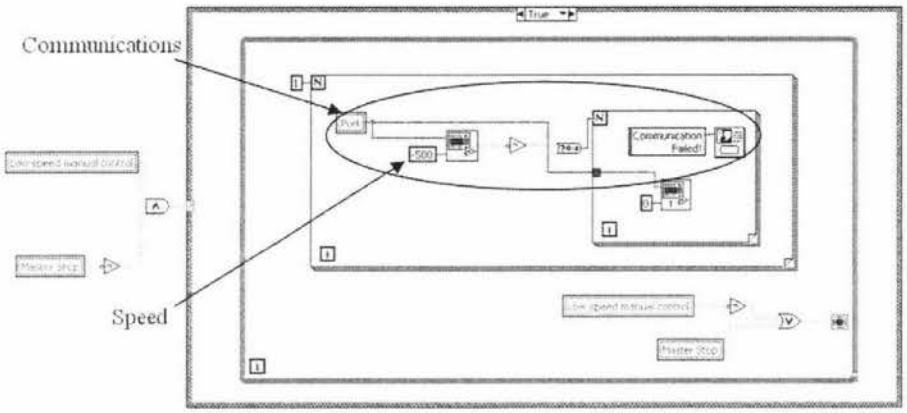

Figure 6-15 The 'low speed manual control' function

The 'low speed manual control' function is activated when its button is pushed. It then passes the velocity value of 500 rpm to the control card. This corresponds to the chewing device performing one chew every five seconds. The function can be stopped by the user by pressing the 'low speed manual control' button again. Once again the status of the communications is also monitored and displays the message 'Communication Failed!' when there is no communication between the software and the control card.

6.3.6 Master stop

The master stop function stops the chewing device no matter what function it is currently performing. It does this by being linked to the stop condition of each function. If the 'master stop' button is pressed it stops the function that it is currently in and enters the 'master stop' function where the velocity of the motor is set to zero. This can be seen in Figure 6-16.

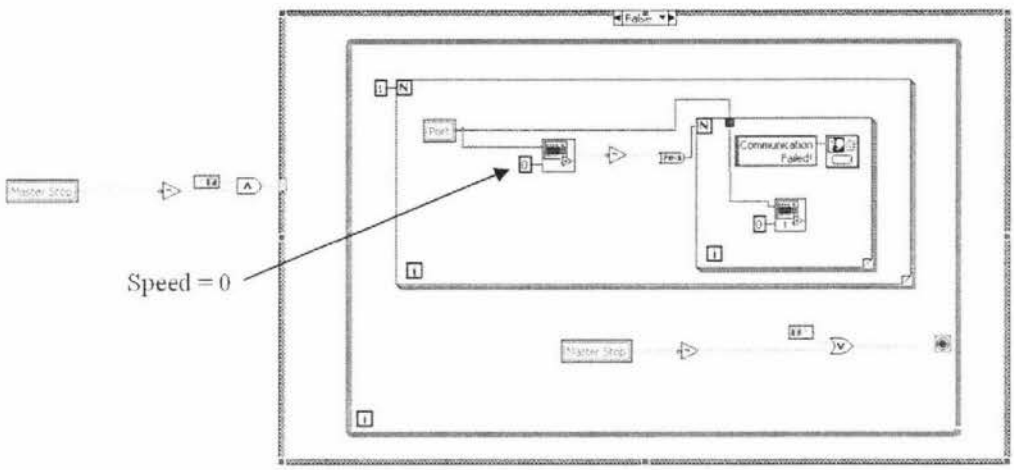

Figure 6-16 The 'master stop' function

6.4 Conclusions

The control of the system functions well and provides the user all the necessary functions to run the chewing device. This is achieved by all the control sub systems doing there job correctly.

The control of the motor allows the desired velocity profiles for chewing to be achieved. Therefore the chewing device will better simulate the mastication system of a human. However as the computer as continuously sends velocities to the control card there is still the possibility for the computer to stop sending the velocity commands. This means that a velocity step may be missed and cause the control card to output the previous velocity for a longer period of time. Therefore the velocity profile may not be as exact as it could be. This however is not noticeable from simple testing of timing it over a large number of cycles and comparing the cycle time to the desired cycle time.

The functions included to run the chewing device are simple and straightforward to use. They include all the operations that were thought could be useful to the operator. The operator also has access to some advanced functions to change the velocity profiles of the chewing device if it is required.

The Hall Effect sensors used to detect when the teeth are at the occlusal position and the open position work well. They perform the task accurately and consistently. They are interfaced to the Labview program through the parallel port. This port can be used

to provide many digital inputs. Therefore additional sensors can be added at a later stage if required.

The line driver circuit made to interface the encoder and therefore the motor to the control card is small enough to be concealed in the encoder housing. This circuit allows the control card to control the motor and does not work without it as it requires a line driven signal. The encoder itself helps the control card to precisely control the motor as it has a 500 pulse per revolution resolution.

7 Conclusions and future work

The chewing device appears to function correctly to the eye. This is due to the fact that it chews food that is inserted between the teeth by following approximate chewing trajectories of a human. However it is not known if the masticated food sample matches the particle size distribution of a food bolus produced by a human. This testing will be carried out in the future by food technologists to more thoroughly evaluate the chewing device. Then it can be determined if the project will be suitable for standardising food testing that involves food samples being chewed.

The prototype so far can perform chewing trajectories during occlusion in the frontal and sagittal planes that closely match what a human does. The six-bar linkage that generates the chewing trajectories has a weakness in the fact that it generates some play in the mechanism that is attached to the slider. This is due to the fact that the linear bushes used for linear guidance all have a little bit of play. The play from these four linear bushes adds up and causes the noticeable play at the actuated teeth. This movement in fact helps the teeth occlude very well. This is due to the fact that this movement allows for some compliance so that if the entry and exit angles do not allow for proper occlusion the actuated teeth get guided by the fixed teeth so that proper occlusion is achieved. However this could be contributing to the fact that the chewing device can not chew foods with elastic properties very well. This was noted when a licorice sample was inserted into the device and the teeth only compressed the licorice rather than reducing the particle size. As the actuating teeth have a small movement in them, they can only work by using their cusps to fracture the food and can not work as blades very well. This can be thought of as a pair of scissors where they do not cut when there is a gap between the two blades. This movement can possibly be removed by changing the linear bushes to linear bearings. The linear bearings use ball bearings to press onto the shafts and rotate to achieve their linear motion. This means that they can be made to have less play.

The method used in the driveline to attach the spur gears to the drive shafts is also a weak point. Currently grub screws are used to press against flat section milled on the shafts. While this method works at the moment it would be a good idea to change this

to a system that uses key ways. This would be far more robust and would definitely withstand constant use.

The overall mechanical design turned out to be far more complex than originally thought. This is due to the fact that two four-bar linkages were made to make the design balanced and also stronger. This meant that the two four-bar linkages had to be kept in time with each other so that they were not counter productive. This as well as the supporting components all had to be manufactured with the exception of gears, bearings, levers etc. If the project was repeated I would suggest that the two-axis robotic system described in chapter 3 be used. This would involve fewer components needing to be constructed and would also allow any two-dimensional trajectory to be achieved within the robots workspace. This robot could then have a third actuator added to it to control the trajectories in the sagittal plane. The chewing device could then be fully controlled by software which as well as being elegant also allows for modifications in the future to be made in software and not by constructing any mechanical parts.

Although the teeth are anatomically correct they are not perfectly aligned. This is due to the fact that a mould was made out of epoxy resin rather than using the plastic study model to hold the teeth. The mould was made based on the study model to try and get the correct alignment of the teeth while having a strong supporting structure. This was made by making a mould of the study model out of plaster of paris and then using this to make the resin mould. The miss alignment problem came about due to the fact that the plaster of paris mould needed to be constructed in two parts. This was required as the plaster mould could not be made in one part due to the fact that the teeth cavities are very small and break off when trying to remove the mould. Therefore the cavities for the teeth were moulded first using a rod that goes into the cavity so that the cavity moulds can be removed from cavities. A mould in the shape of the gum was then made that positions the moulds of the teeth cavities by locating them by the rods. This two part moulding technique lead to a sight error in the alignment of the teeth. Although the teeth seem to occlude fairly well there is a difference of the alignment of the teeth when compared to the study model. This could influence the particle size distribution of the food sample that is chewed.

The teeth used in the chewing device are made out of plastic. Although it is a very hard plastic it is not a very good material to simulate human teeth. It would be a good idea to use teeth that are as close to the real thing as possible. Therefore the teeth used should be made out of substance that is used to create false teeth for humans. Some materials that are used for this include ceramics, and gold. These materials are used to cover the working surface of the teeth and therefore the plastic teeth that are currently used on the chewing device could be coated in one of these substances by a dental technician.

The control of the chewing device is currently done by sending a velocity for the motor to turn at from the computer to the control card. This system would be acceptable if the motor speed did not have to change very often. However the chewing device sends velocity commands to the control card very rapidly to achieve its desired velocity profile. While this works it is not a very good way of achieving the correct motion. This is due to the fact that there could be a delay in the sending of the command to the control card. If this was to occur the motor would turn at the previous speed sent to the control card therefore providing an incorrect velocity profile. No extensive testing has currently been done to determine if this is in fact occurring as the testing so far only involved timing the time taken to perform fifty cycles to compared the desired cycle time and the achieved cycle time. This testing showed that the chewing devices achieved cycle times were very close to that of the desired cycle times. A solution to this problem would be to develop a controller specifically for the chewing device. This would involve developing a micro-processor based circuit that would down load the velocity profile required from the computer before the chewing device starts chewing. This would mean that there would be no interruptions or delays that are possible when transmitting data between two devices. This would also mean that the chewing device would also be stand-alone and would be able to operate without the computer needing to be turned on. However at this stage it is not necessary to include such a system as the human masticatory system does not perform chewing cycles that have the same period all the time.

8 References

ACE Controls. (1996). ACE Controls, Inc. deceleration catalogue, 2005.

Anderson, D.J. (1956). "Measurement of stress in mastication." *Journal of Dental Research 41*, 175-189.

Anderson, K., Throckmorton, G.S., Buschang, P.H. & Hayasaki, H. (2002). "The effects of bolus hardness on the masticatory kinematics." *Journal of Oral Rehabilitation 29*, 689-696.

Ashby, M.F. & Jones, D.R.H. (1996). Engineering Materials, vol. 1, 2nd ED. Oxford:Butterworth Heinemann.

Charbonneau, A., Feraudet, G., Getto, L., Martin, S. & Surrel, T. (2004). "A Linkage Mechanism for Chewing Foods Design, Optimisation and Force Control," Final Year Project, Institute of Technology and Engineering, Massey University.

Craig, J.J. (1989). "Trajectory generation." in *Introduction to Robotics: Mechanics and Control*, 2nd ED. Addion-Wesley, pp.227-261.

Dawson, P.E. (1989). "Evaluation Diagnosis and Treatment of Occlusal Problems." (2nd ED, chapter 24), Mo.:Mosby, St Louis, 85-91.

Erdman,A.G., Sandor, G.N., Kota, S. (2001). "Displacement and Velocity Analysis." in Mechanism Design: Analysis and Synthesis vol. 1, 4th ED, Prentice-Hall, Inc, New Jersey, 119-232.

Every, R.F. (1970). "Sharpness of teeth in man and other primates." *Postilla 143*, 1-20.

Frank, F.C. & Lawn, B.R. (1967) "On the theory of Hertzian fracture." *Proceedings of the Royal Society London series A*, 291-316.

Gibbs, C.H., Lundeen, H.C. (1982). "Jaw Movements and Forces During Chewing and Swallowing and Their Clinical Significance." *Advances in Occlusion*, 2-32.

Gibbs, C.H., Mahan, P.E. & Lundeen, H.E., (1981). "Occlusal forces during chewing – Influences of biting strength and food consistency." *Journal of Prosthetic Dentistry 46*, 561-567.

Gray, H. (1918) "II. Osteology 5b the facial bones." in Anatomy of the human body. Lea and Febiger Philadelphia.

Hannam, A.C. (1997). "Jaw muscle structure and function." in Science and Practice of Occlusion, C.McNeill, ed., Quintessence Publishing Co, Inc, Berlin, 41-49.

Honda Marine. "Vtec information." http://video.google.com/videoplay?docid=-8790857042954658 21&q=vtec, 2005.

J.-S.Pap, (2005). Personal communication.

Koolstra, J.H., van Eijden, T.M.G.J. (1999). "Three-dimensional dynamical capabilities of the human masticatory muscles." *Journal of Biomechanics 32*, 145–152.

Lucas, P.W. (2004a). "The structure of the mammalian mouth." in Dental Functional Morphology: How Teeth Work. Cambridge University Press, United Kingdom, 13-54.

Lucas, P.W. (2004b). "How the mouth operates," in Dental Functional Morphology: How Teeth Work. Cambridge University Press, United Kingdom, 55-86.

Lucas, P.W. (2004c). "Tooth shape," in Dental Functional Morphology: How Teeth Work. Cambridge University Press, United Kingdom, 87-132.

Lund, J.P. (1991). "Mastication and its control by the brainstem." *Critical Reviews in Oral Biology and Medicine 2*, 33-64.

Mongini, F., Tempia-Valenti, G. & Benvegnu, G. (1986). "Computer-based assessment of habitual mastication." *Journal of Prosthetic Dentistry 55*, 638-649.

Norton, R.L. (2004). "Kinematics Fundamentals" in *Design of Machinery: An Introduction to the Synthesis and Analysis of Mechanisms and Machines* (3rd Ed. Chapter 2). McGraw-Hill: New York, 24-85.

Ogawa, T., Ogawa, M. & Koyano, K. (2001). "Different responses of masticatory movements after alteration of occlusal guidance related to individual movement pattern." *Journal of Oral Rehabilitation 28*, 830-841.

Oralb. www.oralb.com/images/learningcenter/teaching/ permanent_teeth_diagram.jpg, 2005.

Palmer, B. (2004). "Occlusion." www.brianpalmerdds.com/pdf/A-Occlusion.pdf, 2005.

Pedersen, A.M., Bardow, A., Beier Jensen, S., Nauntofte, B. (2002). "Saliva and gastrointestinal functions of taste, mastication, swallowing and digestion." *Journal of Oral Diseases 8*, 117–129.

Physik Instrumente. (1996-2005). "Hexapods / Motorized Micropositioning Stages & Actuators." www.physikinstrumente.com/en/products/micropositioning_hexapod/ index.php, 2005.

Stanisic, M.M. "Kinematics and Dynamics of Machinery." www.nd.edu/~stanisic/ ME339/limit.dead.positions.pdf, 2005.

Thompson, T. (1999a). "How to use and interpret the Coupler Curve and Centrode Atlas." www.cedarville.edu/academics/engineering/kinematics/ccapdf/howto.htm, 2005.

Thompson, T. (1999b). "Coupler Curve Atlas." www.cedarville.edu/academics/ engineering/kinematics/ccapdf/ccpagef.htm, 2005.

University of Limerick. "Plate Cam and Knife Edge Follower." www.ul.ie/~kirwanp/knifeedgeanimation.gif, 2005.

Wood, G.D. & Williams, J.E. (1981). "Gnathodynamometer: Measuring opening and closing forces." *Dental Update 8*, 239-250.

Wynne, W.P.D. (2005), "The Art of Articulation." vol. 3 no. 1.

9 Appendix A The instruction manual

Setting up the machine

Turn on the machine

1. Plug in the communications cable to the machine. The port is located at the top of the device near the power supply.
2. Plug the other end of the communications cable into the computers RS-232 serial port and parallel printer port.
3. Plug the power cable into the machine and then into the mains power supply. Turn the power on at the wall.
4. Switch on the power on the machine. The fan should start. If it doesn't check all power connections.

Start up the software

1. Open the chewing device software on the computer.

Check for interference

1. Lower the teeth table height by winding the lower handle to ensure that nothing is interfering with the actuating set of teeth.
2. Make sure that the clamping handles and anything else is not going to interfere with the actuating set of teeth.

Set up the chewing trajectories

1. Wind the upper handle to the desired position by pulling out the locking pin and turning. (clockwise for a lateral chewing motion and anti-clockwise for a vertical chewing motion in the frontal plane)
2. Adjust the incident angle in the side plane by loosening the nut locate opposite the top handle, moving into position and tightening again.

Set up the occlusal position of the teeth

1. Insert the top set of teeth by sliding them into the enclosure on the actuating part of the mechanism. Lock with the locating pin
2. Insert the lower set of teeth into the enclosure located on the teeth table. Lock them in with the locating pin.
3. Click on the 'set to lower position button' on the chewing device software. The top teeth should now move to their lowest position. If it doesn't close the software and check the power and communications cables and start again.
4. Position the teeth so that they occlude (mesh) properly by raising the teeth table and sliding the bottom teeth enclosure into position.

5. Lock the bottom teeth into position by pressing down on the clamping lever that you have access to and turn it clockwise so it is lightly locked into position. Click on the 'set to upper position' button in the software to move the teeth out of the way. Do up the other clamping lever and then tighten the first one and position them out of the way so they don't interfere with the actuating teeth.
6. Check to see if the teeth haven't moved by clicking the 'set to lower position' button in software to see if the teeth still occlude properly. If they have moved start again.
7. Click the 'set to upper position' button in the software to open the mouth.

NOTE: The teeth MUST be reset every time the chewing trajectory settings are changed.

Running the chewing device

1. Ensure that the chewing device has been set up correctly.
2. Insert a food sample onto the pre-molars (front teeth).
3. Inject the correct amount of artificial saliva.
4. Use the software commands to run the device.
5. Move the food sample onto the molars and run again.

Collecting the food sample

1. Remove the locking pins from the upper and lower teeth.
2. Slide out the upper and lower sets of teeth.
3. Collect the food sample by scraping the food off of the teeth.
4. Clean the teeth ready for the next food sample.

The basic software commands

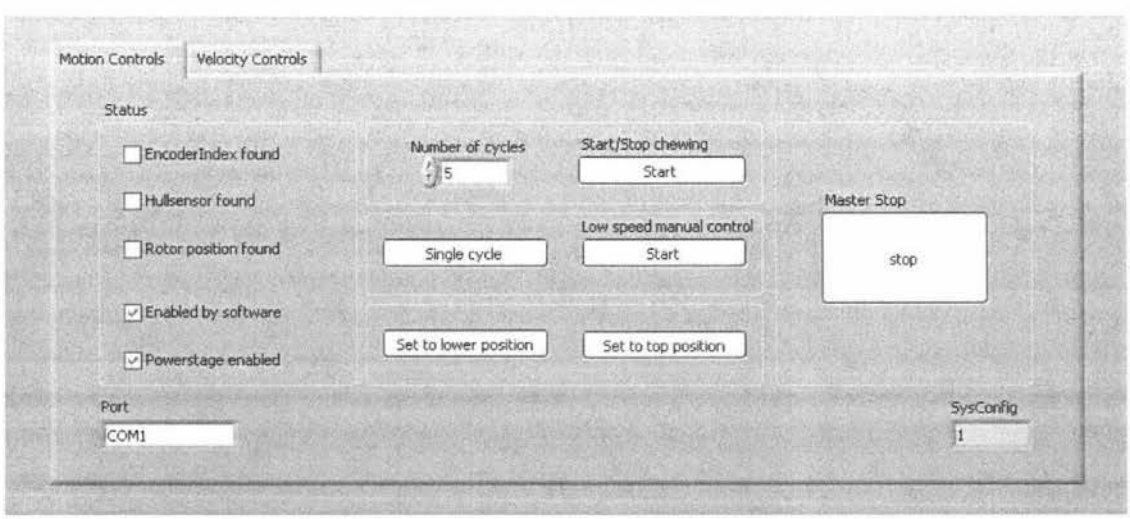

Set to top position: this command opens the mouth

Set to lower position: this command closes the mouth for setting up the teeth.

Single cycle: this command performs one chewing cycle.

Low speed manual control: slowly moves the teeth. Click the button to start it, click again to stop it.

Start chewing: this command starts the device chewing for the number of cycles specified in the 'number of cycles' box.

Master stop: this command stops the chewing device no matter what it is doing. This must be reset to enable the commands to work again. This is done by clicking on the button again.

The advanced software functions

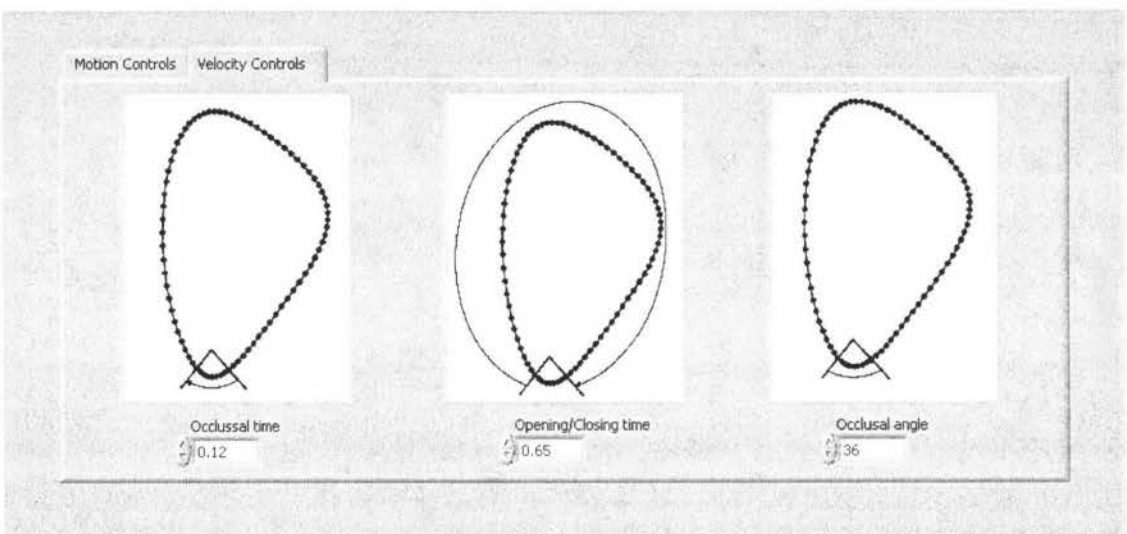

Occlusal time: This specifies the amount of time for the occlusal phase of the chewing cycle. The occlusal phase is where the teeth come together and move over each other.

Opening/Closing time: This specifies the amount of time that it takes to get from the end of the occlusal phase back to the start of the occlusal phase.

Occlusal angle: This is the angle that the crank turns that corresponds to the occlusal phase. The occlusal phase can then be set according to a vertical distance from the maximum intercuspal position. This can be done by using the figure below to determine the occlusal angle that corresponds to the vertical occlusal distance. The standard setting is 36 degrees and corresponds to approximately 0.5mm of

occlusion. This can be adjusted by specifying an occlusal distance and counting the number of points that are between this point and the maximum intercuspal position. Then multiply this number by 8 to get the occlusal angle.

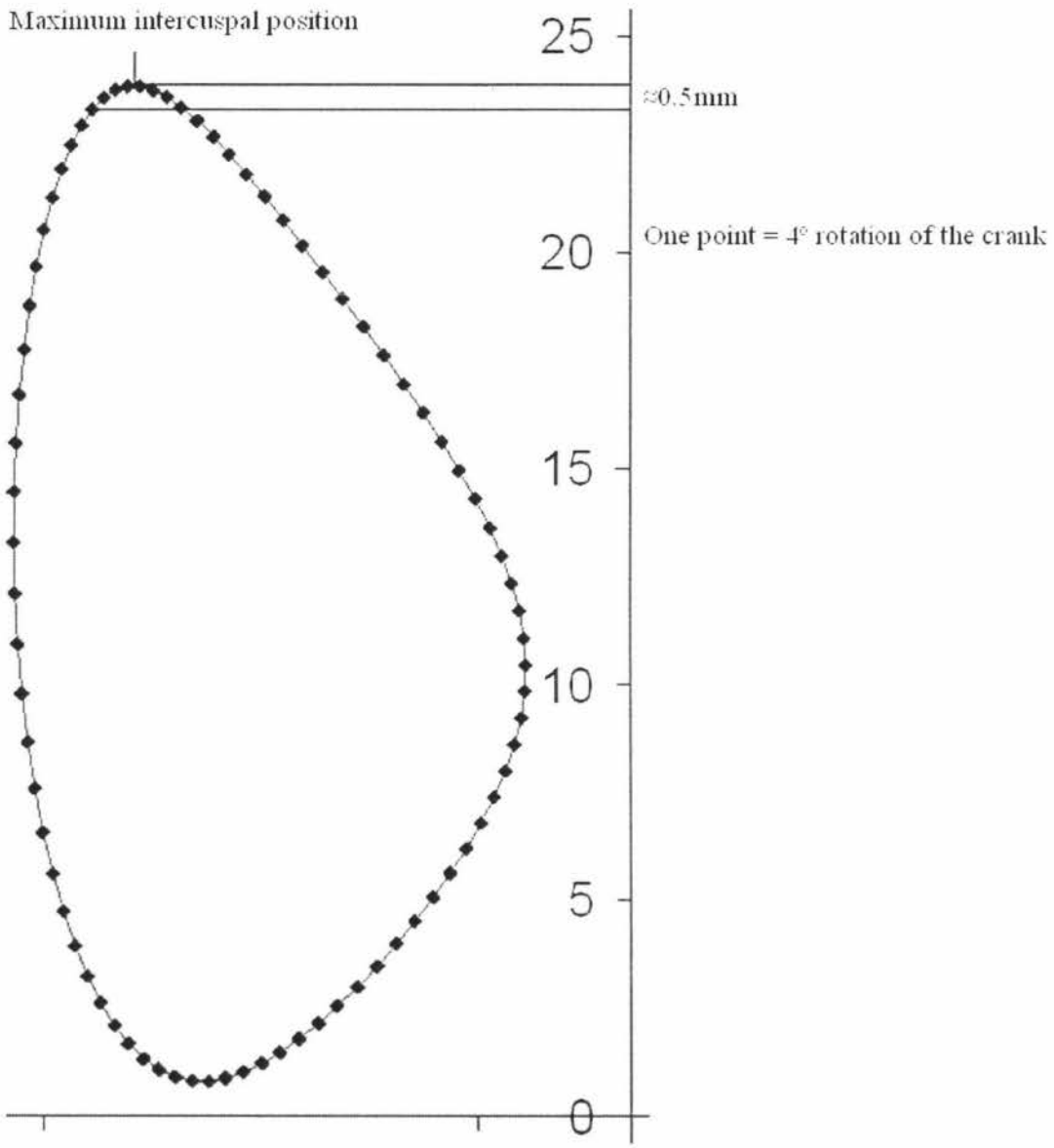

Setting the chewing trajectories

The chewing trajectories can be adjusted to chew different foods by winding the upper handle (clockwise for a lateral chewing motion and anti-clockwise for a vertical chewing motion in the frontal plane). The best position to set the handle is largely unknown but a general rule of thumb applies and is explained below.

The trajectories used to chew different food particles differ depending on both the shape and the texture of the food particles. This is due to the fact that the teeth operate differently depending on the chewing trajectory. If a vertical chewing motion is used, the teeth use their cusps to fracture the food particles. Where as if a more lateral chewing motion is used, the teeth use their sharp edges to function as blades and cut up the food particles (Lucas 2004c). The chewing trajectory used is therefore adjusted to ensure that the teeth are used correctly to chew the desired food particles. The decision of how to use the teeth, and therefore what chewing trajectory to use can be seen in the figure below. It shows that in the first step of deciding on how to use the teeth, the particle shape is detected and if the particles are thin sheets or rods the teeth are used as blades to cut up the food. If however they are thick blocks, then the texture is examined in the mouth. Lucas describes the texture as being $(R/E)^{0.5}$, where R is the food toughness and E is Young's modulus of elasticity. If $(R/E)^{0.5}$ is low, the teeth use their cusps to fracture the food. If $(R/E)^{0.5}$ is high, then the teeth once again use their sharp edges as blades to cut up the food. The application of this model implies foods that require fracturing include peanuts and biscuits as they are not tough and have a relatively high modulus of elasticity and therefore can be chewed with a vertical chewing motion. While foods that require cutting include meats and vegetables and therefore need to be chewed with a lateral chewing motion.

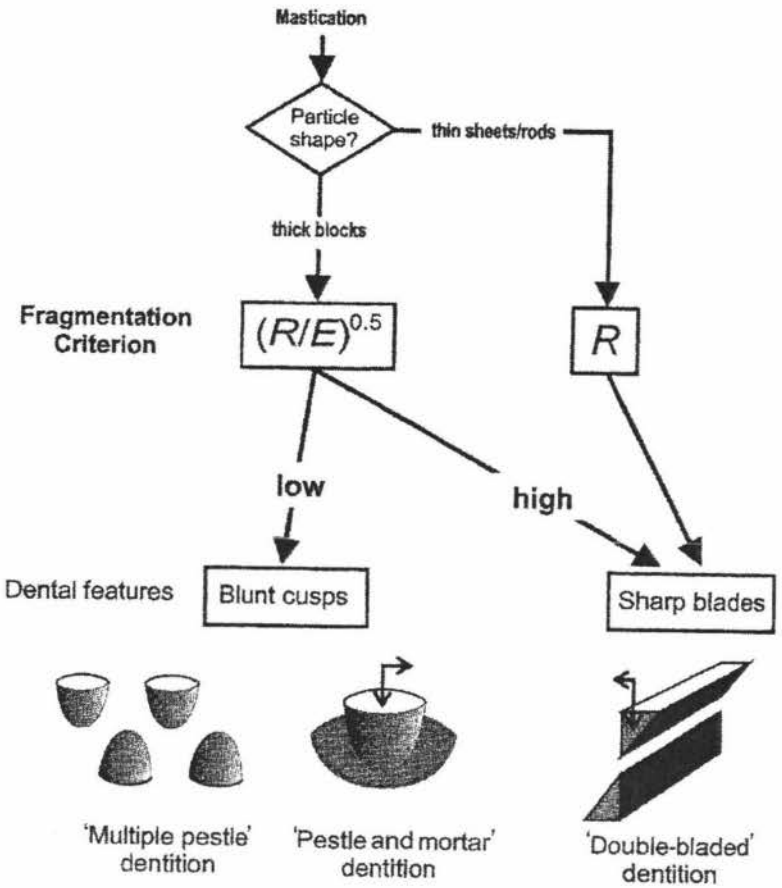
Mastication
Particle shape?
thin sheets/rods
thick blocks
Fragmentation Criterion
$(R/E)^{0.5}$
R
low
high
Dental features
Blunt cusps
Sharp blades
'Multiple pestle' dentition
'Pestle and mortar' dentition
'Double-bladed' dentition

Trouble shooting

Problem	Cause	Fix
Chewing device stalls	To much force trying to be applied	Check to see that no solid objects are jamming it up.
	The teeth are to close together	Lower the teeth until the chewing device starts moving.
	Solid objects are interfering with the actuating teeth	Shut down the software, and reset the power supply of the chewing device by turning the power switch off for 10 seconds and turning it back on. Restart the software.
Software doesn't function correctly	Incorrect power up procedure	Close the software, turn on the chewing device power and re-start the software

10 Appendices B-E

10.1 Appendix B C.A.D files

10.2 Appendix C Labview files

10.3 Appendix D Control card files

10.4 Appendix E Circuit design